



**Doctoral School of Environmental Sciences**

**POLLUTED WATER TREATMENT USING COMPOST MATERIAL AS  
ADSORBENT: BATCH AND CONTINUES COLUMN STUDIES**

**Ph.D. Dissertation**

**By Ramadan Benjreid**

**Gödöllő, Hungary 2019**



Doctoral School of Environmental Sciences

<b>Discipline:</b>	Environmental Sciences
<b>Name of Doctoral School:</b>	Doctoral School of Environmental Sciences
<b>Head:</b>	Csákiné Dr. Michéli Erika, DSc.
<b>Supervisor:</b>	Prof. Dr. György Füleky, CSc.
Environmental Sciences	Faculty of Agricultural and Institute of Environmental Sciences Department of Soil Science and Agrochemistry
Environmental Sciences	Prof. Dr. László Tolner, CSc. Faculty of Agricultural and Institute of Environmental Sciences Department of Soil Science and Agrochemistry
.....	.....
Approval of Head of Doctoral School	Approval of Supervisor

## TABLE OF CONTENTS

<b>CHAPTER 1: INTRODUCTION</b>	<b>1</b>
1.1 Introduction	1
1.2 Research objectives	2
1.3 Thesis organization	3
<b>CHAPTER 2: LITERATURE REVIEW</b>	<b>6</b>
2.1 Sources and health impacts of heavy metals	6
2.2 Wastewater treatment using natural materials	8
2.2.1 Compost materials	9
2.2.1.1 The Composting Process	11
2.2.1.2 Disposing heavy metal adsorbed by compost	13
2.3 Wastewater treatment technology	13
2.3.1 Physical methods	13
2.3.2 Chemical methods	13
2.3.3 Biological treatment	14
2.4 Adsorption	14
2.4.1 Adsorption mechanisms	15
2.4.1.1 Fundamental mechanism of adsorption	16
2.4.1.2 Ion exchange mechanism	17
2.4.2 Types of Adsorption	18
2.4.2.1 Physical adsorption (Vander Waals adsorption)	18
2.4.2.2 Chemisorption	18
2.4.3 Advantages of adsorption	18
2.5 Adsorption isotherms	19
2.5.1 Langmuir isotherm	19
2.5.2 Freundlich isotherm	20
2.5.3 Redlich–Peterson isotherm	20
2.6 Dynamic studies in fixed-bed systems	22
2.6.1 The breakthrough curve	22
2.6.2 Mass transfer zone	25
2.6.3 Mathematical description and adsorption modeling of fixed-bed column studies	26
2.7 Kinetic models for bed column	27
2.7.1 Thomas model	27

2.7.2.	Bohart-Adams model -----	28
2.7.3	Yoon and Nelson model -----	28
<b>2.8</b>	<b>Heavy metal analytical equipment -----</b>	<b>29</b>
2.8.1	SEM/EDX -----	29
2.8.2	Fourier transform infrared spectroscopy -----	30
<b>2.9</b>	<b>Conclusion -----</b>	<b>30</b>
<b>CHAPTER: 3 HEAVY METAL REMOVAL FROM POLLUTED WATER: BATCH AND FIXED BED COLUMN: EXPERIMENTAL STUDY -----</b>		<b>32</b>
<b>3.1</b>	<b>Materials and methods -----</b>	<b>32</b>
3.1.1	Instruments used for experimental analyses -----	32
3.1.2	Preparation of Adsorbent -----	32
3.1.3	Quality control -----	33
3.1.4	Adsorption in batch experiments -----	33
3.1.6	Preparation of synthetic wastewater -----	33
3.1.7	Experimental set up for batch study -----	34
3.1.8	Fixed bed column construction -----	34
<b>3.2</b>	<b>Result and discussion -----</b>	<b>36</b>
<b>3.2.1</b>	<b>Analysis and Characterization of compost -----</b>	<b>36</b>
3.2.1.1	Scanning electron microscopy (SEM) -----	36
3.2.1.2	Energy dispersive X-ray spectroscopy (EDX) -----	40
3.2.1.3.	Fourier transform infrared spectroscopy (FTIR) ---	44
<b>3.2.2</b>	<b>Batch experiment -----</b>	<b>46</b>
3.2.2.1	Langmuir isotherm -----	46
<b>3.2.3</b>	<b>Bed column and breakthrough curve -----</b>	<b>49</b>
<b>3.2.3.1</b>	<b>Mathematical description -----</b>	<b>49</b>
<b>3.2.3.2</b>	<b>Effect of initial inlet concentration on breakthrough curves -----</b>	<b>50</b>
3.2.3.2.1	Effect of $\text{Cu}^{2+}$ concentration on breakthrough curve using Garé compost -----	50
3.2.3.2.2	Effect of $\text{Cu}^{2+}$ concentration on breakthrough curve using Felgyő compost -----	52
3.2.3.2.3	Effect of $\text{Cd}^{2+}$ concentration on breakthrough curve using Felgyő compost -----	53
<b>3.2.3.3</b>	<b>Effect of inlet flow rate on breakthrough curves</b>	

<b>adsorption</b> -----	<b>54</b>
3.2.3.3.1 Effect of Cu <sup>2+</sup> flow rate on breakthrough curve using Garé compost -----	55
3.2.3.3.2 Effect of Cu <sup>2+</sup> flow rate on breakthrough curve using Felgyő compost -----	56
3.2.3.3.3 Effect of Cd <sup>2+</sup> flow rate on breakthrough curve using Felgyő compost -----	57
<b>3.2.3.4 Effect of bed depth on breakthrough curves</b> -----	<b>59</b>
3.2.3.4.1 Effect of bed depth on breakthrough curve after Cu <sup>2+</sup> treated using Garé compost -----	59
3.2.3.4.2 Effect of bed depth on breakthrough curve after Cu <sup>2+</sup> treated using Felgyő compost -----	61
3.2.3.4.3 Effect of bed depth on breakthrough curve after Cd <sup>2+</sup> treated using Felgyő compost -----	63
<b>3.2.4 Kinetic models of fixed bed column adsorption</b> -----	<b>68</b>
<b>3.2.4.1 Adams –Bohart model</b> -----	<b>68</b>
3.2.4.1.1 Adams –Bohart model fitted for Cu <sup>2+</sup> adsorbed by Garé compost -----	69
3.2.4.1.2 Adams –Bohart model fitted for Cu <sup>2+</sup> adsorbed by Felgyő compost -----	72
3.2.4.1.3 Adams –Bohart model fitted for Cd <sup>2+</sup> adsorbed by Felgyő compost -----	74
<b>3.2.4.2 Thomas model kinetics</b> -----	<b>77</b>
3.2.4.2.1 Thomas model fitted for Cu <sup>2+</sup> adsorbed by Garé compost -----	78
3.2.4.2.2 Thomas model fitted for Cu <sup>2+</sup> adsorbed by Felgyő compost -----	80
3.2.4.2.3 Thomas model fitted for Cd <sup>2+</sup> adsorbed by Felgyő compost -----	83
<b>3.2.4.3 Yoon–Nelson kinetic model</b> -----	<b>85</b>
3.2.4.3.1 Yoon–Nelson model fitted for Cu <sup>2+</sup> adsorbed by Garé compost -----	86
3.2.4.3.2 Yoon–Nelson model fitted for Cu <sup>2+</sup> adsorbed by Felgyő compost -----	88

	3.2.4.3.3	Yoon Nelson model fitted for Cd <sup>2+</sup> adsorbed by Felgyő compost -----	90
<b>4</b>		<b>NEW SCIENTIFIC RESULTS -----</b>	<b>93</b>
<b>5</b>		<b>CONCLUSIONS AND FUTURE RESEARCH -----</b>	<b>94</b>
	5.1	Conclusions -----	94
	5.2	Scope for future research -----	94
<b>6</b>		<b>SUMMARY-----</b>	<b>96</b>
<b>7</b>		<b>ÖSSZEFOGLALÁS -----</b>	<b>98</b>
<b>8</b>		<b>REFERENCES -----</b>	<b>100</b>
<b>9</b>		<b>ACKNOWLEDGEMENTS -----</b>	<b>116</b>
<b>10</b>		<b>RELATED PUBLICATIONS -----</b>	<b>117</b>
<b>11</b>		<b>DECLARATION -----</b>	<b>118</b>

**LIST OF FIGURES**

Figure 2.1	Example adsorption isotherm -----	21
Figure 2.2	Typical isotherm models illustration -----	21
Figure 2.3	Ideal breakthrough curves -----	25
Figure 2.4	Typical mass transfer zone -----	26
Figure 3.1	Column experimental set up -----	35
Figure 3.2	Scanning electron microscopy (SEM) for Felgyő compost at 10 $\mu$ m -	37
Figure 3.3	Scanning electron microscopy (SEM) for Felgyő compost loaded with Cu <sup>2+</sup> at 10 $\mu$ m -----	37
Figure 3.4	Scanning electron microscopy (SEM) for Felgyő compost loaded with Cd <sup>2+</sup> at 10 $\mu$ m -----	38
Figure 3.5	Scanning electron microscopy (SEM) for Garé compost at 10 $\mu$ m ---	38
Figure 3.6	Scanning electron microscopy (SEM) for Garé compost loaded with Cu <sup>2+</sup> at 10 $\mu$ m -----	39
Figure 3.7	Scanning electron microscopy (SEM) for Felgyő compost loaded with Cd <sup>2+</sup> at 10 $\mu$ m -----	39
Figure 3.8	Energy dispersive X-ray spectroscopy (EDX), (Felgyő compost unloaded) -----	40
Figure 3.9	Energy dispersive X-ray spectroscopy (EDX) after Cu <sup>2+</sup> loaded (Felgyő compost) -----	41
Figure 3.10	Energy dispersive X-ray spectroscopy (EDX) after Cd <sup>2+</sup> loaded (Felgyő compost) -----	41
Figure 3.11	Energy dispersive X-ray spectroscopy (EDX) (Garé compost unloaded) -----	41
Figure 3.12	Energy dispersive X-ray spectroscopy (EDX) after Cu <sup>2+</sup> loaded (Garé compost) -----	42
Figure 3.13	Energy dispersive X-ray spectroscopy (EDX) after Cd <sup>2+</sup> loaded (Garé compost) -----	42
Figure 3.14	FTIR spectra of raw Garé compost loaded with Cu <sup>2+</sup> and Cd <sup>2+</sup> -----	45
Figure 3.15	FTIR spectra of raw Felgyő compost loaded with Cu <sup>2+</sup> and Cd <sup>2+</sup> -----	45
Figure 3.16	Batch experimental data of Cu <sup>2+</sup> adsorbed by compost (Sioagárd, Garé and Felgyő) fitted to Langmuir model -----	48
Figure 3.17	Batch experimental data of Cd <sup>2+</sup> adsorbed by compost (Sioagárd Garé Felgyő) fitted to Langmuir model -----	48

Figure 3.18	Effect of concentration 20, 100 mg L <sup>-1</sup> at (Garé compost, Cu <sup>2+</sup> treated) different bed heights, flow rate 4 mL min <sup>-1</sup> -----	51
Figure 3.19	Effect of concentration 20, 100 mg L <sup>-1</sup> at (Garé compost, Cu <sup>2+</sup> treated) different bed heights, flow rate 8 mL min <sup>-1</sup> -----	51
Figure 3.20	Effect of concentration 20, 100 mg L <sup>-1</sup> at different bed heights, flow rate 4 mL min <sup>-1</sup> (Felgyő compost, Cu <sup>2+</sup> adsorbed) -----	52
Figure 3.21	Effect of concentration 20, 100 mg L <sup>-1</sup> at different bed heights, flow rate 8 mL min <sup>-1</sup> (Felgyő compost, Cu <sup>2+</sup> adsorbed) -----	53
Figure 3.22	Effect of concentration 20.100 mg L <sup>-1</sup> , flow rate 4 mL min <sup>-1</sup> , different bed heights (Felgyő compost, Cd <sup>2+</sup> treated) -----	54
Figure 3.23	Effect of concentration 20,100 mg L <sup>-1</sup> , flow rate 8ml/min, different bed heights (Felgyő compost, Cd <sup>2+</sup> treated) -----	54
Figure 3.24	Effect of flow rate (Garé compost, Cu <sup>2+</sup> treated) at 20 mg L <sup>-1</sup> concentration at different bed heights, flow rate 4 and 8 mL min <sup>-1</sup> ---	55
Figure 3.25	Effect of flow rate (Garé compost, Cu <sup>2+</sup> treated) at 100 mg L <sup>-1</sup> concentration at different bed heights, flow rate 4 and 8 mL min <sup>-1</sup> ---	56
Figure 3.26	Effect of the flow rate at 20 mg L <sup>-1</sup> Cu <sup>2+</sup> concentration at different bed heights, flow rate 4mL min <sup>-1</sup> and 8 mL min <sup>-1</sup> , (Felgyő compost, Cu <sup>2+</sup> adsorbed) -----	57
Figure 3.27	Effect of the flow rate at 100 mg L <sup>-1</sup> Cu <sup>2+</sup> concentration at different bed heights, flow rate 4 mL min <sup>-1</sup> and 8 mL min <sup>-1</sup> (Felgyő compost, Cu <sup>2+</sup> adsorbed) -----	57
Figure 3.28	Effect of concentration 20.100 mg L <sup>-1</sup> , flow rate 4 m: min <sup>-1</sup> , different bed heights (Felgyő compost, Cd <sup>2+</sup> treated) -----	58
Figure 3.29	Effect of concentration 20,100 mg L <sup>-1</sup> , flow rate 8ml/min, different 71bed heights. (Felgyő compost, Cd <sup>2+</sup> treated) -----	58
Figure 3.30	Effect of bed height (Garé compost, Cu <sup>2+</sup> treated) at concentration 20 mg L <sup>-1</sup> and 4 mL min <sup>-1</sup> flow rate -----	59
Figure 3.31	Effect of bed height (Garé compost, Cu <sup>2+</sup> treated) at concentration 20 mg L <sup>-1</sup> and 8 mL min <sup>-1</sup> flow rate -----	60
Figure 3.32	Effect of bed height (Garé compost, Cu <sup>2+</sup> treated) at concentration 100 mg L <sup>-1</sup> and 4 mL min <sup>-1</sup> flow rate -----	60
Figure 3.33	Effect of bed height (Garé compost, Cu <sup>2+</sup> treated) at concentration 100 mg L <sup>-1</sup> and 8mL min <sup>-1</sup> flow rate -----	61
Figure 3.34	Effect of bed height at concentration 20 mg L <sup>-1</sup> and 4 mL min <sup>-1</sup> flow	

	rate, (Felgyő compost, Cu <sup>2+</sup> adsorbed) -----	62
Figure 3.35	Effect of bed height at concentration 20 mg L <sup>-1</sup> and 4 mL min <sup>-1</sup> flow rate (Felgyő compost, Cu <sup>2+</sup> adsorbed) -----	62
Figure 3.36	Effect of bed height at concentration 100 mg L <sup>-1</sup> and 4 mL min <sup>-1</sup> flow rate (Felgyő compost, Cu <sup>2+</sup> adsorbed) -----	63
Figure 3.37	Effect of bed height at concentration 100 mg L <sup>-1</sup> and 8 mL min <sup>-1</sup> flow rate (Felgyő compost, Cu <sup>2+</sup> adsorbed) -----	63
Figure 3.38	Effect of bed height when concentration 20 mg L <sup>-1</sup> and flow rate 4 mL min <sup>-1</sup> . (Felgyő compost, Cd <sup>2+</sup> treated) -----	64
Figure 3.39	Effect of bed height when concentration 20 mg L <sup>-1</sup> and flow rate 8 mL min <sup>-1</sup> . (Felgyő compost, Cd <sup>2+</sup> treated) -----	65
Figure 3.40	Effect of bed height when concentration 100 mg L <sup>-1</sup> and flow rate 4 mL min <sup>-1</sup> -----	65
Figure 3.41	Effect of bed height when concentration 100 mg L <sup>-1</sup> and flow rate 8 mL min <sup>-1</sup> . (Felgyő compost, Cd <sup>2+</sup> treated) -----	66
Figure 3.42	Adams–Bohart plot (Garé compost, Cu <sup>2+</sup> treated) concentration 20 mg L <sup>-1</sup> and 4 mL min <sup>-1</sup> flow rate and different bed heights -----	70
Figure 3.43	Adams–Bohart plot (Garé compost, Cu <sup>2+</sup> treated) concentration 20 mg L <sup>-1</sup> and 8 mL min <sup>-1</sup> flow rate and different bed heights -----	70
Figure 3.44	Adams–Bohart plot (Garé compost, Cu <sup>2+</sup> treated) concentration 100 mg L <sup>-1</sup> and 4 mL min <sup>-1</sup> flow rate and different bed heights -----	71
Figure 3.45	Adams–Bohart plot (Garé compost, Cu <sup>2+</sup> treated) concentration 100 mg L <sup>-1</sup> and 4 mL min <sup>-1</sup> flow rate and different bed heights -----	71
Figure 3.46	Adams–Bohart plot of felgyő compost, Cu <sup>2+</sup> concentration 20 mg L <sup>-1</sup> and 4 mL min <sup>-1</sup> flow rate and different bed heights -----	73
Figure 3.47	Adams–Bohart plot of felgyő compost, Cu <sup>2+</sup> concentration 20 mg L <sup>-1</sup> and 8 mL min <sup>-1</sup> flow rate and different bed heights -----	73
Figure 3.48	Adams–Bohart plot of felgyő compost, Cu <sup>2+</sup> concentration 100 mg L <sup>-1</sup> and 4 mL min <sup>-1</sup> flow rate and different bed heights -----	73
Figure 3.49	Adams–Bohart plot of felgyő compost, Cu <sup>2+</sup> concentration 100 mg L <sup>-1</sup> and 4 mL min <sup>-1</sup> flow rate and different bed heights -----	74
Figure 3.50	Bohart–Adams plot of Felgyő compost, Cd <sup>2+</sup> treated concentration 20 mg L <sup>-1</sup> and 4 mL min <sup>-1</sup> flow rate and different bed heights -----	75
Figure 3.51	Bohart–Adams plot of (Felgyő compost, Cd <sup>2+</sup> treated) concentration 20 mg L <sup>-1</sup> and 8 mL min <sup>-1</sup> flow rate and different bed heights -----	75

Figure 3.52	Bohart–Adams plot of (Felgyő compost, Cd <sup>2+</sup> treated) concentration 20 mg L <sup>-1</sup> and 4 mL min <sup>-1</sup> flow rate and different bed heights -----	76
Figure 3.53	Bohart–Adams plot of (Felgyő compost, Cd <sup>2+</sup> treated) concentration 20 mg L <sup>-1</sup> and 4 mL min <sup>-1</sup> flow rate and different bed heights -----	76
Figure 3.54	Thomas plot (Garé compost, Cu <sup>2+</sup> treated) concentration 20 mg L <sup>-1</sup> and 4 mL min <sup>-1</sup> flow rate and different bed heights -----	79
Figure 3.55	Thomas plot (Garé compost, Cu <sup>2+</sup> treated) concentration 20 mg L <sup>-1</sup> and 8 mL min <sup>-1</sup> flow rate and different bed heights -----	79
Figure 3.56	Thomas plot (Garé compost, Cu <sup>2+</sup> treated) concentration 100 mg L <sup>-1</sup> and 4 mL min <sup>-1</sup> flow rate and different bed heights -----	79
Figure 3.57	Thomas plot (Garé compost, Cu <sup>2+</sup> treated) concentration 100 mg L <sup>-1</sup> and 4 mL min <sup>-1</sup> flow rate and different bed heights -----	80
Figure 3.58	Thomas plot of felgyő compost, Cu <sup>2+</sup> concentration 20 mg L <sup>-1</sup> and 4 mL min <sup>-1</sup> flow rate and different bed heights -----	81
Figure 3.59	Thomas plot of felgyő compost, Cu <sup>2+</sup> concentration 20 mg L <sup>-1</sup> and 8 mL min <sup>-1</sup> flow rate and different bed heights -----	81
Figure 3.60	Thomas plot of felgyő compost, Cu <sup>2+</sup> concentration 100 mg L <sup>-1</sup> and 4 mL min <sup>-1</sup> flow rate and different bed heights -----	82
Figure 3.61	Thomas plot of felgyő compost, Cu <sup>2+</sup> concentration 100 mg L <sup>-1</sup> and 4 mL min <sup>-1</sup> flow rate and different bed heights -----	82
Figure 3.62	Thomas plot of (Felgyő compost, Cd <sup>2+</sup> treated) concentration 20 mg L <sup>-1</sup> and 4 mL min <sup>-1</sup> flow rate and different bed heights -----	84
Figure 3.63	Thomas plot of (Felgyő compost, Cd <sup>2+</sup> treated) concentration 20 mg L <sup>-1</sup> and 4 mL min <sup>-1</sup> flow rate and different bed heights -----	84
Figure 3.64	Thomas plot of (Felgyő compost, Cd <sup>2+</sup> treated) concentration 20 mg L <sup>-1</sup> and 4 mL min <sup>-1</sup> flow rate and different bed heights -----	84
Figure 3.65	Thomas plot of (Felgyő compost, Cd <sup>2+</sup> treated) concentration 20 mg L <sup>-1</sup> and 4 mL min <sup>-1</sup> flow rate and different bed heights -----	85
Figure 3.66	Yoon–Nelson plot (Garé compost, Cu <sup>2+</sup> treated) concentration 20 mg L <sup>-1</sup> and 4 mL min <sup>-1</sup> flow rate and different bed heights -----	86
Figure 3.67	Yoon–Nelson plot (Garé compost, Cu <sup>2+</sup> treated) concentration 20 mg L <sup>-1</sup> and 8 mL min <sup>-1</sup> flow rate and different bed heights -----	87
Figure 3.68	Yoon–Nelson plot (Garé compost, Cu <sup>2+</sup> treated) concentration 100 mg L <sup>-1</sup> and 4 mL min <sup>-1</sup> flow rate and different bed heights -----	87
Figure 3.69	Yoon–Nelson plot (Garé compost, Cu <sup>2+</sup> treated) concentration 100	

	mg L <sup>-1</sup> and 4 mL min <sup>-1</sup> flow rate and different bed heights -----	87
Figure 3.70	Yoon–Nelson plot (Felgyő compost, Cu <sup>2+</sup> treated) Cu <sup>2+</sup> concentration 20 mg L <sup>-1</sup> and 4 mL min <sup>-1</sup> flow rate and different bed heights -----	89
Figure 3.71	Yoon–Nelson plot (Felgyő compost, Cu <sup>2+</sup> treated) Cu <sup>2+</sup> concentration 20 mg L <sup>-1</sup> and 8 mL min <sup>-1</sup> flow rate and different bed heights -----	89
Figure 3.72	Yoon–Nelson plot (Felgyő compost, Cu <sup>2+</sup> treated) Cu <sup>2+</sup> concentration 100 mg L <sup>-1</sup> and 4 mL min <sup>-1</sup> flow rate and different bed heights -----	89
Figure 3.73	Yoon–Nelson plot (Felgyő compost, Cu <sup>2+</sup> treated) Cu <sup>2+</sup> concentration 100 mg L <sup>-1</sup> and 4 mL min <sup>-1</sup> flow rate and different bed heights -----	90
Figure 3.74	Yoon–Nelson plot of (Felgyő compost, Cd <sup>2+</sup> treated) concentration 20 mg L <sup>-1</sup> and 4 mL min <sup>-1</sup> flow rate and different bed heights -----	91
Figure 3.75	Yoon–Nelson plot of (Felgyő compost, Cd <sup>2+</sup> treated) concentration 20 mg L <sup>-1</sup> and 4 mL min <sup>-1</sup> flow rate and different bed heights -----	91
Figure 3.76	Yoon–Nelson plot of (Felgyő compost, Cd <sup>2+</sup> treated) concentration 20 mg L <sup>-1</sup> and 4 mL min <sup>-1</sup> flow rate and different bed heights -----	92
Figure 3.77	Yoon–Nelson plot of (Felgyő compost, Cd <sup>2+</sup> treated) concentration 20 mg L <sup>-1</sup> and 4 mL min <sup>-1</sup> flow rate and different bed heights -----	92

**LIST OF TABLES**

TABLE 2.1	Heavy metals removal by various adsorbents -----	8
TABLE 2.2	Physical/Chemical Method Advantages and Disadvantages -----	14
TABLE 2.3	Compare of other researches work for removing Cd <sup>2+</sup> with this study -----	26
TABLE 2.4	Compare of other researches work for removing Cu <sup>2+</sup> with this study-----	27
TABLE 2.5	Adsorption models comparison of their strength and weakness -----	29
TABLE 3.1	The chemical composition of raw Felgyő compost after and after loaded with Cu <sup>2+</sup> -----	43
TABLE 3.2	The chemical composition of raw Garé compost and after loaded with Cu <sup>2+</sup> and Cd <sup>2+</sup> -----	43
TABLE 3.3	Content properties of compost materials -----	49
TABLE 3.4	Langmuir Isotherms for Cd <sup>2+</sup> and Cu <sup>2+</sup> ( $q_{max}$ Maximum Adsorption and $K_L$ Equilibrium Constant) -----	49
TABLE 3.5	Removal percentage of Cu <sup>2+</sup> and Cd <sup>2+</sup> , compost (Sioagárd, Garé and Felgyő) -----	49
TABLE 3.6	Mathematical description of column parameters (Garé compost, Cu <sup>2+</sup> treated) -----	66
TABLE 3.7	Mathematical description of column parameters (Felgyő compost, Cu <sup>2+</sup> treated) -----	67
TABLE 3.8	Mathematical description of column parameters (Felgyő compost, Cd <sup>2+</sup> treated) -----	67
TABLE 3.9	Mathematical description of column parameters (Garé compost, Cd <sup>2+</sup> treated) -----	68
TABLE 3.10	Parameters predicted by Adam-Bohart model (Garé compost, Cu <sup>2+</sup> treated) -----	72
TABLE 3.11	Parameters predicted by Adam-Bohart model (Felgyő compost, Cu <sup>2+</sup> treated) -----	74
TABLE 3.12	Parameters predicted by Adam-Bohart model (Felgyő compost, Cd <sup>2+</sup> treated) -----	76
TABLE 3.13	Parameters predicted by Thomas model (Garé compost,	

	Cu <sup>2+</sup> treated) -----	80
TABLE 3.14	Parameters predicted by Thomas model (Felgyő compost loaded with Cu <sup>2+</sup> )-----	83
TABLE.3.15	Parameters predicted by Thomas model (Felgyő compost, Cd <sup>2+</sup> treated) -----	85
TABLE 3.16	Parameters predicted by Yoon-Nelson model (Garé compost, Cu <sup>2+</sup> treated) -----	88
TABLE 3.17	Parameters predicted by Yoon-Nelson model (Felgyő compost, Cu <sup>2+</sup> treated)-----	90
TABLE 3.18	Parameters predicted by Yoon-Nelson model. (Felgyő compost, Cd <sup>2+</sup> treated) -----	92

## CHAPTER 1: INTRODUCTION

### 1.1 Introduction

Water pollution is the contamination of water bodies such as lakes, rivers, oceans, and groundwater caused by human activities, which can be harmful to organisms and plants which live in these water bodies. Water pollution by toxic heavy metals through the discharge of industrial waste is a worldwide environmental problem. The presence of heavy metals in streams, lakes, and groundwater reservoirs has been responsible for several health problems with plants, animals, and human beings (Huang et al. 2008). Copper is widely applied in the electrical wiring, selenium rectifier, plumbing, gear wheel and roofing industries for its electrical and thermal conductivity, good corrosion resistance and ease of installation and fabrication. The copper is essential and healthy to humans. However, like all heavy metals, it is potentially toxic as well. The potential sources of copper in industrial effluent are from pulp and paperboard mills, plating baths and metal cleaning, the fertilizer industry, and wood pulp production (Subbaiah et al. 2011). In recent decades, the annual global release of heavy metal reached 22,000 tons (metric tons) for cadmium, 939,000 tons for copper, 783,000 tons for lead and 1,350,000 tons for zinc (Singh et al. 2003). The excessive intake of copper results in its accumulation in the liver and produces gastrointestinal problems, kidney damage, anemia and continued inhalation of copper-containing sprays which is linked with an increase in lung cancer among exposed workers (Sunarso and Ismadji 2009). Cadmium is one such heavy metal which is added to water and soil through the effluent from battery, catalyst, paint, mining and many other industries. It affects human being adversely when injected into human bodies. It can cause both long term and short-term diseases in human beings and other aquatic life (Laniyan et al. 2011). Consequently, it became very important to remove such contaminants from industrial wastewater before they are discharged into the environment. The removals of these hazardous materials may be performed using various techniques, including precipitation, membrane filtration, ion exchange, sorptive flotation and adsorption. However, these methods are known for their high cost and ineffective when dealing with low heavy metal concentration. While a number of researchers have attempted to resolve this problem through the use of different technologies, an efficient and cost-effective approach for heavy metal removal remains a challenge. Among many methods, adsorption techniques have been found appropriate for wastewater treatment because of their cost

effectiveness and uncomplicatedness. Adsorption has been recognized as an effective process in most of the industrial water and wastewater treatment (Mohammadi et al. 2005). Adsorption is the process of the attraction and accumulation of gas or liquid particles on the surface of another substance. Whereas the absorbed particles are called the adsorbate, the substance applied for adsorption is called the adsorbent. The foremost benefits of biosorption technology are its efficacy in reducing the concentration of heavy metal ions to very low levels and the use of low-cost biosorbent materials. Compost is an effective technology of retaining bio waste and generating effective fertilizer. The process of composting has also become an effective method of reducing the toxicity of heavy metals from solid waste and soils. The composts were applied to soils, which could increase the mineral nutrients and humic substances content, as well as the microbial activities (Aranda et al. 2015). Studies have found that as compost is processed, the content of dissolved heavy metals decreases, while the content of stable forms of heavy metals increases (Hanc et al. 2012). In addition, the morphological variations of heavy metals have a certain relevance to the fluctuations of organic matter and humus development throughout the composting progress. This paper evaluates the adsorption of  $\text{Cd}^{2+}$  and  $\text{Cu}^{2+}$  by using compost material as an adsorbent application. Batch experiments were carried out to examine the ability of different compost material of removing heavy metal from industrial waters. The experimental data was applied to one for the most used adsorption models, and its function fitted well.

## **1.2. Research objectives**

The objective of this research was to investigate heavy metal removal from industrial wastewater using various adsorbent materials in a series of batch and fixed-bed column studies under various experimental conditions. In order to achieve this objective, two different approaches conducted in laboratory studies with the following methods:

1. A batch adsorption study using different compost material was conducted to investigate the capability of removing  $\text{Cu}^{2+}$  and  $\text{Cd}^{2+}$  from industrial water.
2. A fixed bed column system adsorption study was operated using different compost material with different conditions of concentration of heavy metal, bed depth and flow rate to remove heavy metal from the aqueous solution.
3. Applying the most commonly used models for adsorption prediction.

4. Studying the compost material capacity and their chemical characteristics by relating analytical instrumental technologies.

### **1.3 Thesis organization**

The experiments and tasks were defined, designed and are presented in this study in the following manuscript format:

#### **Experimental**

##### **Batch study (Part I)**

Laboratory examination for the part I was carried out in batch experiments. The determined concentration from 0 to 50000  $\mu\text{g mL}^{-1}$  of the solution was tested with a different type of compost material. The weight of 1 g of compost material mixed with 10 mL solution concentration flask was investigated. Langmuir model was fitted to the data and its coefficient was determined.

##### **Continuous fixed bed (Part II)**

Laboratory experiments for part II were carried out to determine the efficiency of compost material in continuous adsorption mode versus different adsorption column depths, flow rate, adsorbent concentration and different time as well. The experimental work was carried out to verify the kinetic models with fixed bed columns. The investigation conducted to evaluate the compost material of removal different heavy metals which discussed in chapter 3.

#### **Chapter 1: Introduction**

The introduction part of this thesis is giving a general overview of heavy metal contamination and the work carried out.

#### **Chapter 2: The literature review**

A literature review is presented in Chapter 2 which touches on various aspects of this research. Since this research is focused on heavy metal removal from aqueous solution using adsorption, general treatment methods including adsorption were reviewed. Adsorption fundamentals, adsorption approaches and adsorbent materials for heavy metal removal were reviewed and presented.

### **Chapter 3: Batch and continuous fixed bed experiments**

Batch experiments were implemented in a set of flasks containing 10 mL of solution to investigate the effects, biosorbent dosage (1 g), initial metal ion concentration (0 to 50000  $\mu\text{g mL}^{-1}$ ) and contact time (24 hours). The suspensions were then filtered and metal ion concentrations in the supernatant solutions were measured by Atomic Absorption Spectrophotometer. Series of batch experiments were conducted using  $\text{Cu}^{2+}$  and  $\text{Cd}^{2+}$ . This chapter aimed to compare different compost material and different adsorbates. The data were fitted to Langmuir isotherm and coefficient were obtained and compared. Fundamental information on the adsorption capacities of these adsorbent materials was discussed. Batch experimental was run for the removal of several heavy metals using different compost material as treatment. The fixed bed system is dedicated to kinetics study of the ability of compost material for removing copper from wastewater by Felgyő and Garé compost for removing  $\text{Cu}^{2+}$  from wastewaters and  $\text{Cd}^{2+}$  treatment by Felgyő compost is also presented. The main objective of the fixed bed column was to investigate the adsorption of heavy metals  $\text{Cu}^{2+}$  and  $\text{Cd}^{2+}$  using different flow rate and different concentration at various volume (bed depth) ratios. A laboratory bench-scale fixed-bed column study was operated in a down-flow method to evaluate low-cost adsorbents for the removal of heavy metals based on the adsorption media, which was packed at different column depths (5, 10 and 15 cm). Effluent metal concentrations were set at 20, 100 mg/L and monitored its flow into the column bed, while metal breakthroughs as a function of volumetric throughput in the columns were reported and compared to each other. The results of these fixed-bed column investigations could provide useful insights into the design of larger scale metal removal applications using these types of natural adsorbents. Metal removal efficiencies and adsorbent adsorption capacities for each of the columns was estimated to assess the suitability of these adsorption media and the preferred operating conditions for the treatment of heavy metals. From the results of this work, observations regarding the potential use of these natural adsorbents for the heavy metal removal were discussed.

### **Chapter 4: Recommendations and further studies**

#### **Instruments used during this study**

The importance of using analytical equipment has been used by various researchers in order to give broad pictures of the mechanism of adsorption and the relationship of

adsorbent-adsorbate. Amongst many techniques, the usage of the below equipment was beneficial to this study, below are the methods used and further elaborated in Chapter 1.

1. Atomic absorption spectrophotometry.
2. Energy dispersive X-ray spectroscopy (EDX)
3. Fourier transform infrared spectroscopy (FTIR)
4. Scanning electron microscopy (SEM)

## CHAPTER 2: LITERATURE REVIEW

The purpose of this literature review is to identify and summarize some of the research regarding the removal of heavy metals from aqueous solutions and from wastewaters, using low-cost natural adsorbents. Concentration solution in different conditions using adsorption were studied, with a major emphasis on adsorption methods for heavy metal confiscation. Adsorption fundamentals, adsorption mechanisms, adsorbent materials for heavy metal removal, as well as different research investigations are reviewed and discussed. Isotherm and kinetic models were also considered in this study. Our understanding of the mechanisms of metal biosorption now allows the process to be scaled up and used in field applications, with packed-bed sorption columns being perhaps the most efficient for this purpose. Regenerating the biosorbents increases the process economy by allowing their reuse in multiple sorption cycles. The process results in metal-free effluents and small volumes of solutions containing concentrated metals, which can be easily recovered.

### 2.1 Sources and health impacts of heavy metals

Toxic heavy metals of particular concern in the treatment of industrial wastewaters include zinc, copper, nickel, mercury, cadmium, lead and chromium. Copper does essential work in animal metabolism. But the excessive ingestion of copper brings about serious toxicological concerns, such as vomiting, cramps, convulsions, or even death (Paulino et al. 2006). Cadmium compound as compared to other heavy metals is relatively water soluble therefore mobile in soil and tends to bioaccumulate. The long-lifetime PVC-window frames, plastics and plating on steel are the basic sources of cadmium in the environment. Cadmium accumulates in the human body especially in kidneys, thus leading to disfunction of the kidney (Volesky & Holan 1995). Metal contamination issues are becoming increasingly common worldwide, with many documented cases of metal toxicity in mining industries, foundries, smelters, coal-burning power plants and agriculture. Heavy metals, such as cadmium, copper, lead, chromium and mercury are major environmental pollutants, particularly in areas with high anthropogenic pressure. Heavy metal accumulation in soils and water is of concern in agricultural production due to the adverse effects on food safety and marketability, crop growth due to phytotoxicity, and environmental health of soil organisms. The influence of plants and their metabolic activities affects the geological and biological redistribution of heavy metals through pollution of the air,

water and soil. Here is a highlighted detail of heavy metals, their occurrence and toxicity for plants. Metal toxicity has high impact and relevance to plants and consequently, it affects the ecosystem, where the plants form an integral component. Plants growing in metal-polluted sites exhibit altered metabolism, growth reduction, lower biomass production and metal accumulation. Various physiological and biochemical processes in plants are affected by metals. The contemporary investigations into toxicity and tolerance in metal-stressed plants are prompted by the growing metal pollution in the environment. A few metals, including copper, manganese, cobalt, zinc and chromium are, however, essential to plant metabolism in trace amounts. It is only when metals are present in bioavailable forms and at excessive levels, they have the potential to become toxic to plants. Excessive accumulation of heavy metals in agricultural soils through wastewater irrigation, may not only result in soil contamination, but also lead to elevated heavy metal uptake by crops, and thus affect food quality and safety (Muchuweti et al. 2006). Heavy metal accumulation in soils and plants is of increasing concern because of the potential human health risks. This food chain contamination is one of the important pathways for the entry of these toxic pollutants into the human body. Heavy metal accumulation in plants depends upon plant species, and the efficiency of different plants in absorbing metals is evaluated by either plant uptake or soil-to-plant transfer factors of the metals (Rattan et al. 2005). Vegetables cultivated in wastewater-irrigated soils take up heavy metals in large enough quantities to cause potential health risks to the consumers. In order to assess the health risks, it is necessary to identify the potential of a source to introduce risk agents into the environment, estimate the amount of risk agents that come into contact with the human-environment boundaries, and quantify the health consequence of the exposure (Ma et al. 2006). According to the (National Research Council (NRC), 1983), this process consists of four steps, hazard identification, exposure assessment, dose/response assessment, and risk characterization. Chronic level intake of toxic metals has adverse impacts on humans and the associated harmful impacts become apparent only after several years of exposure (Ikeda et al. 2000). However, the consumption of heavy metal-contaminated food can seriously deplete some essential nutrients in the body that are further responsible for decreasing immunological defences, intrauterine growth retardation, impaired psycho-social faculties, disabilities associated with malnutrition and high prevalence of upper gastrointestinal cancer rates (Türkdoğan et al. 2003). Wastewater irrigation is a widespread practice in the world and recently a

number of articles have been published on wastewater-irrigated soils contaminated with heavy metals (Rothenberg et al. 2007). However, additional insight into metal uptake, accumulation and assessment of human health risks associated with wastewater-irrigated soils is still needed

## 2.2 Wastewater treatment using natural materials

Vieira et al. (2014) reported a list of removal of heavy metal ions using low-cost abundantly available adsorbents such as agricultural wastes such as tea waste and coffee, hazelnut shells, peanut hull, red fir and maple. Saw dusts, pinus bark and different bark samples, palm kernel husk and coconut husk, peanut skins, modified cellulosic materials, chemically modified cotton, corncobs and modified corncob, rice hulls, apple wastes, coffee grounds, bark, modified bark, wool fibers, tea leaves, and wool, olive cake, pine needles, almond shells, cactus leaves, charcoal, modified lignin, banana and orange peels, modified sugar beet pulp modified sunflower stalk, palm fruit bunch, maize leaf and different agricultural by-products. Other different types of adsorbents also used for varieties of heavy metal removal, below are reported in table 2.1.

Table 2.1. Heavy metals removal by various adsorbents

Adsorbent materials	Metal treated	Removal percentage	References
Wheat shell	Cu (II)	99%	(Basci et al. 2003)
Wheat bran	Cd (II)	87.15%	(Singh et al. 2005)
Water hyacinth	Pb (II), Cu (II), Co (II), Zn (II)	70-80%	(Kamble and Patil, 2001)
Waste tea leaves	Pb (II), Fe (II), Zn (II), Ni (II)	92%, 84%, 73%	(Ahluwalia and Goyal, 2007)
Three kinds treated rice husk	Cd (II)	80-97%	(Kumar and Bandyopadhyay, 2006)
Steam activated sulphurised carbon from bagasse pith	Cd (II)	98.80%	(Krishnan and Anirudhan, 2003)
Rose biomass pretreated with NaOH	Pb, Zn (II)	75%	(Nasir et al. 2007)
Rice bran	Pb (II), Cd (II), Cu (II), Zn (II)	>80.0%	(Montanher et al. 2005)
Peels of peas, fig leaves, broad beans, medlar peel	Cd (II)	70-80%	(Benaissa, 2006)
<i>Oriza sativa</i> husk	Pb (II)	98%	(Zulkali et al. 2006)
Husk of black gram Straw, saw dust, datesnut	Cd (II) Cd (II)	99%	(Saeed and Iqbal, 2003)
Dried parthenium powder	Cd (II)	>99%	(Ajmal et al. 2006)
Bagasse fly ash	Cd (II), Ni (II)	65 & 42%	(Srivastava et al. 2007)
Bagasse	Cd (II), Zn (II)	90-95%	(Mohan and Singh, 2002)
Agricultural by product <i>Humulus lupulus</i>	Pb (II)	75%	(Gardea-Torresdey et al. 2000)

### 2.2.1 Compost materials

Composting is a pacifying method to manage all forms of wastes (such as sewage sludge, municipal solid waste, tannery waste, pig manure, poultry manure etc.) which are biodegradable. The use of compost formed by above waste material to land can be used as soil fertilizer/conditioner due to presence of nitrogen, phosphorus, potassium and other nutrients. Composting is the process in which organic matter is transformed into compost by aerobic microorganisms, it comprises three major phases: mesophilic, thermophilic and cooling phase (the compost stabilization phase) (Neklyudov et al. 2008). It can reduce the solid waste volume by 40-50%, pathogens are destroyed by the metabolic heat generated by the thermophilic phase, which degrades a big number of hazardous organic pollutants and make available a final product that can be used as a soil improvement or fertilizer (Cai et al. 2007). If the final product contains high level of heavy metals, it often hinders agriculture land application of sewage sludge compost and it may be noxious to soil, plants and human health. Heavy metals uptake by plants and successive accumulation in human tissues and biomagnifications . The thermophilic phase of composting, which is the first step of composting, affects the exchangeable fraction. The toxic and anoxic conditions (produced by acetic acid and ammonia) at the first step of composting, affect the reducible and organic fractions. (Zorpas et al. 2000) reported the content of exchangeable Pb increased during the later thermophilic stage, but dropped again in the cooling period. The relative percent of residual Zn increased 3.38% during mesophilic and thermophilic phases but decreased 1.07% in the cooling stage. The exchangeable and carbonate Cu only accounted for the small parts of total Cu. Their concentrations increased, although a decrease tendency appeared during thermophilic phase. The composting process is currently viewed primarily as a waste management method to stabilize organic waste, such as manure, yard trimmings, municipal biosolids, and organic urban wastes. The stabilized end-product (compost) is widely used as a soil amendment to improve soil structure, provide plant nutrients, and facilitate the revegetation of disturbed or eroded soil (Cole et al. 1994). Mature compost also provide an inexpensive and technologically straightforward solution for managing hazardous industrial waste streams (solid, air, or liquid) and for remediating soil contaminated with toxic organic compounds (such as solvents and pesticides) and inorganic compounds (such as toxic metals). For example, a large number of hydrocarbons, which are common industrial contaminants found in soil

and exhaust gas, degrade rapidly during the composting process or in other compost-based processes. Furthermore, the addition of mature compost to contaminated soil accelerates plant and microbial degradation of organic contaminants and improves plant growth and establishment in toxic soils. When mature compost is added to contaminated soils, remediation costs are quite modest in comparison to conventionally used methods. Mature compost also controls several plant diseases without the use of synthetic fungicides or fumigants. Compost is an effective technique for utilizing biowaste and producing effective fertilizer. Composting has also become an effective method of reducing the toxicity of heavy metals from wastewater and soils. When compost is applied to soils could improve the mineral nutrients and humic substances content, as well as the microbial activities. Studies have found that as compost is processed, the content of dissolved heavy metals decreases, while the content of stable forms of heavy metals increases. In addition, the morphological changes of heavy metals have a certain relevance to the changes in organic matter and humus formation during the composting progress (Castaldi et al. 2006). Therefore, the fixation and adsorption of heavy metals by humus formed in the composting process is an economical and effective method of decreasing the bioavailability of heavy metals and reducing the risk of heavy metals in soils and wastewaters. As the humus composition and content change during the composting process, the molecular structure and the condensation degree also change greatly. In composting, there are significant reductions in the fat and polysaccharide structures but an increase in the aromatic structure (Huang et al. 2006). Functional groups such as phenolic hydroxyl and carboxyl increase, which means that the composting process can promote humic substances and provide more adsorption sites for chelating heavy metals (Veeken et al. 2000). Changes in the organic matter structure and humus functional groups during the composting process have been studied, and the stability of the organic matter has been found to increase as the aromatic structure in the humus increases (Fuentes et al. 2007). After composting, the humic acid (HA)/fulvic acid (FA) ratio will increase and the organic matter could further decompose and change the composition and structure after the secondary composting process. The composting process will change the structural characterization and adsorption properties of organic materials. As the previous study reported, composting can improve the adsorption efficiency of renewable bio-adsorbents of plant sources (Anastopoulos et al. 2013). A number of studies have studied that humus extracted from different types of soils, sludge and compost showed complexation with heavy

metal ions (Li et al. 2010). Previous studies have shown that high-molecular-weight humus, such as humin, is considered to be an active ingredient for the fixed adsorption of heavy metals (Mohee and Soobhany, 2014). To date, extensive researches focused on the addition of composts reduce leachability and mobility of heavy metals due to aerobic biological processes. It has been investigated that the application of manure composts changed the speciation of Zn and Pb in soil (Pardo et al. 2011). The change in the  $\text{Cd}^{2+}$  speciation had been explored in compost-amended soil (Rajaie et al. 2006). Moreover, waste-compost humus with a strong sorption capacity is a potential organic fertilizer resource. The application of composts as a soil amendment, and the adsorption rules and mechanisms for heavy metals in soil solutions need to be further investigated. Studies concerning the effect of the composting process on improving the properties of compost granule adsorbents have rarely been conducted. Changes of compost maturity over the composting stages also have important effects on the humus composition and morphology characterization, and thus affect the adsorption efficiency of heavy metals, and this mechanism requires further examination. Taken together, the multi-metal adsorption needs to deepen the knowledge of the interactions between composts and heavy metals. Compost maturity can also be enhanced by secondary fermentation, which is the process with the increase of the humus content and the more complex and stable structure for the humic substance (Spaccini and Piccolo, 2009). However, there are few types of research conducted for compost application and heavy metal adsorption.

### **2.2.1.1 The Composting Process**

Composting is a managed system that uses microbial activity to degrade raw organic materials, such as yard trimmings, so that the end-product is relatively stable, reduced in quantity (when compared to the initial amount of waste), and free from offensive odors. Composting can be done on a large or small scale, with the management requirements and intensity increasing dramatically as system size increases. In its simplest form, compostable material is arranged in long rows (windrows) and turned periodically to ensure good mixing. This process can handle large quantities of input, such as yard trimmings of up to 100,000 cubic yards per year, on only a few acres of land. Raw materials that tend to be very odorous during composting, such as municipal waste sludge (biosolids), can be processed in more elaborate systems and in a confined facility where odorous air can be treated. These systems use rotating drums, trenches, or enclosed tunnels for initial processing,

followed by a covered curing period. Mature compost can be substituted for the soil filter. A compost filter has several advantages over a soil filter, including a higher adsorptive capacity for volatile organic compounds and better air permeability properties. All composting methods share similar characteristic features and processes. Initially high microbial activity and heat production cause temperatures within the compostable material to rise rapidly into the thermophilic range (50 °C and higher). This temperature range is maintained by periodic turning or the use of controlled air flow (Viel et al. 1987). After the rapidly degradable components are consumed, temperatures gradually fall during the "curing" stage. At the end of this stage, the material is no longer self-heating, and the finished compost is ready for use. Substantial changes occur in microbial populations and species abundance during the various temperature stages (Gupta et al. 1987). Mesophilic bacteria and fungi are dominant in the initial warming period, thermophilic bacteria (especially actinomycetes) during the high temperature phase, and mesophilic bacteria and fungi during the curing phase (Finstein et al. 1975). The resulting compost has a high microbial, with microbial populations much higher than fertile, productive soils and many times higher than in highly disturbed or contaminated soils. Therefore, compost bioremediation takes far less time than natural attenuation of toxic materials (land farming). Microbial populations in soil (both fertile and contaminated) substantially vary from season to season. In most cases, the addition of compost greatly increases microbial populations and activity. Since the microbes are the primary agents for degradation of organic contaminants in soil (Alexander, 1994), increasing microbial density can accelerate degradation of the contaminants. In soil systems, microbial composition is greatly modified by organic input composition (Martin et al. 1992); the same degree of variation can be expected in composting systems. Dramatic changes in chemical composition occur during the composting process. Most starting materials for composting are plant-derived residues and contain carbon in the form of polysaccharides (cellulose and hemicellulose), lignin, and tannin. The end-product has a low polysaccharide content, most of which is microbial cell wall and extracellular gums (Macauley et al. 1993). With about 25 percent of the initial carbon content present in the form of highly stabilized humic substances. Organic matter content ranges from 30 to 50 percent of dry weight, with the remainder being minerals. The combination of high organic content and a variety of minerals makes compost an excellent adsorbent for both organic and inorganic chemicals.

### **2.2.1.2 Disposing heavy metal adsorbed by compost**

(Sas-Nowosielska et al. 2004) proposed the following disposal possibilities: composting, compaction, pyrolysis, direct disposal, leaching, and incineration (combustion and gasification). Kovacs and Szemmelveisz (2017) also suggested other alternative disposal option; total heavy metal content can be minimized by mixing the metal-enriched biomass with high proportions of uncontaminated dry matter and other biodegradable substances. The technology requires the close and continuous monitoring of mixture composition. The positive aspect of this method is that the phytoextracted metals are returned into the soil in small doses which contributes to nutrient recovery. Ex-situ composting post-harvest was proposed as a more effective method for the disposal of hazardous biomass.

## **2.3 Wastewater treatment technology**

There are three methods for treating waste water, namely physical, chemical and biological.

### **2.3.1 Physical methods**

Physical methods are the widely used and comprise of membrane filtration and adsorption technique. The major disadvantage of membrane technology is its high cost of periodic replacement. Moreover, it has limited lifetime as membrane fouling occurs very quickly. Filtration by using membrane was frequently used for exclusion of metallic contaminants from paper mill waste waters (Merrill et al. 2001). The perusal of literature reflects that liquid-phase adsorption is one of the most popular methods for the purification of the waste stream. This is an attractive alternative technique. By implementation of proper process design, high quality treated effluents can be produced. For this some inexpensive raw materials can be used. Thus, among the other methods, adsorption can be considered as an effective sequestration process for decontamination of process effluents (Dabrowski 2001).

### **2.3.2 Chemical methods**

Chemical techniques for the separation of toxic metals are rapid and efficient and no loss of sorbent is observed due to regeneration. But these methods are expensive. Accumulation and disposal of metal bearing sludge create secondary pollution problem. Recently, advanced oxidation technique by generating hydroxyl radicals is

used for degradation of pollutants but this is not economically feasible as high energy and chemical costs are involved (Mourao et al. 2006). Challenged with more and more strict regulations, currently, heavy metals are the environmental primacy pollutants and are becoming one of the most serious environmental concerns. So, these toxic heavy metals should be removed from the wastewater to protect the people and the environment. Many methods that are being used to remove heavy metal ions include chemical precipitation, ion-exchange, electroflotation, adsorption, coagulation-flocculation, membrane filtration, chemical precipitation, and electrochemical treatment technologies. (Adil 2006) summarized the advantage and disadvantage of some methods as listed in table 2.2.

Table 2.2. Physical/Chemical Method Advantages and Disadvantages

Methods	Usages	Disadvantages
Ozonation	Applicable for gaseous phase	Half life is short (20 min)
Oxidation	Rapid Process	Byproduct formation and high energy cost
Photochemical	No sludge generation	Byproduct formation
Ion Exchange	No adsorbent loss	Not effective for all types of heavy metals
Membrane Filtration	Removes all contaminants	Concentrated sludge is produced
Coagulation	Economically viable	High sludge production
Activated Carbon	Highly effective	Very expensive, non renewable
Precipitation	Low cost	Byproduct formation
Adsorption	Good % Removal Percentage	Adsorbent requires regeneration and disposal

### 2.3.3 Biological treatment

Biosorption is often considered as the most attractive alternative when compared with physical and chemical methods (Keskinan et al. 2003). Biological treatment involving microbial degradation of pollutants is a commonly used technique for waste water treatment. Due to some technical constrains, their application is restricted. The process is time consuming and requires a large area. Besides, that it is constrained by lack of flexibility in design and operation (Bhattacharyya and Sharma, 2003).

### 2.4 Adsorption

Adsorption has been proved to be an excellent way to treat industrial waste effluents, offering significant advantages like the low-cost, availability, profitability, ease of

operation and efficiency, in comparison with conventional methods especially from economic and environmental points of view. Adsorption has emerged as a promising technique for metal removal. The processes can occur at an interface between any two phases, such as liquid, gas-liquid, or liquid-solid interfaces (Barakat 2011). Moreover, adsorption is coming to be regarded as a practicable separation method for purification or bulk separation in newly developed material production processes of, for example, high-tech materials and biochemical and biomedical products. Surface characteristics and pore structures of adsorbents are the main properties in determining adsorption equilibrium and rate properties which are needed for plant design. New adsorbents are continuously being developed, introducing new applications for adsorption technology. Adsorption equilibrium is the fundamental factor in designing adsorption operations. When adsorption takes place with suspended adsorbent particles in a vessel, adsorbate is transported from the bulk fluid phase to the adsorption sites in the adsorbent particle. In this type of situation, changes in the amount adsorbed or concentration in the fluid phase can be predicted by solving the set of differential equations describing the mass balances in the particle, at the outer surface and between the particle and the fluid phase. Determination of diffusion parameters should be done with a simple kinetic system. These discussions are also applicable to the analysis and design of adsorption operation in a vessel or differential reactor. Another powerful technique for determining the rate parameters involved in an adsorption packed column gives the basic relations used for calculation of breakthrough curves.

#### **2.4.1 Adsorption mechanisms**

The complexity of the adsorbent structure implies that there are many ways for the metal to be captured by the adsorbed media. Adsorption mechanisms are therefore various, and, in some cases, they are still not very well understood. Metal adsorption and biosorption onto agricultural wastes is a rather complex process affected by several factors. Mechanisms involved in the biosorption process include chemisorption, complexation, adsorption-complexation on surface and pores, ion exchange, microprecipitation, heavy metal hydroxide condensation onto the biosurface, and surface adsorption (Semerjian 2010). The adsorption process of the adsorbate molecules from the bulk liquid phase into the adsorbent surface is presumed to involve the following stages:

- I. Mass transfer of the adsorbate molecules across the external boundary layer towards the solid particle.
- II. Adsorbate molecules' transport from the particle surface into the active sites by diffusion within the pore-filled liquid and migrate along the solid surface of the pore.
- III. Solute molecules adsorption on the active sites on the interior surfaces of the pores.
- IV. Once the molecule adsorbed, it may migrate on the pore surface through surface diffusion.

#### **2.4.1.1 Fundamental mechanism of adsorption**

The surface binding-sites of the adsorbent and the presence of hydrogen ion in solution are known to have a significant effect on the adsorptive uptake of metal ions. Due to the value of solution pH, the adsorbent surface undergoes protonation or deprotonation (Banerjee et al. 2007). At lower pH values, stiff competition between hydrogen and cadmium cations for the active sites could reduce Cd(II) adsorption. In this situation, high positive charge density of the adsorbent made the Cd(II) adsorption unfavorable due to electrostatic repulsion. Reversely, at higher pH values, the presence of hydrogen ions in the aqueous solution was reduced and the adsorbent surface was also deprotonated, thereby resulting in the increased adsorption of Cd(II). It is necessary to point out that according to the above discussion and some preliminary experiments, the results of adsorption were obtained at pH 6. Finally, deprotonation of the adsorbent surface underwent electrostatic attraction for Cd(II), resulting in the formation of metal–ligand complexes. On the other hand, the functional groups present in biomass molecules such as carbonyl, phenolic and carboxyl had the affinity for metal complexation (Sud et al. 2008). In the present work, carboxyl groups on compost, as perceived by FTIR spectra, played the main role in the Cu and Cd adsorption. As a result, complexation and ion exchange appeared to be the governing mechanism of the adsorption. Fall in pH of metal solution as it passes through the biomass packed column is a result of ion-exchange dependent sorption of metal ions onto the biomass. Functional groups of biomass, such as, carboxyl, release their hydrogen ions in the metal solution and electrostatically capture metal cations (Mehta and Gaur, 2005). However, in a few

cases, pH of effluent is higher than that of influent due probably to leaching of some anionic forms of minerals, such as, carbonate ions from the packed biosorbent. Nonetheless, fall of pH within the column is a matter of concern as it may adversely affect the metal removal performance of the biosorbent packed column, especially for cationic forms of metal ions. This aspect, unfortunately, remains unexplored till date. Our knowledge about fall in pH of the metal solution as it flows through the column under varying experimental conditions, such as, biomass type, metal ions, bed height, and flow rate is either lacking or inadequate. There is no technique that can be used to adjust the pH of the metal solution during its flow through the biomass-filled column. But, maintenance of pH in column during operation may maximize metal removal by a biosorbent packed bed. Nonetheless, the problem of lowering of pH of the metal solution can be avoided to a little extent by taking slightly higher pH of the influent metal solution, in comparison to pH which is mentioned as the optimum under batch condition. However, such a tactic needs proper experimental optimization and adequate approval. Here, it seems important to mention that we can take influent pH only by 6.5, because pH N 6.5 may cause precipitation of metal ions in the form of hydroxides (Eccles 1999).

#### **2.4.1.2 Ion exchange mechanism**

The metal cations (including  $\text{Cd}^{2+}$  are mainly bound through their interaction with various negatively charged groups in the compost formed through deprotonation. The most important are the carboxyl groups which are present in the byproducts of the decomposition such as humic acids but can also be present in the original structure of the organic matter - other negatively charged groups are also likely to present in lower concentrations, but this depends on the source/chemical composition of the organic matter used for composting. Similarly, phenolic hydroxyl groups in humic acids can also participate in the complexation. The cations can also interact with the surface of the inorganic clay particles, though its extent and mechanism depend on the inorganic content and the clay type; for example, in case of the very common silicates, they mostly react with the hydroxyl groups on the surface. (Liu et al. 2018) conducted research for removing  $\text{Cu}^{2+}$ ,  $\text{Cd}^{2+}$ ,  $\text{Zn}^{2+}$  and  $\text{Ni}^{2+}$  by compost material and reported that the complex surface structure and organic matter complexation were the main mechanisms of adsorption. (Covelo et al. 2004) stated that the greater percentage of  $\text{Cd}^{2+}$  in the adsorbents was associated with the residual fractions. The possible explanation for the residual state of adsorbed  $\text{Cd}^{2+}$  by compost may be due

to the existence of strong chemical bonds between  $\text{Cd}^{2+}$  and compost organic matter; organo-metal complexes exhibited higher stability and reduced the mobility of heavy metal ions. (Horsfall and Spiff, 2005) reported that complexation and ion exchange appeared to be the governing mechanism of the adsorption. In this regard, the sorption of Pb (II) and Cd (II) ions by nitric acid-treated wild cocoyam biomass was studied and the sorption was reported to occur by ion-exchange mechanism containing hydroxyl groups. (Sud et al. 2008) confirmed that the functional groups present in biomass molecules such as carbonyl, phenolic, and carboxyl had the affinity for metal complexation.

## **2.4.2 Types of Adsorption**

There are two types of adsorption phenomena, physical adsorption and chemical adsorption

### **2.4.2.1 Physical adsorption (Van der Waals adsorption)**

Physical adsorption is the result of intermolecular forces of attraction between molecules of the solid adsorbent and the substance adsorbed. It is a readily reversible phenomenon. In industrial adsorption operations, this reversibility is used for the recovery of adsorbent for reuse, for recovery of adsorbed substance or for the fractionation of the mixtures.

### **2.4.2.2 Chemisorption**

Chemisorption is the result of chemical interaction between the solid adsorbent and the adsorbed substance. The adhesive force and the heat liberated are much greater those that found in physical adsorption. The process is frequently irreversible. Some substances which under the condition of low temperature undergo only physical adsorption substantially. But they exhibit chemisorption at high temperatures and sometimes both the phenomena may occur at the same time. Chemisorption is of particular importance in catalysis.

### **2.4.3 Advantages of adsorption:**

- I. The removal efficiency of high and low concentration.
- II. The system is effective over a temperature range of 4-90°C.
- III. Economically low cost operated with low capital investment.

- IV. Convert metal pollutant to metal product.
- V. Easy to design and operate for heavy metal treatment.
- VI. Adsorption is an approved operation by many researchers and shows a good trend of heavy metal removal.

## 2.5 Adsorption isotherms

Isotherms studies provide information on the capacity of adsorbent which is a most important parameter for an adsorption system. Adsorption isotherms are characterised by certain constants and describe the mathematical relationship between the quantity of adsorbate and concentration of adsorbate remaining in the solution at equilibrium. There are several isotherm equations describing the equilibrium and the most common of them are Langmuir, Freundlich and Redlich–Peterson models. Fig. 2.1 is an example of ideal adsorption isotherm, while Fig. 2.2 is showing the most used adsorption isotherm curves found in the literature. Sorption isotherms obtained by using batch method have been traditionally used for preliminary screening of the systems before running more costly tests. The procedure is well known and gives an indication, both of effectiveness of sorbents and for removing specific impurities and maximum uptake that can be taken up by a particular unit of sorbent material. The sorption studies by the batch method have been reported for many pollutants on many sorbents. However, the practical utility of a sorbent in removing the pollutants from the wastewater is mainly judged by column operations.

### 2.5.1 Langmuir isotherm

Langmuir adsorption isotherm is the most widely used model for the adsorption process and based on monolayer coverage of adsorbate on the surface of adsorbents. According to Langmuir theory, it has been assumed that adsorption occurs at a specific homogenous site within adsorbent, each site is occupied by only an adsorbate molecule, all sites are equivalent and there are no interactions between adsorbate molecules. The non-linear form of Langmuir isotherm model (Langmuir 1918) can be represented by Eq. (3):

$$q_e = \frac{q_{\max} K C_e}{1 + K C_e} \quad (2.1)$$

The linear form of Eq. (4) is:

$$\frac{C_e}{q_e} = \frac{q_{\max} K C_e}{K q_{\max}} + \frac{C_e}{q_{\max}} \quad (2.2)$$

Where  $C_e$  ( $\text{mg L}^{-1}$ ) is the equilibrium concentration of the adsorbate,  $q_e$  ( $\text{mg g}^{-1}$ ) the amount adsorbed per unit mass of adsorbent at equilibrium,  $q_{\max}$  ( $\text{mg g}^{-1}$ ) and  $K$  ( $\text{L mg}^{-1}$ ) are the Langmuir constants related to maximum adsorption capacity and the affinity of binding sites or bonding energy for adsorption processes, respectively.

### 2.5.2 Freundlich isotherm

The empirical Freundlich isotherm (Freundlich 1906) is used to describe multi-side adsorption isotherm for heterogeneous surfaces and expressed by the following equation:

$$q_e = K_f C_e^{1/n} \quad (2.3)$$

Where  $K_f$  and  $n$  are the Freundlich constant related to adsorption capacity and intensity, respectively. Eq. (2.4) is generally used in the linear form, represented by

$$\ln q_e = \ln K_f + \frac{1}{n} \ln C_e \quad (2.4)$$

### 2.5.3 Redlich–Peterson isotherm

Redlich–Peterson isotherm (Redlich and Peterson, 1959) which incorporates the features of both Freundlich and Langmuir models has three-parameters known as Redlich–Peterson constants. The non-linear form of the Redlich–Peterson model is expressed as follows:

$$q_e = \frac{A C_e}{1 + C_e^g} \quad (2.5)$$

Where  $A$  ( $\text{L g}^{-1}$ ),  $B$  ( $\text{L mg}^{-1}$ )g and  $C$  are the Redlich Peterson constants.

The exponent  $g$  lies between 0 and 1. If  $g$  equals 1, Eq. (2.6) converts to the Langmuir form. Linear form of Eq. (2.6) can be described as follows:

$$\ln \left( A \frac{C_e}{q_e} - 1 \right) = g \ln C_e + \ln B \quad (2.6)$$

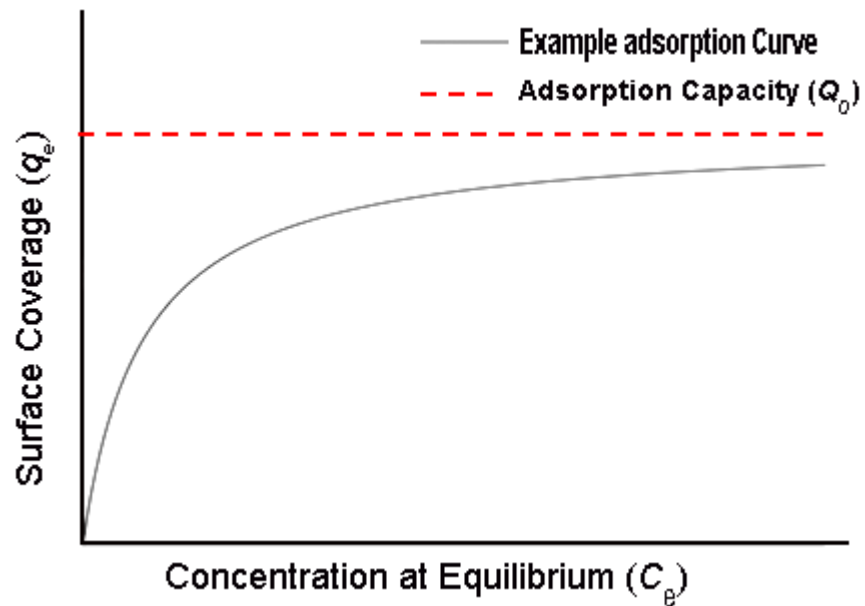


Fig. 2.1 Example adsorption isotherm

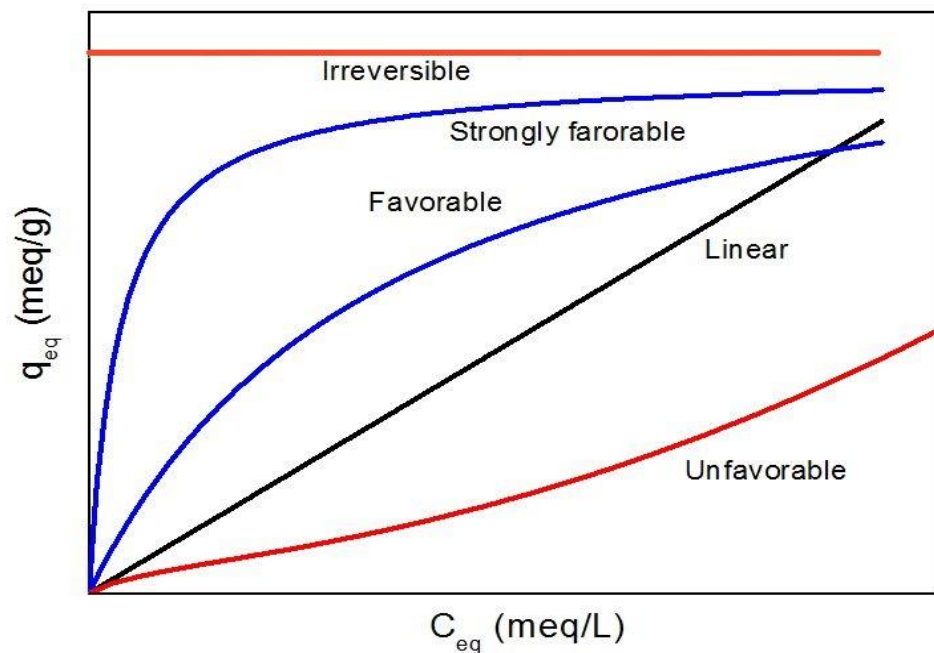


Fig. 2.2 Adsorption general isotherm curves

There are various isotherm models used for adsorption in literature such as Henry's Isotherms, Dubinin-Radushkevich, Hill Isotherm, Temkin Isotherm, Halsey, Sips and Toth Isotherm. However, Langmuir, Redlich-Peterson and, Pseudo first and second order are still widely used. Although several methods have been adopted to determine the isotherm, the most widely used one is the conventional static method proceeding in a closed system. Actually, due to the complexity of the structure of

adsorbent and the interaction between each corpuscle, isotherms can present diverse shapes. The Langmuir sorption isotherm, which is probably the best known and most widely applied, supposes monolayer sorption by physical forces with a homogeneous distribution of sorption sites and sorption energies, without any interaction between the sorbed molecules. In contrast to the Langmuir model, the Freundlich isotherm is originally empirical in nature, but was later interpreted as sorption to heterogeneous surfaces or surfaces supporting sites of varied affinities i.e. multilayer adsorption (Pino et al. 2006).

## **2.6 Dynamic studies in fixed-bed systems**

### **2.6.1 The breakthrough curve**

Most adsorption and/or ion exchange operations, whether in a laboratory or in plant-scale processes, are carried out in columns. A solution is passed through a bed of adsorbent beads where its composition is changed by adsorption. The composition of the effluent and its change with time depending on the properties of the adsorbent, the composition of the feed, and the operating conditions (flow rate, temperature etc.). Plots of the ratio  $C/C_0$  (outlet adsorbate concentration/adsorbate feed concentration) versus time are called breakthrough curves. As the run starts, most of the mass transfer takes place near the inlet of the bed, where the fluid first contacts the sorbent. If the solid contains no adsorbate at the start, the concentration in the fluid drops exponentially to zero before the end of the bed is reached. The typical breakthrough curve is shown in Figure 2.3. As the run proceeds, the solid near the inlet is nearly saturated, and most of the mass transfer takes place further from the inlet. The concentration gradient is S-shape. The region where most of the change in concentration occurs is called the mass-transfer zone. This is the real behavior of the mass transfer process in fixed beds. When the axial or radial mass transfer resistances are neglected, adsorption occurs homogeneously and this is the ideal case. In fact, mass transfer resistances can be minimized but not effectively eliminated (McCabe et al. 2001). The limits of the breakthrough curve are often taken as  $C/C_0$  values of 0.05 to 0.95, unless any other recommendation is fixed. They are related to the breakpoint ( $t_b, C_b$ ) and saturation point ( $t_s, C_s$ ), respectively. In most of cases  $C_s = C_0$ . This is the case of wastewater treatment of highly toxic adsorbates. When the concentration reaches the limiting permissible value, say, 1 ppm, it is considered as the break point. The flow is stopped, the column is regenerated, and the inlet

concentration is redirected to a fresh sorbent bed (McCabe et al. 2001). Most separation and purification processes that use sorption technology involve continuous flow operations. In this operating mode, the saturated solid sorbent zone gradually extends throughout the column where the sorbate is adsorbed. The adsorption experimental data show a typical S-shaped curve where the slope is a result of three factors: the equilibrium sorption isotherm relationship, mass transfer effects throughout the sorbent in the column, and the influence of axial mixing, which determines deviation from the ideal plug-flow behaviour (Silva et al. 2002a). Fixed bed column systems with continuous flow allow the regenerating cycles operation. Using an appropriate eluent solution, the sorbent can be regenerated. The regeneration process liberates small volumes of concentrated metal solutions, which are more appropriate for conventional recovery processes (Kratochvil and Volesky, 1998). To represent a dynamic heavy metals ions removal in fixed bed columns, a mathematical analysis of the system was performed, and S-shaped experimental curves were evaluated. A typical breakthrough curve can be represented as a ratio of the effluent ( $C$ ) and inlet concentration ( $C_0$ ) versus time. The efficiency of the adsorption process can be estimated by the sharpness of the breakthrough curve. The correct design of a fixed bed column used for biosorption is not an easy task and to reduce the costs of implementation of such equipment mathematical models have to be applied as the most robust and powerful tool. The model validation is performed on the bases of experimental data collected from laboratory scale, and the statistical criterion is used during the non-linear parameter identification procedure. The developed models then may be applied for designing and process optimization in a pilot plant and industrial scale (Silva et al. 2003b). The residence time is a key parameter in the design procedure of adsorption in a fixed bed column (McKay and Bino, 1990). When operating with low flow rates, the process is controlled by the external mass transfer (fluid around the particles surface) limitation. To avoid such a control, it is suggested for the process to operate in the range of higher flow rates. High flow rates may be applied in a process that is controlled by the internal mass transfer velocity (diffusion inside the particles). However, this will result in low residence times for adsorption and therefore, a decreasing of flow rates is suggested. It is obvious that the two effects are antagonistic, and the optimal flow rate has to be searched in the intermediate region of flow rates. Hence, the mass transfer coefficients have to be determined correctly to guarantee an optimal column design (Ko et al. 2000). The mathematical models used to describe the adsorption process

can be divided into three categories: models of equilibrium stage, theory of the interference, and models of rate equation. The models of rate equation are more realistic compared to the others. These models are based on the species mass balances of interest in both, the fluid and the stationary phase (sorbent particles). They generally consider the effect of mass transfer in the liquid film, intraparticle diffusion, and equilibrium isotherms. Due to the complexity and non-linearity of these models, general analytical solutions are usually impossible to be achieved (Robinson et al. 1994). There are several mathematical models in the literature, which have been used to represent the dynamics of the fixed bed column. Models with analytical solutions are often used for fitting the breakthrough curve. Full-scale column operation was designed according to the data collected in the laboratory level. Many mathematical models have been used for the evaluation of efficiency and applicability of the column models for full scale operations. To design a column sorption process, it was necessary to predict the breakthrough curve or concentration time profile and sorption capacity of the sorbent for the selected sorbate. Many models have been developed to predict the sorption breakthrough behaviour with a high degree of accuracy. In this study the Thomas, Bohart-Adams and Yoon- Nelson models were used to evaluate the behaviour of the selected adsorbent-adsorbate system. The ideal model should predict the breakthrough curve, including the breakthrough time, exhaustion time, breakthrough concentration, and exhaustion concentration, as mentioned in Figure 2.3. The efficiency of column can be explained by means of breakthrough curves. A breakthrough curve is obtained by plotting the column effluent concentration versus volume treated or time of treatment. Breakthrough capacity, exhaustion capacity and degree of column utilization are the important features of the breakthrough curves. The breakthrough capacity is defined as the mass of sorbate removed by the sorbent at breakpoint concentration, which is also termed as the maximum acceptable concentration of the sorbates. The degree of column utilization is defined as the mass sorbed at the breakthrough point divided by the mass sorbed at complete saturation. The exhaustion capacity is defined as the mass of the sorbate removed by unit weight of the sorbent at a saturation point.

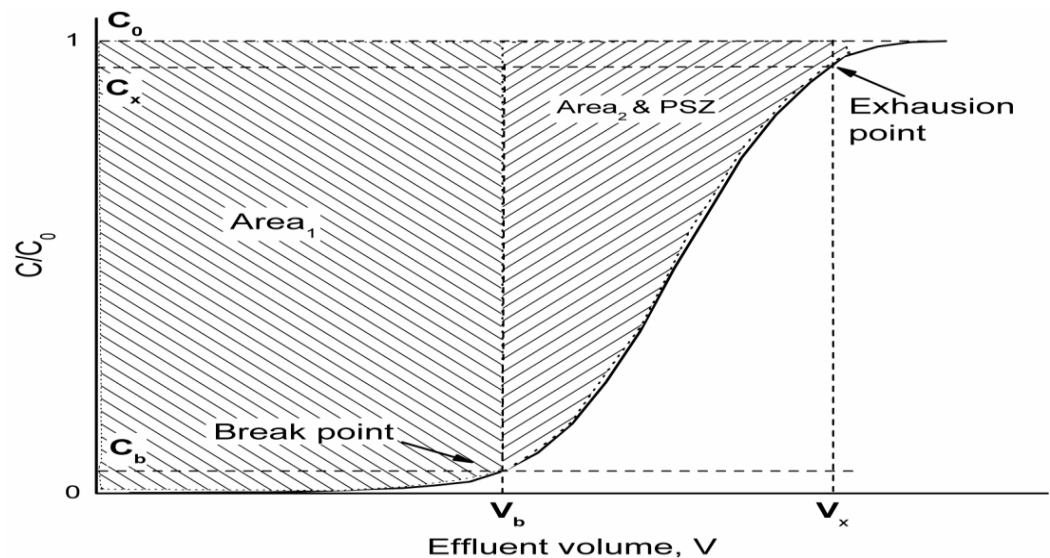


Fig. 2.3 Ideal breakthrough curves

Where  $t_b$  = Breakthrough time,  $t_x$  = Exhaustion time,  $C_b$  = Breakthrough concentration,  $C_x$  = Exhaustion concentration,  $C_0$  = Inlet concentration,  $M_s$  = Adsorption zone from the breakpoint to exhaustion

### 2.6.2 Mass transfer zone

The mass transfer zone (MTZ) is the active surface of the adsorbent in the bed where adsorption occurs (Fig. 2.4). The fluid flowing into the column gets through a fresh bed. The top of the adsorbent in interaction with the fluid rapidly adsorbs the pollutant throughout the first contact. Consequently the fluid exit the column is basically free of metallic ions (points P1, P2 and P3 in Fig. 2.4). As the bulk of contaminated fluid getting through the bed column increases, an adsorption zone of mass transfer (MTZ) gets defined. In this MTZ, adsorption is complete and the concentration of pollutant in the bed column varies from 100% of  $C_0$  (corresponding to complete saturation) to approximately 0% of  $C_0$  (corresponding to the virgin adsorbent). This adsorption zone then transfers downwards through the bed column in relation to time until the breakthrough occurs. When this zone reaches the bottom of the bed the pollutant dissolved in the solution cannot yet be adsorbed any longer. This moment is called “breakpoint”. The plot obtained after this point gives the concentration history and is called breakthrough profile or breakthrough curve. From a practical point of view, this point allows determining the solute concentration in the effluent and the volume treated ( $V_b$ ). For most adsorbent–pollutant systems, the breakthrough curve is obtained after an effluent concentration of 50% has been reached.

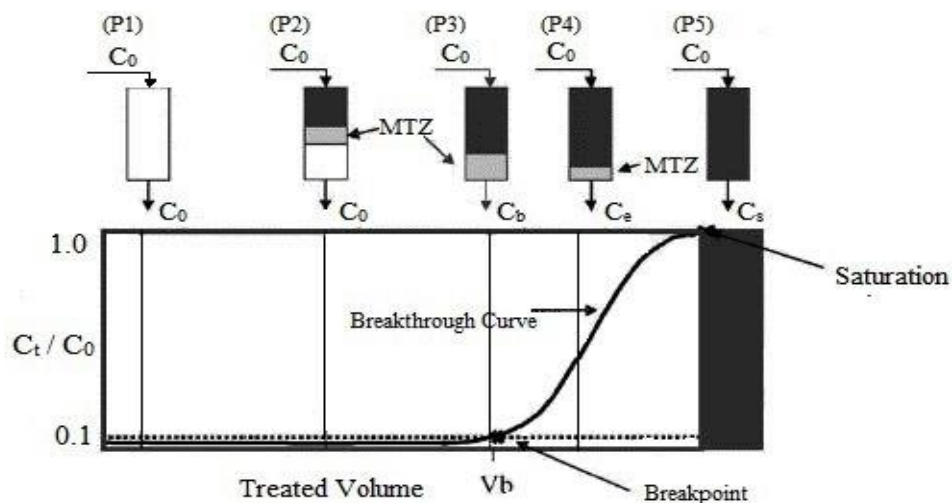


Fig. 2.4 (MTZ: mass transfer zone). Typical breakthrough curve for activated carbon showing the movement of the mass transfer zone according to the throughput volume

### 2.6.3 Mathematical description and adsorption modeling of fixed-bed column studies

Estimation of breakthrough curves and determination of kinetic constants are the most important parameters for the fitted models. The values of the maximum adsorption capacity for the adsorption of  $\text{Cd}^{2+}$  and  $\text{Cu}^{2+}$  cations on different adsorbents used in the literature with adsorbents of the present study are summarized in table 2.3 and 2.4

Table 2.3. Compare of other researches work for removing  $\text{Cd}^{2+}$  with this study

Type of adsorbent	Bed (cm)	Q (min $\text{L}^{-1}$ )	$C_0$ (mg $\text{L}^{-1}$ )	Models used	$q_{\max}$ (mg $\text{g}^{-1}$ )	References
Oil Palm Shell-derived Activated Carbon	3	3	200	Yoon, Thomas, Bohart, BDST	22.2	(Ling et al. 2016)
Compost	1.1	8	100	Yoon, Thomas, Bohart	17.2	This study
PAN oxime-nano $\text{Fe}_2\text{O}_3$	20	7	50	Thomas and BDST	24.4	(Jahangiri-rad et al. 2014)
Alga	6	2.3	60	Thomas, Yan and Belter	318	Ghasemi et al. 2011)
dead calcareous skeletons	2.2	10	100	Thomas, Yoon and Bohart	26.4	(Lim and Aris, 2014)
macrofungus <i>Pleurotus platypus</i>	4	5	10	Bohart–Adams	13.3	(Vimala et al. 2011)
Peat	10	1.5	209	Langmuir	8.15	(Li and Champagne, 2009)
iron-coated zeolite	12	8	5	Thomas	0.93	(Nguyen et al. 2015)

Table 2.4. Compare of other researches work for removing Cu<sup>2+</sup> with this study

Type of adsorbent	Bed (cm)	Q (mL min <sup>-1</sup> )	C <sub>0</sub> (mg L <sup>-1</sup> )	Models used	q <sub>max</sub> (mg g <sup>-1</sup> )	References
Pine cone shell	13.4	2	50	N/A	9.38	(Martín-Lara et al. 2016)
Felgyő compost	4	2	100	Thomas, Bohart-Adamas and Yoon-nelson	8.58	This work
Marula seed husk (Sclerocarya birrea)	10	20	70	Pseudo-first-order model, Pseudo-second-order	7.22	(Moyo et al. 2015)
Cystoseira crinitophylla	30	16.5	50	Thomas, Clark	N/A	(Christoforidis et al. 2015)
Zeolite	20	5. 1hr	10	Yoon-Nelson	10.29	(Upadhyaya et al. 2017)
expanding rice husk	9	10	50	Bohart- Adams	6.33	(Luo et al. 2011)
Activated charcoal and bone charcoal	36	30	200	Thomas, Bohart-Adamas and Yoon-Nelson	N/A	(Murthy and Srinivas, 2016)

## 2.7 Kinetic models for bed column

With the purpose of identifying particular criteria for determining when the kinetic model should be combined to the fixed-bed adsorber model to calculate breakthrough curves for a determined adsorbent-adsorbate system. Kinetics provides information regarding the mechanism and rate of adsorption of the adsorbate on a specific adsorbent. The development of a kinetic model is needed for designing and elevating an adsorption process.

### 2.7.1 Thomas model

Thomas model (Thomas 1944) is used for the determination of adsorption capacity of an adsorbent which is essential for the design of column for effective wastewater treatment. It also assumes plug flow behavior in the bed and uses Langmuir kinetics of sorption-desorption and no axial dispersion is derived with the sorption that the rate driving force obeys second-order reversible reaction kinetics. This model is suitable for adsorption processes where the external and internal diffusion limitations are absent.

$$\ln \left[ \frac{C_0}{C_{eff}} - 1 \right] = 1 + \frac{k_{th} q_0 m}{Q} - k_{th} q_0 t \quad (2.7)$$

Where  $C_{eff}$ ,  $C_o$  = the effluent and inlet solute concentrations (mg/l),  $q_o$  = the maximum adsorption capacity (mg g<sup>-1</sup>),  $M$  = the total mass of the adsorbent (g),  $Q$  = volumetric flow rate (ml/min),  $V$  = the throughput volume (ml) and  $K_{th}$  = the Thomas rate constant (ml/min/mg).

### 2.7.2 Bohart-Adams model

This model is based on physically measuring the capacity of the bed at various percentage breakthrough values. The BDST model constants can be helpful to scale up the process for other flow rates and concentrations without further experimentation. It is used to predict the column performance for any bed length, if data for some depths are known. It states that the bed depth,  $Z$  and service time ( $t$ ) of a column bears a linear relationship. The rate of adsorption is controlled by the surface reaction between adsorbate and the unused capacity of the adsorbent. (Bohart and Adams 1920).

$$\ln \left[ \frac{C_{eff}}{C_o} \right] = k_{AB} C_o t - \frac{K_{AB} N_o Z}{U_o} \quad (2.8)$$

### 2.7.3 Yoon and Nelson model

This model is based on the assumption that the rate of decrease in the probability of adsorption for each adsorbate molecule is proportional to the probability of adsorbate adsorption and the probability of adsorbate breakthrough on the adsorbent. (Yoon and Nelson 1984) The Yoon and Nelson equation is expressed as:

$$\ln \left[ \frac{C_o}{C_o - C_{eff}} \right] k_{YN} t - \tau k_{YN} \quad (2.9)$$

Where  $k_{YN}$  is the rate constant (L min<sup>-1</sup>),  $\tau$  is the time required for 50% adsorbate breakthrough (min) and  $t$  is the breakthrough (sampling) time (min). The breakthrough curve of the continuous fixed-bed system is used to evaluate the column performance. Generally, the breakthrough curve is described by  $C_{eff}/C_o$ , in which  $C_{eff}$  and  $C_o$  represent the effluent and influent concentrations, respectively. The adsorbed metal ion concentrations in the column are observed by a plot of the adsorbed metal concentration,  $C_{ad}$  (1) or normalized concentration defined as the ratio of effluent metal concentration to influent concentration ( $C_{eff}/C_o$ ) as a function

of time or volume of effluent ( $V_{\text{eff}}$ ). Table 2.5 is a general overview of these models with their strength and weakness.

Table 2.5. Adsorption models comparison of their strength and weakness

Models	Strength	Weakness
Thomas	Best fitting for longer bed height, lower flow rate and higher influent concentration	Not well-described for shorter column
Yoon-Nelson	Less parameters required for calculation	Not well-fitted for shorter bed depth of adsorbent
Adam-Bohart	Provides the prediction for saturation concentration of adsorbate	Requires more parameters for model application
BDST	Simple model	Only studies the effect of bed depth

## 2.8 Heavy metal analytical equipment

### 2.8.1 SEM/EDX

The Scanning Electron Microscopy (MEB or SEM) is a technique of electronic microscopy based on the electrons-material interactions, capable of producing images of the sample surface. The principle of the MEB is based on the fact that an electron beam bombards the surface of the sample to be analyzed which re-emits certain particles. These particles are analyzed by various detectors which give a three dimensions image of the surface. Due to the excited state of the atoms present in the material by interaction with the incidental electrons, photons X are emitted (de-excitation process). The emission volume of photons X, ( $\mu\text{m}^3$ ) depends upon the energy of the incidental electrons, the atomic number of the sample and the level energy initially ionized. The chemical analysis by EDX (Energy Dispersive X-ray analysis) consists of a detection of these photons by using a solid detector Si-Li (detection by energy dispersion). The energy of these photons X is characteristic of its atoms; the possibility to realize an elemental analysis. A lines spectre (peaks) is obtained, each corresponding to the photons X of the given energy, thus has a given element. The intensity of the characteristic lines is proportional to the concentration of the element in the analytical volume, this analysis is quantitative. However, there is factors of correction depending on the experimental parameters (energy of the incidental beam, its angle...), the sample composition, and that it is difficult to calculate. Thus, only a semi-quantitative analysis is considered. The detection limit is situated at concentrations about 0.1 - 1 % (for elements having average or light atomic weight and except unfavourable superposition of characteristic peaks). The

detectors allow to detect the light elements (C, O, N) and even at limited degree the boron, but the yield is very weak because the photons of boron are absorbed by the window which protects the detector (Mohamed 2011).

### **2.8.2 Fourier transform infrared spectroscopy**

Fourier transform infrared spectroscopy (FTIR) was used to determine the vibration frequency changes in the functional groups on the adsorbents. FTIR spectroscopy offers a vast array of analytical opportunities in academic, analytical, QA/QC and forensic labs. Deeply ingrained in everything from simple compound identification to process and regulatory monitoring, FTIR covers a wide range of chemical applications, especially for polymers and organic compounds. When IR radiation is passed through a sample, some radiation is absorbed by the sample and some passes through (is transmitted). The resulting signal at the detector is a spectrum representing a molecular ‘fingerprint’ of the sample. The usefulness of infrared spectroscopy arises because different chemical structures (molecules) produce different spectral fingerprints (Thermo Fisher Scientific 2013).

### **2.9 Conclusion**

Adsorption is an effective method for heavy metal ion removal from aqueous solution and from wastewaters. In order to assess the performance of adsorbents, batch experiments should be conducted to determine and compare the adsorption capacities of different adsorbents for various heavy metal ions. After the batch adsorption investigations, small column testing should be undertaken as an efficient means of evaluating and estimating adsorbent capacities for pilot-scale or full-scale column applications. Compost requires almost no further treatment, and more important it is very effective in removing heavy metals from aqueous solution, wastewater from industries and even at some scientific laboratories such as biological, pharmaceutical, medical. Although all the heavy metal wastewater treatment techniques can be employed to remove heavy metals, they have their inherent advantages and limitations. Heavy metals removal from aqueous solutions has been traditionally carried out by chemical precipitation for its simplicity process and inexpensive capital cost. However, chemical precipitation is usually adapted to treat high concentration wastewater containing heavy metal ions and it is ineffective when metal ion concentration is low. And chemical precipitation is not economical and can produce a large amount of sludge to be treated with great difficulties. Ion

exchange has been widely applied for the removal of heavy metal from wastewater. However, ion-exchange resins must be regenerated by chemical reagents when they are exhausted, and the regeneration can cause serious secondary pollution. And it is expensive, especially when treating a large amount of wastewater containing heavy metal in low concentration, so they cannot be used at a large scale. Adsorption is a recognized method for the removal of heavy metals from low concentration wastewater containing heavy metal. The high cost of AC limits its use in adsorption. Many varieties of low-cost adsorbents have been developed and tested to remove heavy metal ions. However, the adsorption efficiency depends on the type of adsorbents. Biosorption of heavy metals from aqueous solutions is a relatively new process that has proven very promising for the removal of heavy metal from wastewater

## CHAPTER: 3

### HEAVY METAL REMOVAL FROM POLLUTED WATER: BATCH AND FIXED BED COLUMN: EXPERIMENTAL STUDY

#### 3.1 Materials and methods

##### 3.1.1 Instruments used for experimental analyses

The functional groups of the compost were characterized by a Fourier transform infrared (FTIR) spectrometer (FTIR – Mattson Research Series). The spectra of compost were measured within the range of 4,000–500  $\text{cm}^{-1}$  wave number. Morphological analysis of the adsorbent was done by using the scanning electron microscope SEM + EDX– JEOL JSM-5600LV + EDS-2000. The acceleration voltage of the instrument was set at 5 kV, with an image point resolution of 10  $\mu\text{m}$ , with x35 and x50 magnification. The metal concentration was analysed using atomic absorption spectrophotometer (AAS; model GBC 935).

##### 3.1.2 Preparation of adsorbent

Adsorbents were provided by laboratory of bio combustibles from Szent István University, Gödöllő (Hungary). Each compost was ground and sieved into fractions below 2 mm. The fractions collected below mesh size of 2 mm were designated for the characterization and biosorption investigations without any pre-treatment. Felgyő compost is a green waste and sewage sludge, 2. Garé is communal sewage sludge, slurry mud and chicken manure with straw. 3. Sioagárd is green biomass/bio waste. For batch experiments, the particular weight of compost sample was one gram. 13 samples were prepared for a single set, and 3 replications were conducted to carry the test for one single metal followed by the same steps for other composts besides the heavy metals. Finally, every set of samples has 10 mL of concentrated solution per each bottle plus one gram of compost. The concentration solution ranges from 0 to 50000  $\mu\text{g g}^{-1}$  of one single metal and the homogeneous mixture was ready to be investigated.

### 3.1.3 Quality control

The distilled water was digested and analysed with every sample group to track any possible contamination source and obtain a baseline value. Triplicate runs for batch mode adsorption experiments were made for each adsorbent to determine the relative deviation of the experiments.

### 3.1.4 Adsorption in batch experiments

After each adsorption, the residual  $\text{Cd}^{2+}$  and  $\text{Cu}^{2+}$  were determined by digesting the filtered synthetic wastewater followed by AAS analysis as a standard method. The percentage of the adsorbed metal ions was estimated using the following equation:

$$R (\%) = \frac{(C_0 - C_e)}{C_0} \times 100 \quad (3.1)$$

Where  $C_0$  and  $C_e$  are metal ions concentrations ( $\text{mg L}^{-1}$ ) before and after adsorption respectively.

Adsorption capacity estimated using the bellow equation:

$$X = \frac{V(C_0 - C_e)}{M} \quad (3.2)$$

Where,  $V$  = Volume of solution (mL),  $M$  = mass of adsorbent (mg),  $C_0$  = Initial metal Concentration ( $\mu\text{g g}^{-1}$ ),  $C_e$  = Final metal Concentration at equilibrium ( $\mu\text{g g}^{-1}$ ),  $X$  = The adsorbate Concentration / adsorption Capacity of compost ( $\mu\text{g g}^{-1}$ )

### 3.1.5 Preparation of synthetic wastewater

Cd and Cu added separately to distilled water in the laboratory and the value of concentration was determined in a range from 50 to 50000  $\mu\text{g g}^{-1}$ . The stock solution of 1000  $\text{mg L}^{-1}$   $\text{Cu}^{2+}$  was prepared by dissolving  $\text{CuSO}_4 \cdot 5\text{H}_2\text{O}$  and  $\text{Cd}(\text{NO}_3)_2 \cdot 4\text{H}_2\text{O}$  in different flasks of 1.0 L deionized water and further diluted to the desired concentration with deionized water. The concentration solution was determined in a range of (0–50000  $\mu\text{g g}^{-1}$ ) for each metal in batch experiments and 20, 100  $\text{mg L}^{-1}$  for bed column experiments. The chemicals used throughout this study were of analytical reagent grade

provided by Reanal Ltd, Hungary. The individual metal ion concentrations in solution were analysed using an atomic absorption spectrophotometer (AAS) Varian Spectra AA-20 at the Analysis Service Unit of Szent Istvan University, Hungary.

### 3.1.6 Experimental set up for batch study

Batch adsorption experiments were carried out by shaking a series of samples containing the same amounts of different concentration solution with a mixture of 3 different composts used to sorb the heavy metal separately. The compost materials used were mixed with concentration range of (50, 100, 250, 500, 1000, 2500, 5000, 10000, 25000, 30000, 40000, and 50000  $\mu\text{g g}^{-1}$ ) of  $\text{Cu}^{2+}$  and  $\text{Cd}^{2+}$ . After the composts have been collected, the product was ground and sieved to 2 mm which transferred to a small flask with a screw cap which contained 1 g compost plus 10 ml of concentrated solution, and then immersed in a shaking machine as a complete set containing 13 samples at a constant speed of 125 rpm. The shaking was run for every set of the experiment for 24 hours. All the experiments were performed in triplicate method, the adsorbate and adsorbent were separated by high speed centrifugation at 6000 rpm for 7 minutes. In this stage of the experiment the adsorbent particles were separated from the suspensions by filtration through 0.43  $\mu\text{m}$  filter paper. The residual concentration of heavy metals was determined by the Atomic absorption photometer. The measured data were fitted to Langmuir function.

### 3.1.7 Fixed bed column construction

The glass columns were 30 cm long, 1.2 cm internal diameter with a porous ending at the bottom. The column packed with the desired amount of compost representing the height of the bed column with two supporting layers of glass wool at the top and the bottom.  $\text{Cu}^{2+}$  was tested on two compost Felgyő and Garé, packed with 5, 10 and 15 g of compost with bed heights (1.1, 2 and 3.1cm), (2.4, 3.1 and 6.5cm). respectively. Cadmium was investigated by using Felgyő compost into three different bed height (1.1, 2 and 3.1cm). Columns positioned vertically and adsorption tests were performed in continuous down flow method, the experiments were conducted at room temperature. The schematic diagram is illustrated in Fig. 3.1. Wastewater kept in an overhead container and the only driving force of the solution through the column is the gravity and

it is manually controlled for its flow operation. A flow control valve was used to adjust the flow at 4 and 8 mL min<sup>-1</sup>. The initial heavy metal concentration of 20 and 100 mg L<sup>-1</sup> of Cu<sup>2+</sup> was prepared using analytical grade (CuSO<sub>4</sub>·5H<sub>2</sub>O) and Cd(NO<sub>3</sub>)<sub>2</sub>·4H<sub>2</sub>O provided by Reanal Ltd company. The solution was prepared by dissolving the individual required quantity of copper sulfate and cadmium nitrate in distilled water. It was further diluted to obtain standard solutions. 1000 mL of aqueous solution was filled on the overhead tank and then charged into fixed bed columns. The samples were collected at different time intervals to analyze Cu<sup>2+</sup> and Cd<sup>2+</sup> concentration using atomic absorption spectrophotometer.

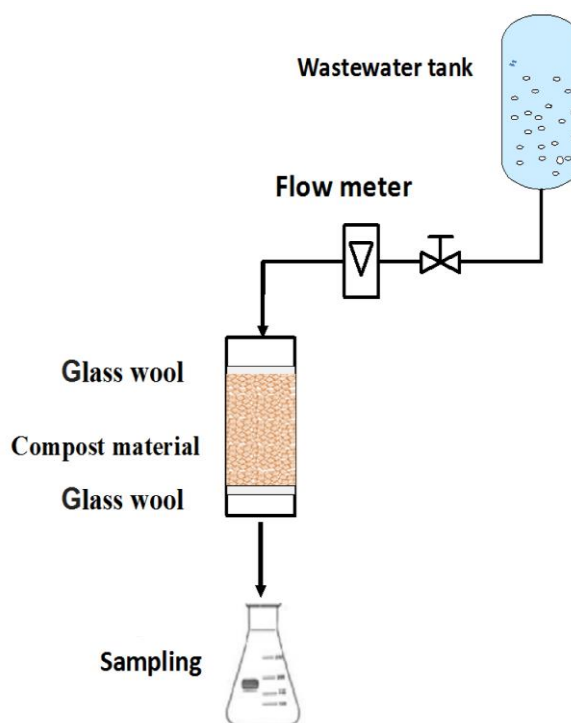


Fig. 3.1 Column experimental set up

## 3.2 Result and discussion

### 3.2.1 Analysis and Characterization of compost for bed column

#### 3.2.1.1 Scanning electron microscopy (SEM)

Studies are available which have reported the utilization of the scanning electron microscopy analysis for showing the surface modification changes in the adsorbent Fig. 3.2 to 3.7 before and after adsorption show how an irregular surface, which is heterogeneously shaped and cracked probably favours the sorption of  $\text{Cu}^{2+}$  and  $\text{Cd}^{2+}$  on different parts of the adsorbent; making it a propitious adsorption technique. The scanning electron microscope was set at x35 and x50 magnification, while the accelerated voltage was set at 5 kV in order to obtain high-resolution micrographs at different adsorbent spots. SEM figures are indicating that the compost had good characteristics to be used as an adsorbent for metal ion uptake due to its heterogeneous distribution and particle sizes which perhaps favour the adsorption mechanisms. The composition of Felgyő and Garé was very similar despite the large differences in the morphology (Garé compost containing much larger particles as seen on the SEM images). The carbon content was roughly half of the concentration observed at the two compost samples, indicating significantly higher organic matter content. The differences between the compost samples could be observed in Fig 3.2 and 3.5 for raw compost. Nevertheless, the treatment affected the concentration of some elements, leading to a decrease especially in the Na, Cl, S and K content. Because of the heterogeneous structure and composition of the compost, the chemical elemental analysis was expected to show the chemical constituents which could influence the heavy metal adsorptive capacity of the adsorbent. The differences are relatively small; they consist mostly of organic matter in varying shapes (often as fibers), larger particles (a part of them with a certain extent of symmetry) and a large number of smaller particles (often forming aggregates). Their ratio varies significantly, but the comparison of these samples is difficult due to the large heterogeneity (likely low magnification optical microscopy would be more suited for this). This is also indicated by the large differences between the compositions of the specimens originating from the same compost sample. At larger magnifications next to none differences can be observed between regions consisting of different particles, thus the adsorption did not affect noticeably the surface morphology.

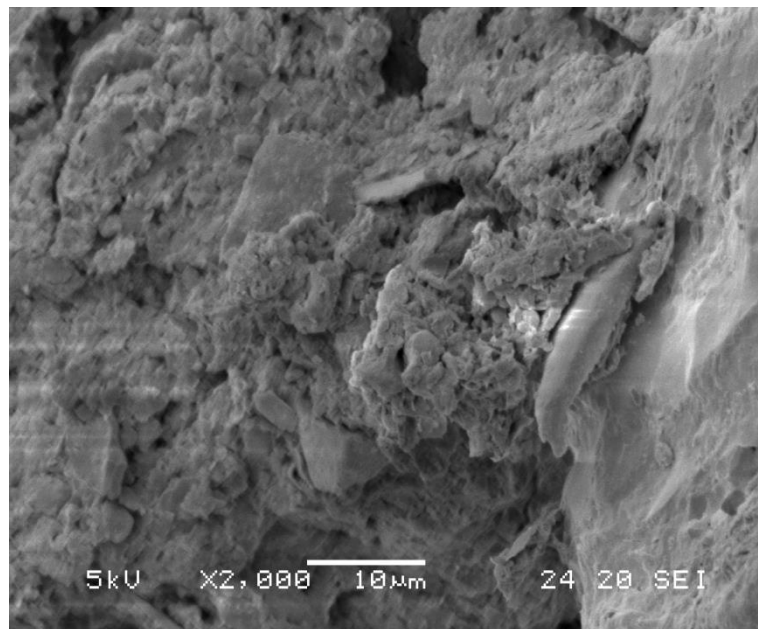


Fig. 3.2 Scanning electron microscopy (SEM) for Felgyő compost at 10µm

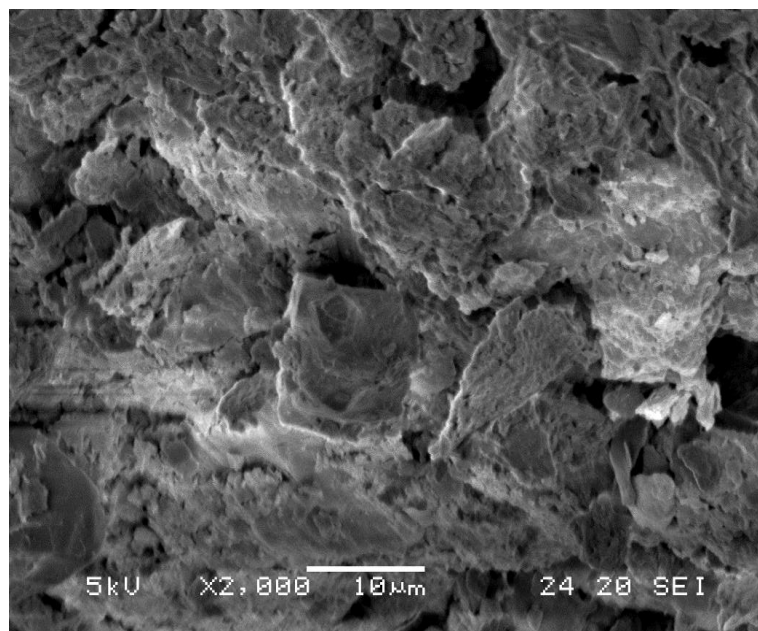


Fig. 3.3 Scanning electron microscopy (SEM) for Felgyő compost loaded with Cu<sup>2+</sup> at 10 µm

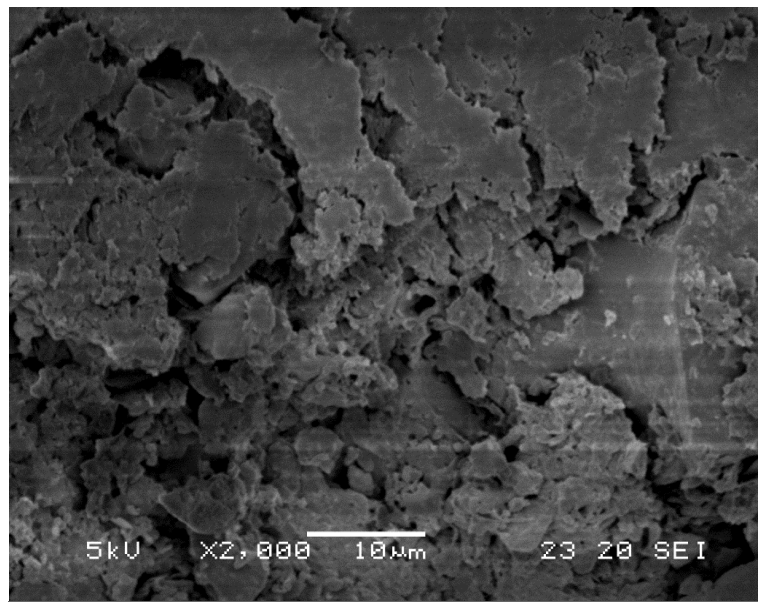


Fig. 3.4 Scanning electron microscopy (SEM) for Felgyó compost loaded with Cd<sup>2+</sup> at 10 μm

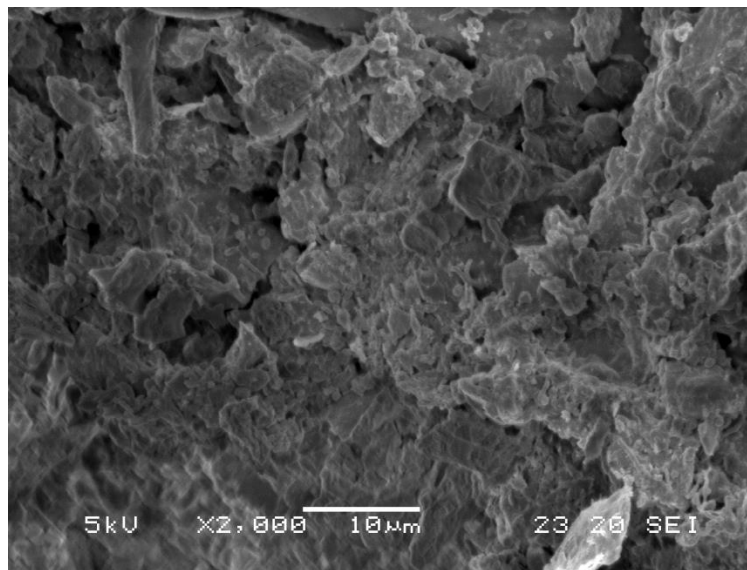


Fig. 3.5 Scanning electron microscopy (SEM) for Garé compost at 10 μm



Fig. 3.6 Scanning electron microscopy (SEM) for Garé compost loaded with  $\text{Cu}^{2+}$  at  $10 \mu\text{m}$

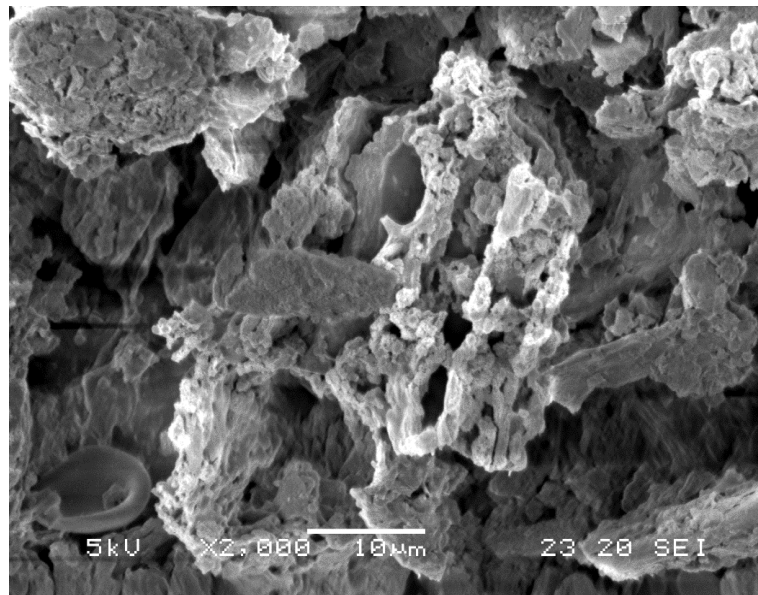


Fig. 3.7 Scanning electron microscopy (SEM) for Garé compost loaded with  $\text{Cd}^{2+}$  at  $10 \mu\text{m}$

### 3.2.1.2 Energy dispersive X-ray spectroscopy (EDX)

EDX analysis was used to determine qualitatively the elemental composition of the raw compost and after treatment as depicted in Fig 3.8 to 3.13 before and after adsorption for  $\text{Cu}^{2+}$  and  $\text{Cd}^{2+}$  using Felgyő and Garé respectively. The samples were coated with gold prior to analysis to avoid electron charging. Fig 3.7 to 3.13 is an illustration for the adsorption of heavy metals onto different compost materials. The elemental composition percentages of these samples are given in Table 3.1 and 3.2. Figures 3.9, 3.10, 3.12 and 3.13 shows the main peaks of silicate, carbon and oxygen in the compost after loaded with heavy metals. For the compost, two regions are analysed, showing very different results concerning the presence of significant amounts of C, Si and O and the absence of Na and Cl as indicated on table 3.1 and 3.2. The appearance of  $\text{Cu}^{2+}$  and  $\text{Cd}^{2+}$  features can be observed on EDX spectrum at different energy values indicates that the biosorbents studied were able to bind metal ions. This indicates that the catalyst is not uniformly distributed on the compost substrate; this fact can also be seen in all SEM micrographs. The disappearance of some metal after metal ion adsorption may be due to the ion-exchange mechanism; this is also incurred with (Kamari et al. 2014). EDX analysis provided direct confirmation for the heavy metal adsorption onto the compost material.

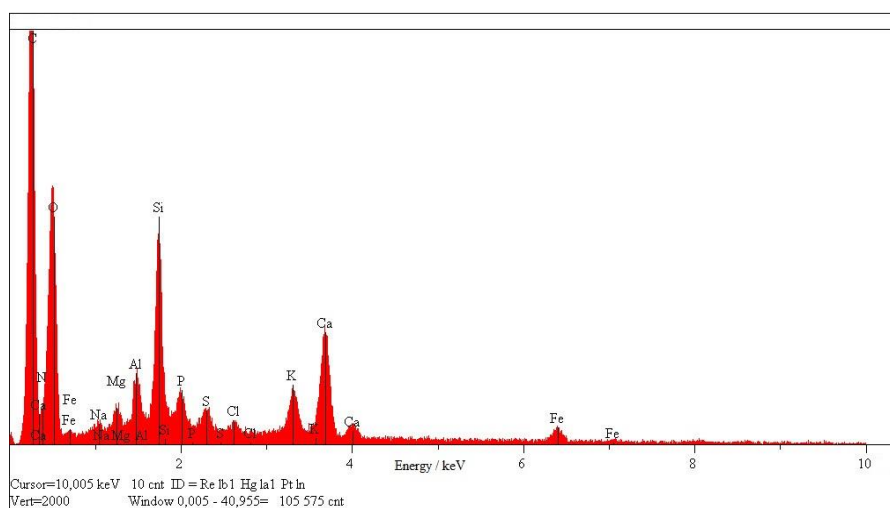


Fig. 3.8 Energy dispersive X-ray spectroscopy (EDX), (Felgyő compost unloaded)

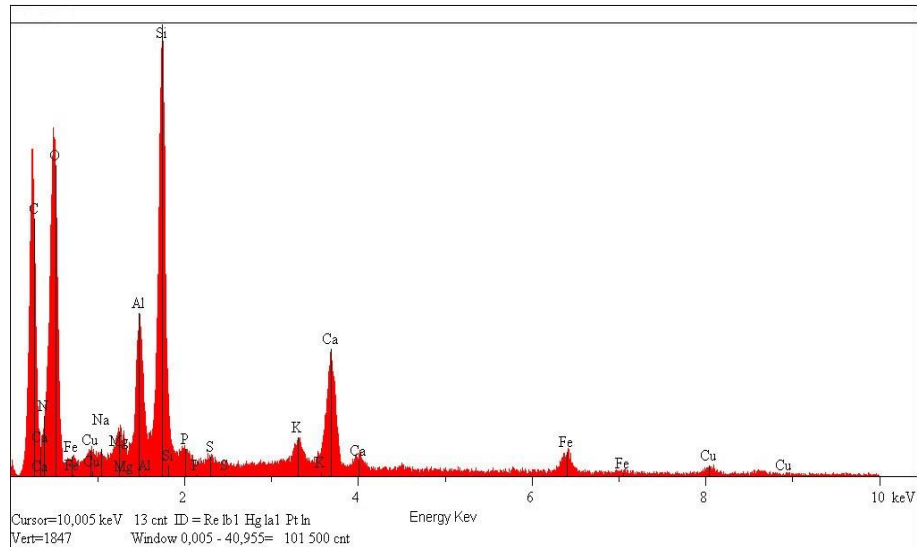


Fig. 3.9 Energy dispersive X-ray spectroscopy (EDX) after  $\text{Cu}^{2+}$  loaded (Felgyó compost)

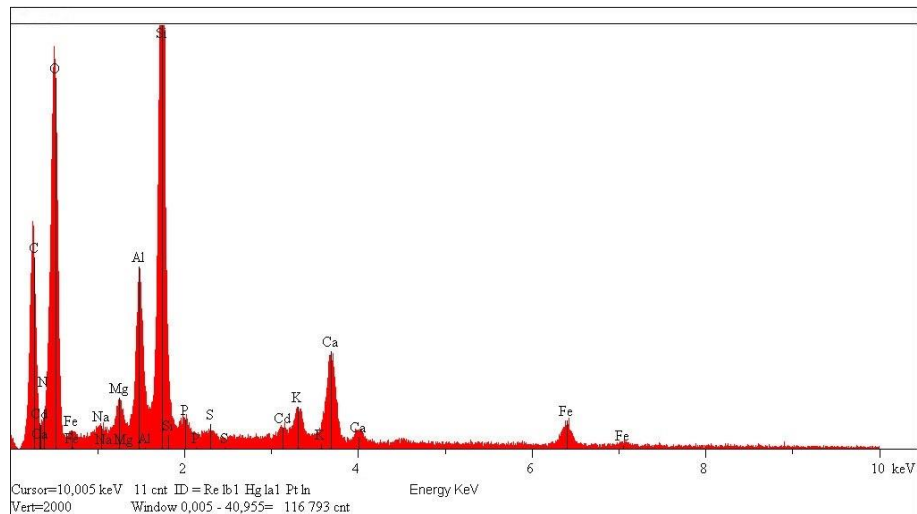


Fig. 3.10 Energy dispersive X-ray spectroscopy (EDX) after  $\text{Cd}^{2+}$  loaded (Felgyó compost)

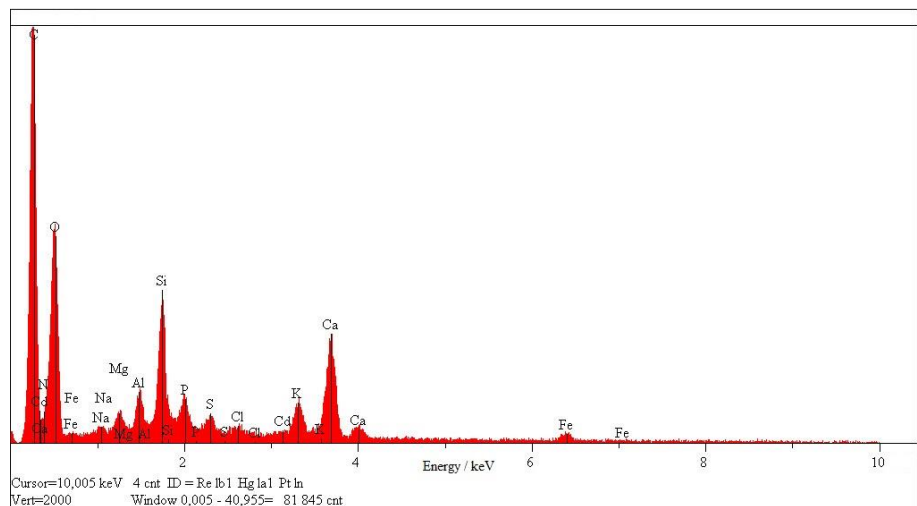


Fig. 3.11 Energy dispersive X-ray spectroscopy (EDX) (Garé compost unloaded)

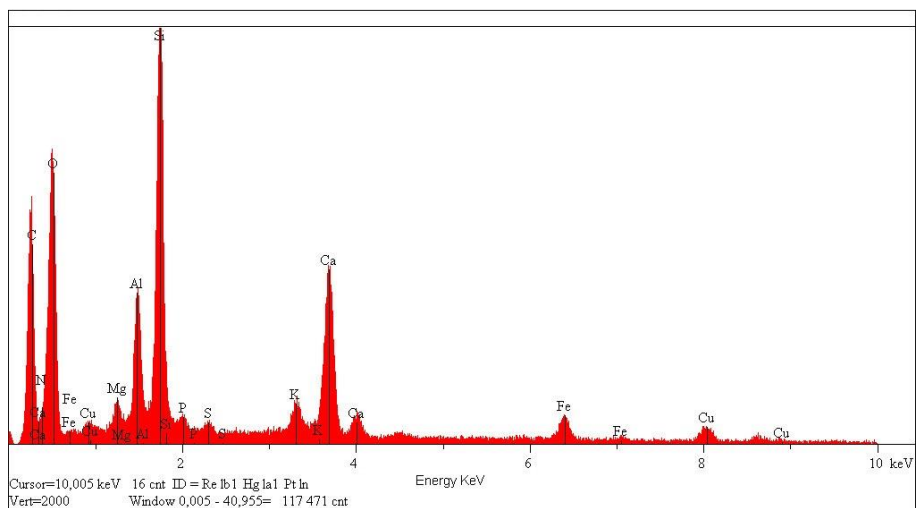


Fig. 3.12 Energy dispersive X-ray spectroscopy (EDX) after  $\text{Cu}^{2+}$  loaded (Garé compost)

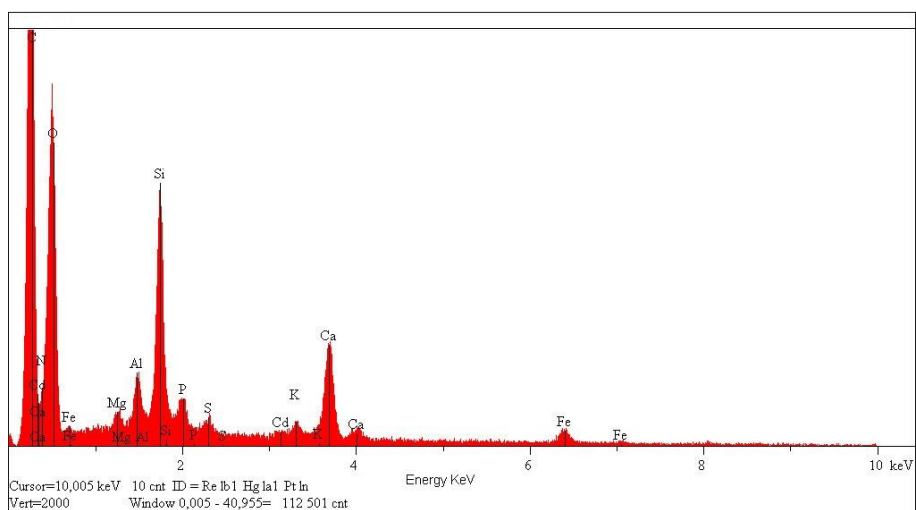


Fig. 3.13 Energy dispersive X-ray spectroscopy (EDX) after  $\text{Cd}^{2+}$  loaded (Garé compost)

Table 3.1. The EDX chemical composition of raw Felgyő compost before and after loaded with  $\text{Cu}^{2+}$  and  $\text{Cd}^{2+}$ 

Sample	Raw compost		Raw compost		$\text{Cu}^{2+}$ loaded		$\text{Cd}^{2+}$ loaded	
Mag	x35		x50		x50		x50	
Element	At. Ratio	Wt %	At. Ratio	Wt %	At. Ratio	Wt %	At. Ratio	Wt %
C	41.22	32.164	44.708	35.233	29.235	21.398	29.235	21.398
N	12.9	11.738	10.048	9.235	13.81	11.79	13.81	11.787
O	38.163	39.667	38.043	39.936	44.618	43.502	44.618	43.502
Na	0.267	0.399	0.197	0.297	-	-	-	-
Mg	0.395	0.623	0.357	0.57	0.535	0.792	0.535	0.792
Al	0.771	1.351	0.806	1.428	2.26	3.72	2.261	3.718
Si	2.759	5.035	2.552	4.703	7.158	12.25	7.158	12.252
P	0.444	0.893	0.442	0.899	0.18	0.339	0.18	0.339
S	0.288	0.599	0.352	0.74	0.096	0.188	0.096	0.188
Cl	0.124	0.286	0.097	0.225	-	-	-	-
K	0.69	1.753	0.639	1.64	0.329	0.783	0.329	0.783
Ca	1.652	4.301	1.302	3.423	0.98	2.38	0.976	2.384
Fe	0.328	1.19	0.456	1.672	0.53	1.81	0.532	1.809
Cu	-	-	-	-	0.27	1.046	-	-
Cd	-	-	-	-	-	-	0.27	1.046

Table 3.2. The EDX chemical composition of raw Garé compost and after loaded with  $\text{Cu}^{2+}$  and  $\text{Cd}^{2+}$ 

Sample	Raw compost		Raw compost		$\text{Cu}^{2+}$		$\text{Cd}^{2+}$	
Mag	x35		x50		x50		x50	
Element	At. Ratio	wt%	At. ratio	wt%	At. ratio	wt%	At. ratio	wt%
C	42.478	33.232	44.960	36.711	41.372	33.629	43.788	35.276
N	10.427	9.513	10.054	9.574	11.433	10.838	12.409	11.658
O	39.605	41.275	40.439	43.985	42.915	46.467	38.569	41.39
Na	0.243	0.364	0.287	0.449	-	-	-	-
Mg	0.484	0.767	0.349	0.577	0.154	0.253	0.252	0.411
Al	0.739	1.298	0.528	0.968	0.753	1.376	0.656	1.187
Si	2.338	4.277	1.565	2.988	2.15	4.087	2.289	4.311
P	0.598	1.207	0.310	0.653	0.269	0.563	0.375	0.779
S	0.274	0.573	0.240	0.522	0.125	0.272	0.163	0.35
Cl	0.135	0.311	0.084	0.202	-	-	-	-
K	0.613	1.562	0.298	0.793	0.098	0.259	0.104	0.274
Ca	1.841	4.807	0.733	1.996	0.495	1.344	1.099	2.954
Fe	0.224	0.816	0.153	0.583	0.18	0.678	0.219	0.822
Cu	-	-	-	-	0.055	0.235	-	-
Cd	-	-	-	-	-	-	0.078	0.589

### 3.2.1.3 Fourier transform infrared spectroscopy (FTIR)

While the characteristic peaks of the main organic components are present in all spectra, no significant differences can be observed: the different ratio of the various peaks (indicating different composition from the major organic substances) is probably simply related to the very heterogeneous compost sample as very low amounts of sample (less than 10 mg) is required for a pellet. Moreover, there were no major changes such as the appearance or disappearance of peaks was observed in the treated samples when compared to the references. Supposing that the metal binding is mainly due to the ionic interaction of the metal cations with the carboxyl groups in the humic substances, a shift in the ratio of the peaks related to the protonated and dissociated carboxyl groups could indicate the metal binding. However, the peak related to the protonated carboxyl around  $1720\text{ cm}^{-1}$  is not observed even in the reference, probably due to the salt formation occurring with other present cations (such as Na, K etc.), and during the treatment only the change of the cation occurs; thus, the metal binding has no noticeable effect on the spectra. Fig. 3.14 and 3.15 indicated the peak of  $3400\text{ cm}^{-1}$  is wide band related to the OH and NH groups and  $2930\text{ cm}^{-1}$  C-H stretching in the  $-\text{CH}_2-$  groups;  $1630\text{ C}=\text{O}$  bond (mainly in the carboxyl groups), though the relative wide peak probably indicates the presence of C=C and amide groups as well,  $1430$  related to the O-H and C-O bonds, then  $1380$  probably CH bonds, although other peaks related to other groups such as nitrate may also be present, which is indicated by the non-steep curve at lower wavelengths.  $1070$ ,  $1030$  relatively wide band related to the C-O-C bonds in various polysaccharides, the size and relativity of the two peaks is simply related to the differences in the polysaccharide ratio (such as the starch, cellulose, etc. content; the presence of clay minerals may also affect the band). There are likely more characteristic peaks, which overlap with the most intensive ones mentioned above, thus making their identification difficult in a complex sample like compost, which contains a wide variety of organic compounds. The figure 3.14 and 3.15 show no significant differences were observed. Theoretically, the adsorption may lead to the shift of the peaks related to the groups participating in the adsorption, but in this case the differences were minimal and showed no trend, thus likely only the result of the heterogeneity of the compost material. Thus, the spectra could be mainly used for an explanation of the differences between the adsorption of different samples, i.e. if peaks related to the metal binding groups (as

mentioned in the explanation) are larger, they can bind more ions, hence the larger adsorption capacity of the specimen.

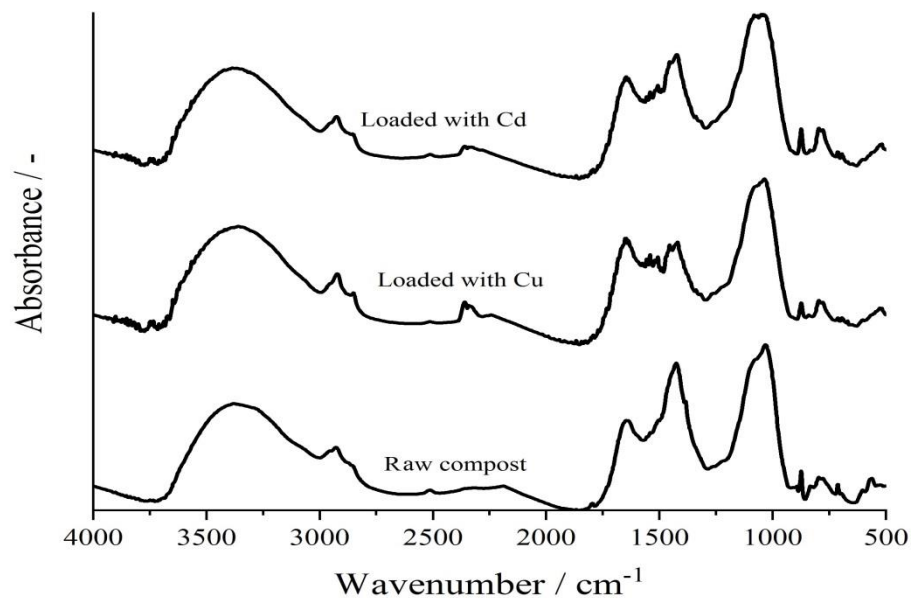


Fig. 3.14 FTIR spectra of raw Garé compost loaded with Cu<sup>2+</sup> and Cd<sup>2+</sup>.

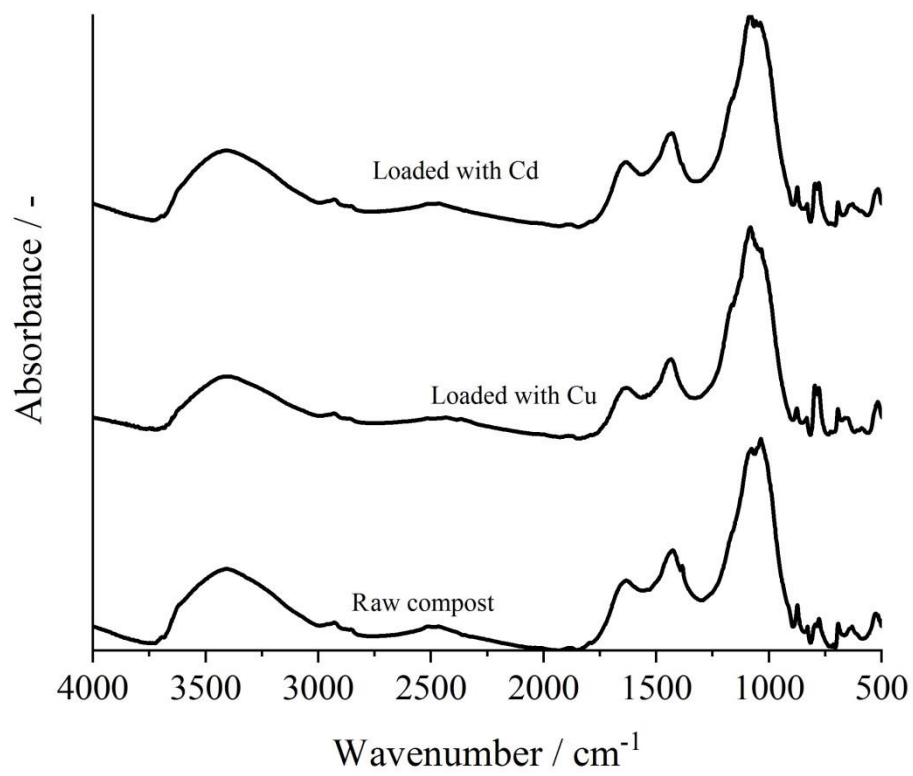


Fig. 3.15 FTIR spectra of raw Felgyő compost loaded with Cu<sup>2+</sup> and Cd<sup>2+</sup>.

### 3.2.2 Batch experiment

#### 3.2.2.1 Langmuir isotherm

The Langmuir isotherm deals with the unimolecular thick layer of adsorbate upon the surface of adsorbents without having any interactions between adsorbed molecules. Its mathematical form is given by (Langmuir, 1918).

$$q_e = \frac{q_{max} K C_e}{1 + K C_e} \quad (3.3)$$

Where  $C_e$  is the equilibrium concentration ( $\text{mg L}^{-1}$ ),  $q_e$  and  $q_{max}$  are respectively the amount and maximum amount of metal ion sorbed at equilibrium per unit weight of sorbent ( $\text{mg L}^{-1}$ ) and  $K_L$  is the equilibrium adsorption constant. The compost has a significant impact on the uptake of heavy metals in this research. The results obtained are shown in Fig. 3.16 and 3.17 and in terms of compost effect on the sorption of  $\text{Cd}^{2+}$  and  $\text{Cu}^{2+}$  from the aqueous solution onto the different sorbents in relation of the metal ions removed percentage. It is clear that  $\text{Cd}^{2+}$  and  $\text{Cu}^{2+}$  ions were effectively adsorbed in the composts and the maximum adsorption of  $\text{Cd}^{2+}$  and  $\text{Cu}^{2+}$  ions using compost occurred at 0 to  $10000 \mu\text{g g}^{-1}$  by 100%. The results in Fig. 3.16 and 3.17 show that the equilibrium capacity of cadmium, copper removal by the different adsorbents increased significantly as the concentration of the solution increased as seen in table 3.5. The adsorption capacities of  $\text{Cu}^{2+}$  and  $\text{Cd}^{2+}$  ions increased rapidly as the concentration value increased. Above  $10000 \mu\text{g g}^{-1}$  the adsorptive capacities of  $\text{Cd}^{2+}$  and  $\text{Cu}^{2+}$  ions increased, but at a slower rate. This is because of the competitive adsorption between hydrogen ion and the heavy metal cation (Amarasinghe and Williams, 2007). The adsorption equilibrium was analysed for Langmuir models using non-linear regression. It was observed that the metal uptake by composts varied with varying of initial solution concentration and composts as shown in Fig 3.16 and 3.17. The cadmium in Fig 3.17 adsorbed was higher in compost 2. Garé then 3. Sioagárd and less in 1. Felgyő, the maximum adsorbed capacity in compost 2. Garé was recorded  $40107 \mu\text{g g}^{-1}$  while in 3. Sioagárd was  $30669 \mu\text{g g}^{-1}$  and recorded less amount adsorbed in 1. Felgyő with  $26594 \mu\text{g g}^{-1}$ , the equilibrium constant presented in table 3.4 is 0.037 for compost 1. Felgyő, 0.027 at compost 3. Sióagárd and less steep for compost 2. Garé. From table 3.5, the

greater percentage of  $\text{Cd}^{2+}$  in the adsorbents was associated with the residual fractions. The possible explanation for the residual state of adsorbed  $\text{Cd}^{2+}$  by compost may be due to the existence of strong chemical bonds between  $\text{Cd}^{2+}$  and compost organic matter; organometal complexes exhibited higher stability and reduced the mobility of heavy metal ions (Haroun et al. 2007). In Table 3.3 is depicted the organic matter content of the 3 composts. Copper has recorded the highest amount in Fig 3.16 of  $44242 \mu\text{g g}^{-1}$  adsorbed into compost 2. Garé and  $30237 \mu\text{g g}^{-1}$  in compost 3. Sióagárd finely in compost 1. Moreover, the content of  $\text{Cu}^{2+}$  adsorbed by both composts exceeded  $\text{Cd}^{2+}$ , indicating the competitive adsorption advantage of Cu and further illustrated the selective adsorption order. This was consistent with the adsorption order of heavy metals by humus substances (Covelo et al. 2004). Felgyő was the lowest amount sorbed of copper with a record of  $26350 \mu\text{g g}^{-1}$  as depicted in table 3.4. The curves in Fig. 3.16 and 3.17 and equilibrium constant K in table 3.4 have shown higher steepness in compost 3. Sióagárd, 0.05, then 1. Felgyő, 0.04 and lesser in 2. Garé 0.02, respectively. The initial concentration provides an important driving force to overcome all mass transfer resistances of solutes between the aqueous and solid phases. The impact of initial heavy metal concentration on the rate of sorption is shown in Fig 3.16 and 3.17, from those figures we can learn that metal removal differs with varying of initial heavy metal concentration. As shown in Fig. 3.16 and 3.17, when the initial cations concentration increased, the uptake capacity of compost increased respectively. The ion exchange was believed to be a principle mechanism of the sorption where metals originally attached onto the biomass structure was replaced by the heavy metal ions (Apiratikul and Pavasant, 2008). Content properties of compost materials are given in table 3.3.

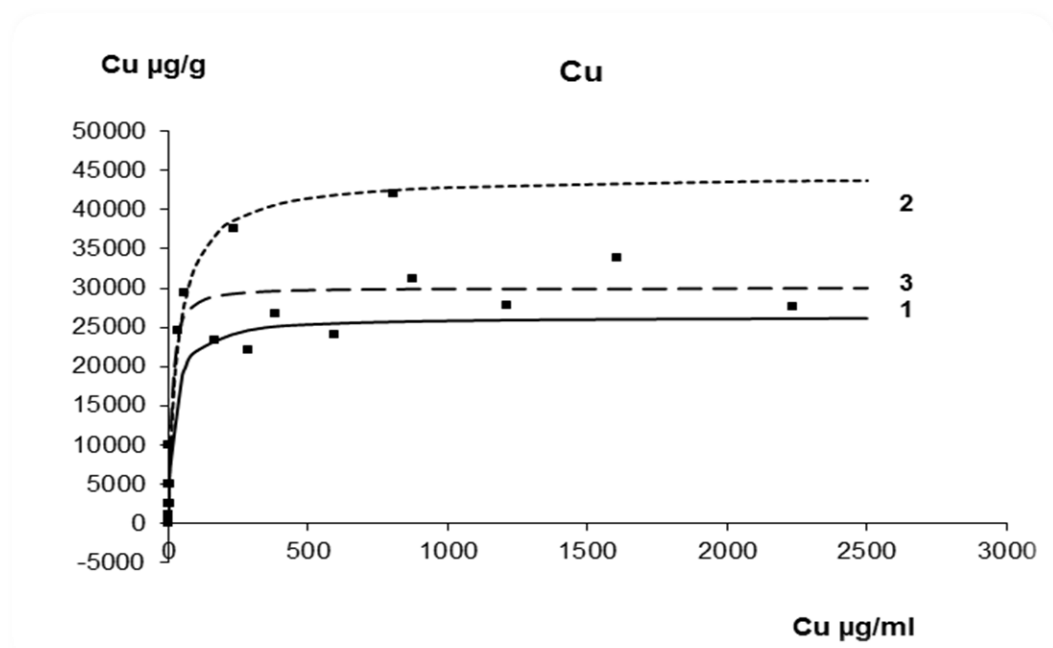


Fig. 3.16 Experimental data of Cu<sup>2+</sup> adsorbed by compost (Sioagárd, Garé and Felgyő) fitted to Langmuir model

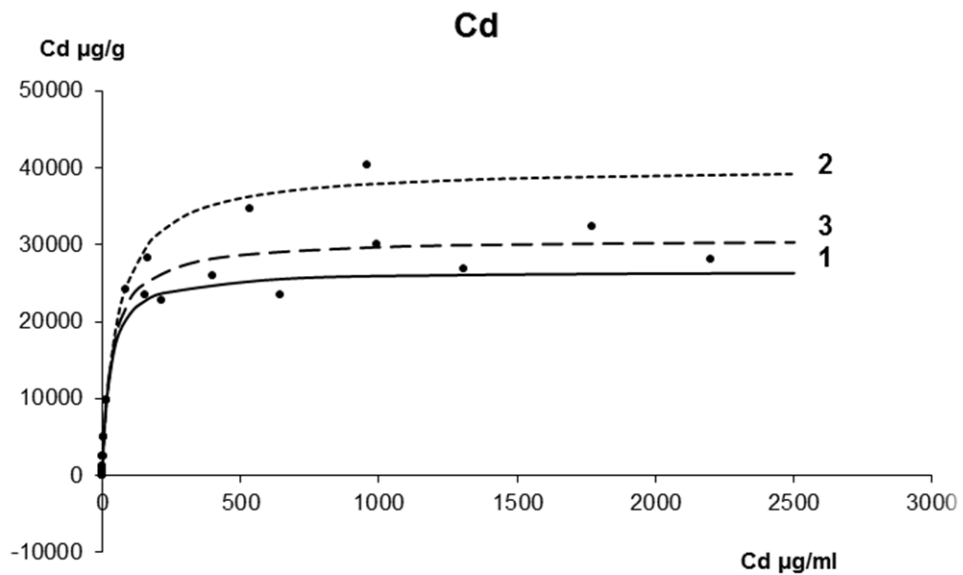


Fig. 3.17 Experimental data of Cd<sup>2+</sup> adsorbed by compost (Sioagárd, Garé and Felgyő) fitted to Langmuir model

Table 3.3. Content properties of compost materials

Compost Material	Dry mater	pH <sub>KCl</sub>	pH <sub>H<sub>2</sub>O</sub>	Organic Mater %	NH <sub>4</sub> -N mg/kg	NO <sub>3</sub> -N mg/kg	Salt %	Total N %	Total P <sub>2</sub> O <sub>5</sub> %	Total K <sub>2</sub> O%
1.Felgyő	64.3	6	6.6	24.7	17.8	942	1.8	1.1	0.7	0.7
2. Garé	46.3	5.1	5.4	50.0	95.8	2175	4.5	2.6	31233	13453
3. Sióagárd	61.7	7	7.3	62.2	16.5	1461	1.3	1.0	16554	9998

Table 3.4. Langmuir Isotherms for Cd<sup>2+</sup> and Cu<sup>2+</sup> ( $q_{max}$  Maximum Adsorption and  $K_L$  Equilibrium Constant)

Metal	Cd <sup>2+</sup>		Cu <sup>2+</sup>	
	$q_{max}$ µg-1	$K_L$	$q_{max}$ µg-1	$K_L$
1. Felgyő	26594	0.037	26350	0.049
2. Garé	40107	0.017	44242	0.028
3. Sióagárd	30669	0.027	30273	0.058

Table 3.5. Removal percentages of Cu<sup>2+</sup> and Cd<sup>2+</sup>, compost (Sioagárd, Garé and Felgyő)

C <sub>0</sub>	Removal percentage of Cadmium			Removal percentage of copper		
	Felgyő Compost	Garé Compost	Sioagárd Compost	Felgyő Compost	Garé Compost	Sioagárd Compost
50	97	96	97	90	86	86
100	98	97	97	93	92	92
250	98	97	98	95	93	96
500	98	98	98	97	96	97
1000	98	98	99	97	97	98
2500	99	98	99	98	98	99
5000	99	98	99	99	98	99
10000	98	98	98	99	99	99
25000	91	96	94	88	98	93
30000	78	94	86	80	98	87
40000	67	86	75	69	94	78
50000	56	80	63	55	83	67

### 3.2.3 Bed column and breakthrough curve

#### 3.2.3.1 Mathematical description

The performance of the bed column system can be estimated using the shape of the breakthrough curve attained from the plot of  $C_{eff}/C_0$  contrary to time  $t$ , where  $C_{eff}$  and  $C_0$  are the effluent and influent concentrations. The adsorbed metal ion concentrations in the column are observed by a plot of the adsorbed metal concentration,  $C_{ad} = (1)$  or

normalized concentration defined as the ratio of effluent metal concentration to influent concentration ( $C_{eff}/C_0$ ) as a function of time or volume of effluent  $V_{eff}$ . The essential dynamics for column demonstration at various operating a breakthrough curve study are the bed height, flow rate, and initial inlet concentration. The effects of these factors on the profile of the breakthrough curve and column performance were studied and illustrated in table 3.6, 3.7 and 3.8.

$$C_{ad} = \text{Inlet concentration } (C_0) - \text{Outlet concentration } (C_{eff}) \quad (3.4)$$

$$V_{eff} \text{ (mL)} = Q_{total} \quad (3.5)$$

where  $Q$  = Volumetric flow rate ( $\text{mL min}^{-1}$ )

$t_{total}$  = Total flow time (min)

$$q_{total} \text{ (mg)} = \frac{Q}{1000} = \frac{Q}{1000} \int_{t=0}^{t=t_{total}} C_{ad} dt \quad (3.6)$$

$$q_{eq} \left( \frac{\text{mg}}{\text{g}} \right) = \frac{q_{total}}{X} \quad (3.7)$$

The metal removal percentage was determined from the relationship (3.8):

$$\%R = [(C_0 - C_{eff}) Q \cdot t / mt] \times 100 \quad (3.9)$$

### 3.2.3.2 Effect of initial inlet concentration on breakthrough curves.

The effect of the initial inlet concentration on breakthrough curves was evaluated using 20 and 100  $\text{mg L}^{-1}$  of  $\text{Cu}^{2+}$  inlet concentration solutions, while setting up the bed height at 2.4, 3.1 and 6.5 cm of Garé absorbent respectively, the flow rate was manipulated at 4  $\text{mL min}^{-1}$  and 8  $\text{mL min}^{-1}$ .

#### 3.2.3.2.1 Effect of $\text{Cu}^{2+}$ concentration on breakthrough curve using Garé compost

Table.3.6 is demonstrating the results obtained from the columns. The breakthrough times of these curves decrease, and the curves dispersed and emerged slowly with increasing initial inlet concentration as demonstrated in Fig 3.18 and 3.19 at 20  $\text{mg L}^{-1}$  concentration this effect was also observed by (Abdolali et al. 2017). Higher removal percentage was observed with the decrease of inlet concentration (Oguz and Ersoy,

2014). Both  $q_{eq}$  and  $q_{total}$  increased considerably by the increase of inlet concentration.  $q_{total}$  increased from 19.77 mg at  $Cu^{2+}$  concentration of 20 mg L<sup>-1</sup> to 95.12 mg when the inlet concentration was 100 mg L<sup>-1</sup> and  $q_{eq}$  increased from 3.88 mg g<sup>-1</sup> to 17.55 mg g<sup>-1</sup> at 20 mg L<sup>-1</sup> and 100 mg L<sup>-1</sup> respectively as shown in table 3.6. A similar tendency has been reported by other researchers (Martín-Lara et al. 2016). This increase in the IE capacity could be explained by the fact that a higher influent  $Cu^{2+}$  concentration results in a higher driving force for the transfer process to overcome the mass transfer resistance (Sun et al. 2014).

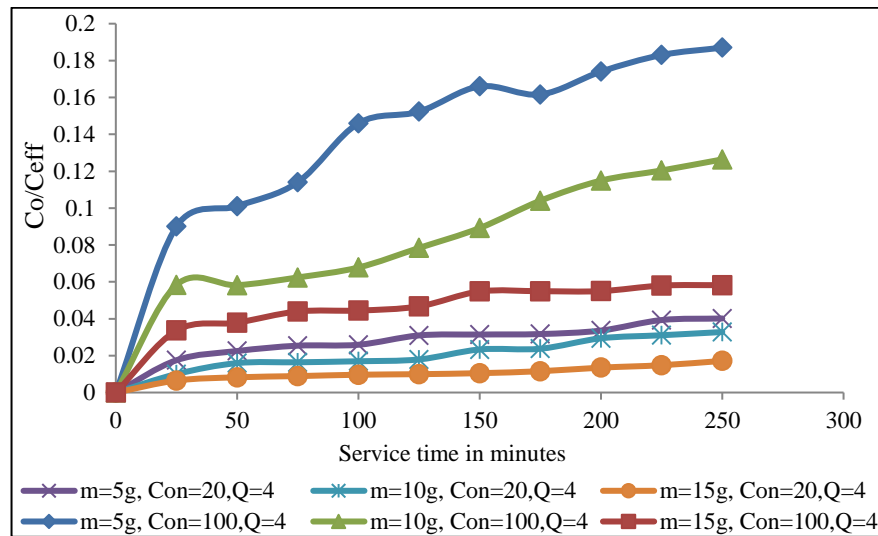


Fig. 3.18 Effect of concentration 20, 100 mg L<sup>-1</sup> at (Garé compost, Cu<sup>2+</sup> treated) different bed heights, flow rate 4 mL min<sup>-1</sup>

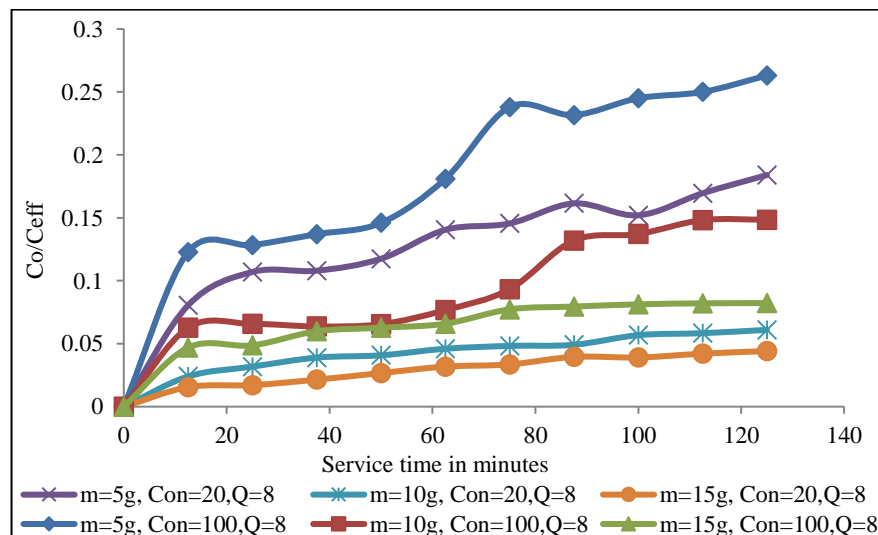


Fig. 3.19 Effect of concentration 20, 100 mg L<sup>-1</sup> at (Garé compost, Cu<sup>2+</sup> treated) different bed heights, flow rate 8 mL min<sup>-1</sup>

### 3.2.3.2.2 Effect of $\text{Cu}^{2+}$ concentration on breakthrough curve using Felgyő compost

The results of  $\text{Cu}^{2+}$  treated by Felgyő (1.1, 2 and 3.1 cm) compost is demonstrated on table 3.7, which indicated that both  $q_{\text{eq}}$  and  $q_{\text{total}}$  improved significantly by the increase of inlet concentration.  $q_{\text{total}}$  increased from 19.23 g at  $\text{Cu}^{2+}$  concentration of 20  $\text{g L}^{-1}$  to 78.24 g when the inlet concentration was 100  $\text{mg L}^{-1}$ .  $q_{\text{eq}}$  increased from 1.95  $\text{mg g}^{-1}$  to 8.58  $\text{mg g}^{-1}$  at 20 and 100  $\text{mg L}^{-1}$  respectively. A similar tendency has been conveyed by other researches (Kumar et al. 2011). Fig. 3.20 and 3.21 are demonstrating the results obtained from the column which indicated the breakthrough times of these curves were decreased with increasing initial inlet concentration. At lower inlet concentrations, breakthrough curves dispersed, and breakthrough emerged slowly, this effect was also observed (Oguz and Ersoy, 2014). Higher deduction percentage was detected with the reduction of inlet concentration. The decrease in metal removal efficiency was observed with increase in influent metal concentration (Foo et al. 2013).

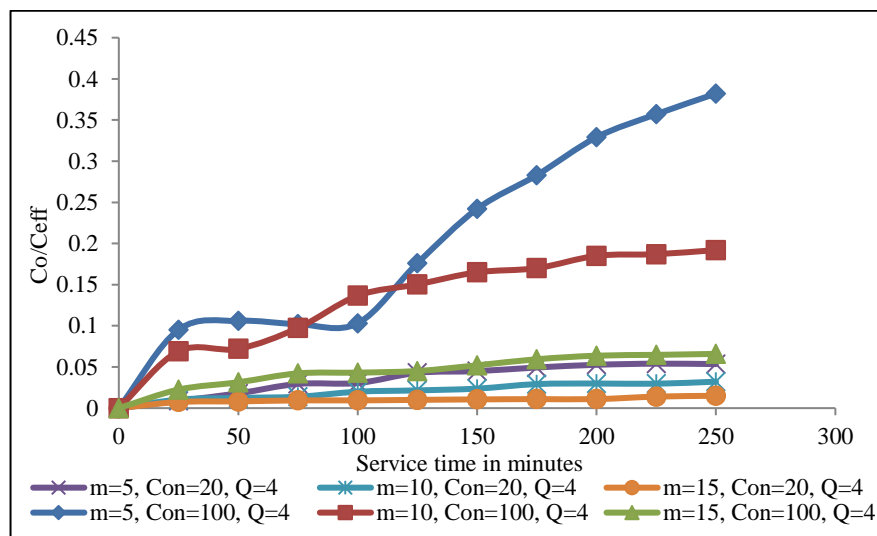


Fig. 3.20 Effect of concentration 20, 100  $\text{mg L}^{-1}$  at different bed heights, flow rate 4  $\text{mL min}^{-1}$  (Felgyő compost,  $\text{Cu}^{2+}$  adsorbed)

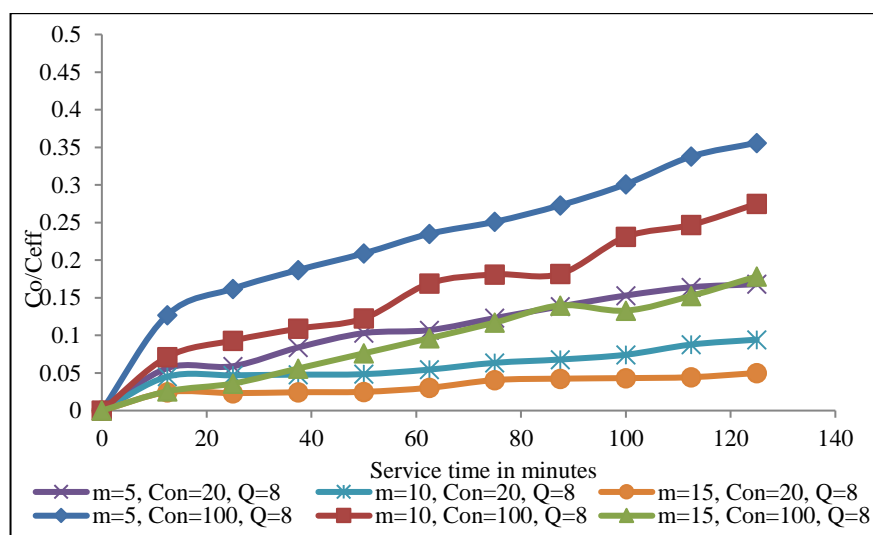


Fig. 3.21 Effect of concentration 20, 100 mg L<sup>-1</sup> at different bed heights, flow rate 8 mL min<sup>-1</sup> (Felgyő compost, Cu<sup>2+</sup> adsorbed)

### 3.2.3.2.3 Effect of Cd<sup>2+</sup> concentration on breakthrough curve using Felgyő compost

The results shown in table 3.8 for treating Cd<sup>2+</sup> by using Felgyő compost further indicated that both  $q_{eq}$  and  $q_{total}$  increased considerably by the increase of inlet concentration.  $q_{total}$  increased from 19.9 g at Cd<sup>2+</sup> concentration of 20 mg L<sup>-1</sup> to 97.33 g when the inlet concentration was 100 mg L<sup>-1</sup>.  $q_{eq}$  increased from 1.98 mg g<sup>-1</sup> to 9.47 mg g<sup>-1</sup> at 20 and 100 mg L<sup>-1</sup> respectively. Similar tendency has been reported by other researches (Sun, 2014). On increasing the initial ion concentration, the breakthrough curves became steeper and breakthrough volume decreased because of the lower mass-transfer flux from the bulk solution to the particle surface due to the weaker driving force (Baek et al. 2007). The breakthrough times of these curves decrease with increasing initial inlet concentration as depicted on Fig 3.22 and 3.23. At lower inlet concentrations, breakthrough curves spread, and breakthrough occurred gradually. Higher removal percentage was observed with the decrease of inlet concentration.

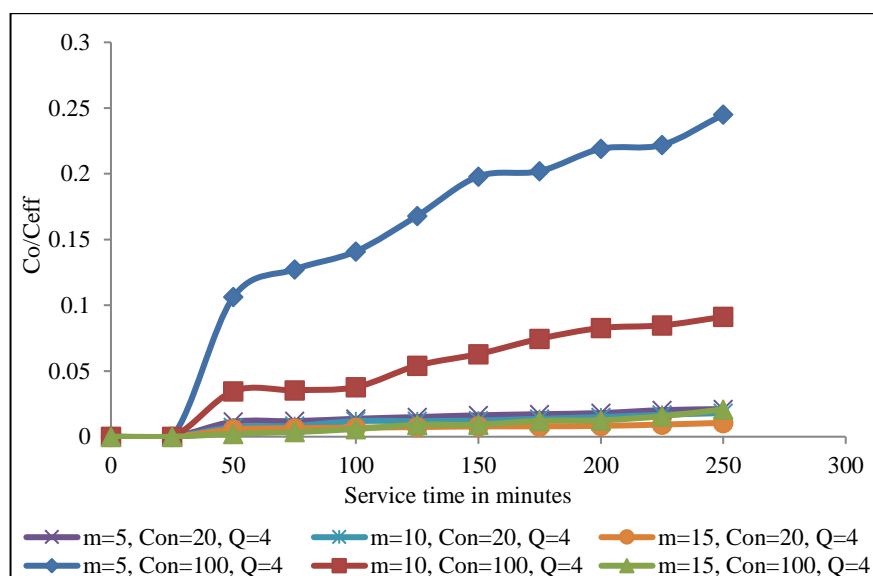


Fig.3.22 Effect of concentration 20, 100 mg L<sup>-1</sup>, flow rate 4ml/min, different bed heights (Felgyó compost, Cd<sup>2+</sup> treated)

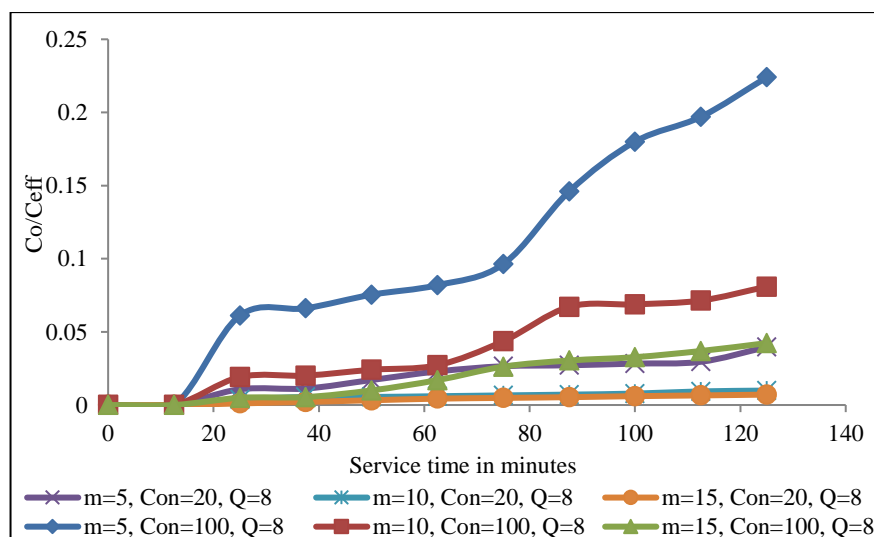


Fig. 3.23 Effect of concentration 20, 100 mg L<sup>-1</sup>, flow rate 8ml/min, different bed heights (Felgyó compost, Cd<sup>2+</sup> treated)

### 3.2.3.3 Effect of inlet flow rate on breakthrough curves adsorption.

The flow rate is a very crucial parameter for column operation because it determines the duration the sorbate is in contact with sorbent packed in the column. Generally, the column attains a breakthrough point early at a high flow rate (Kumar et al. 2016). The effect of the initial inlet concentration on breakthrough curves was evaluated using 20 and 100 mg L<sup>-1</sup> of Cu<sup>2+</sup> and Cd<sup>2+</sup> inlet concentration solutions, by applying different compost material. The flow rate was manipulated at 4 ml min<sup>-1</sup> and 8 ml min<sup>-1</sup>.

### 3.2.3.3.1 Effect of $\text{Cu}^{2+}$ flow rate on breakthrough curve using Garé compost

The results obtained by treating  $\text{Cu}^{2+}$  by Garé compost is demonstrated in table 3.6, which shows the column parameters at various operating conditions and its effect on adsorption process. This table also gives the removal percentage of ions at different operation conditions. Fig. 3.24 and 3.25 demonstrate the breakthrough curve which became steeper and elevated when the flow rate changed from 4 to 8  $\text{mL min}^{-1}$ . At higher flow rate, it takes additional time for the bed to get saturated; whereas for lower flow rate there was sufficient time for the  $\text{Cu}^{2+}$  solution to get adsorbed on adsorbent. The column performed well at the lowest flow rate (Ozdemir et al. 2009). The percentage of  $\text{Cu}^{2+}$  removal also decreases with increasing in flow rate and higher removal percentage occurred at slower flow rate. Table 3.6 shows the effect of flow rate on the adsorption capacity ( $q_{total}$ ) and equilibrium adsorption ( $q_{eq}$ ). When the flow rate rise, both  $q_{total}$  and  $q_{eq}$  decreases, a similar observation has been observed by Riazi et al. (2016), however,  $q_{eq}$  was not reported with significant effect considerably. At higher flow rate, the residence time of effluent in the bed is low. This is due to a decrease in contact time between the metal ions and the compost at higher linear flow rates. As the adsorption rate is controlled by intra-particulate diffusion, an early breakthrough occurs leading to a low bed adsorption capacity (Taty-Costodes et al. 2005).

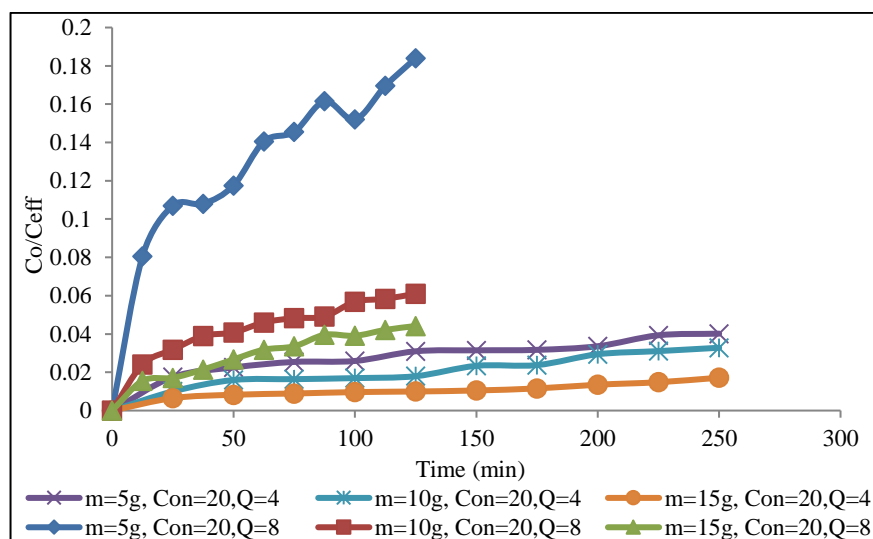


Fig. 3.24 Effect of flow rate (Garé compost,  $\text{Cu}^{2+}$  treated) at  $20 \text{ mg L}^{-1}$  concentration at different bed heights, flow rate 4 and 8  $\text{mL min}^{-1}$

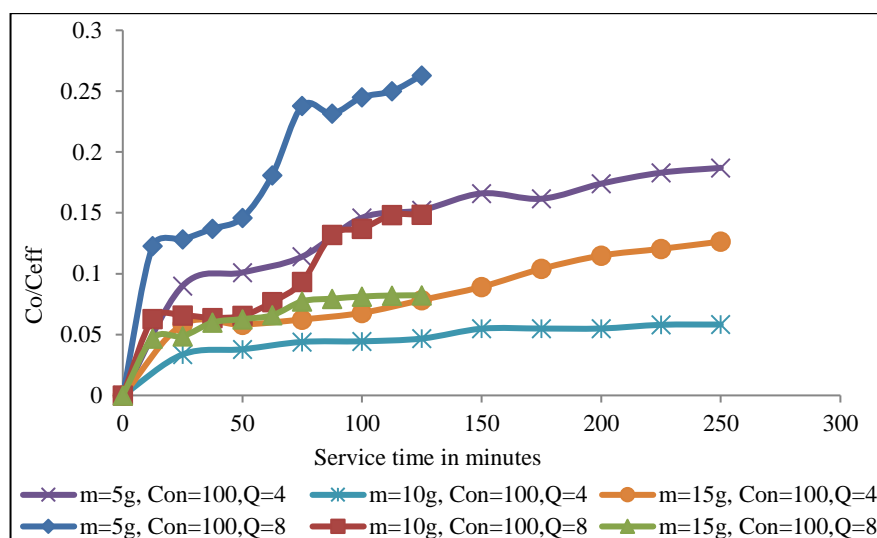


Fig. 3.25 Effect of flow rate (Garé compost,  $\text{Cu}^{2+}$  treated) at  $100 \text{ mg L}^{-1}$  concentration at different bed heights, flow rate 4 and  $8 \text{ mL min}^{-1}$

### 3.2.3.3.2 Effect of $\text{Cu}^{2+}$ flow rate on breakthrough curve using Felgyő compost

In  $\text{Cu}^{2+}$  case treatment by Felgyő compost, once could notice from Fig. 3.26 and 3.27 that the breakthrough curve became steeper and elevated when the flow rate boosted from  $4$  to  $8 \text{ mL min}^{-1}$ , similar observation noticed by Gupta (1998), for removal of  $\text{Cu}^{2+}$  by biosorption onto coconut shell in fixed-bed column systems. The results also show that the shape of the breakthrough curve is saturated earlier at higher flow rates as shown in figure 3.26 and 3.27 because the front of the adsorption zone quickly reached the top of the column. In contrast, a lower flow rate and longer contact time resulted in a shallow adsorption zone (Suksabye et al. 2008). Table 3.7 shows the effect of flow rate on the adsorption capacity  $q_{\text{total}}$  and equilibrium adsorption ( $q_{\text{eq}}$ ). When the flow rate rose, both  $q_{\text{total}}$  and  $q_{\text{eq}}$  decreased, similar observation by (Chao et al. 2014), however,  $q_{\text{eq}}$  was not affected considerably. In addition, the percentage of  $\text{Cu}^{2+}$  removal also decreased with an increase in flow rate and higher removal percentage occurred at a slower flow rate. This is due to the decrease in contact time between the metal ions and the compost at higher linear flow rates. At higher flow rate, the residence time of effluent in the bed was less.

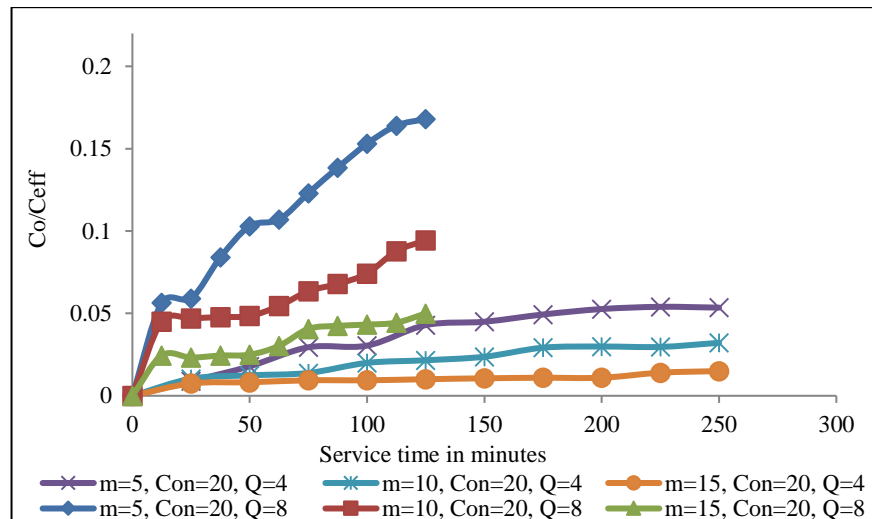


Fig. 3.26 Effect of the flow rate at  $20 \text{ mg L}^{-1} \text{ Cu}^{2+}$  concentration at different bed heights, flow rate  $4 \text{ mL min}^{-1}$  and  $8 \text{ mL min}^{-1}$ , (Felgyő compost,  $\text{Cu}^{2+}$  adsorbed)

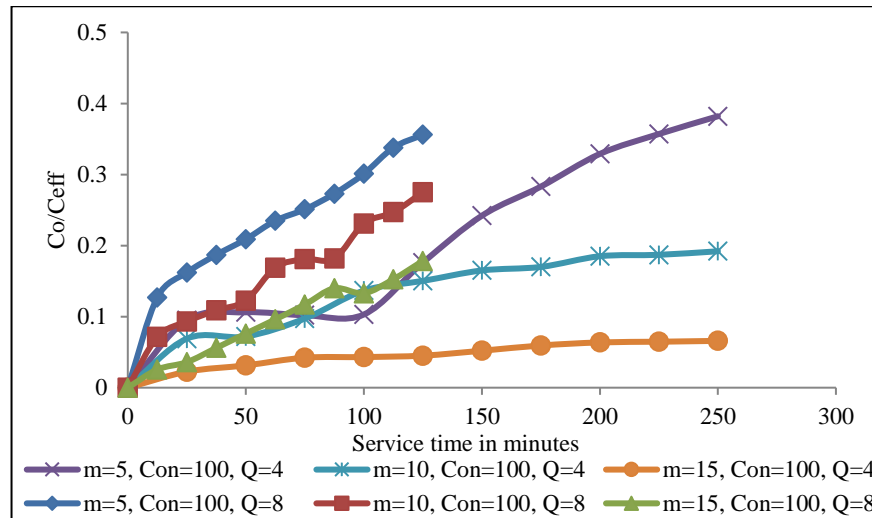


Fig. 3.27 Effect of the flow rate at  $100 \text{ mg L}^{-1} \text{ Cu}^{2+}$  concentration at different bed heights, flow rate  $4 \text{ mL min}^{-1}$  and (b)  $8 \text{ mL min}^{-1}$  (Felgyő compost,  $\text{Cu}^{2+}$  adsorbed)

### 3.2.3.3.3 Effect of $\text{Cd}^{2+}$ flow rate on breakthrough curve using Felgyő compost

Fig. 3.28, 3.29 and table 3.8 are demonstrating the results obtained from the column for  $\text{Cd}^{2+}$  treated by Felgyő compost. The breakthrough times of these curves decrease with increasing initial inlet concentration. At lower inlet concentrations, breakthrough curves spread and breakthrough occurred gradually. This is because of the residence time of the adsorbate in the column, which is long enough for adsorption equilibrium to be reached at high flow rate. This means that the contact time between the adsorbate and the adsorbent is minimized, leading to early breakthrough (Sivakumar and Palanissamy, 2009). Higher removal percentage was experimental with the reduction of inlet

concentration (Biswas and Mishra, 2015). Both  $q_{eq}$  and  $q_{total}$  increased considerably by the increase of inlet concentration.  $q_{total}$  increased from 19.9 g at  $Cd^{2+}$  concentration of 20 mg L<sup>-1</sup> to 97.33 g when the inlet concentration was 100 mg L<sup>-1</sup>.  $q_{eq}$  increased from 1.98 mg/g to 9.47 mg g<sup>-1</sup> at 20 and 100 mg L<sup>-1</sup> respectively. When the volumetric flow rate decreased more favourable ion exchange conditions were achieved (Kananpanah et al. 2009).

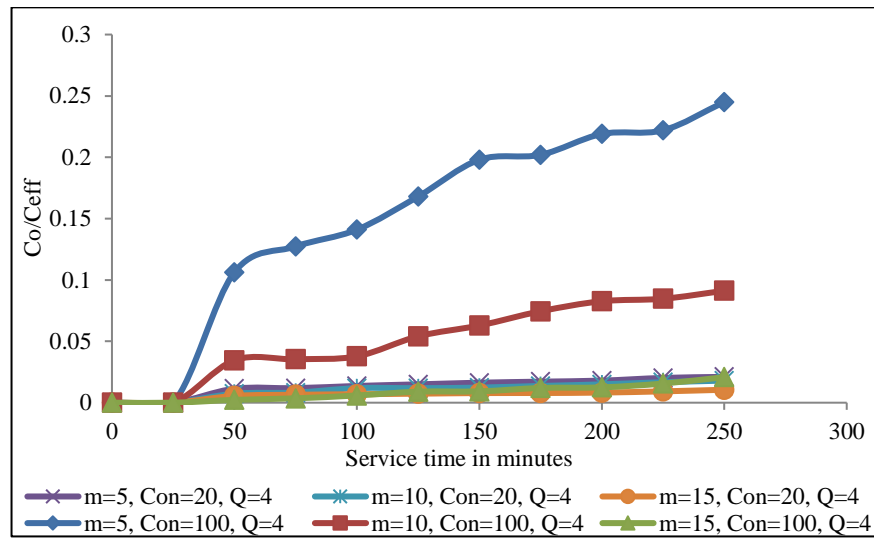


Fig. 3.28 Effect of concentration 20, 100 mg L<sup>-1</sup>, flow rate 4 ml/min, different bed heights (Felgyő compost, Cd<sup>2+</sup> treated)

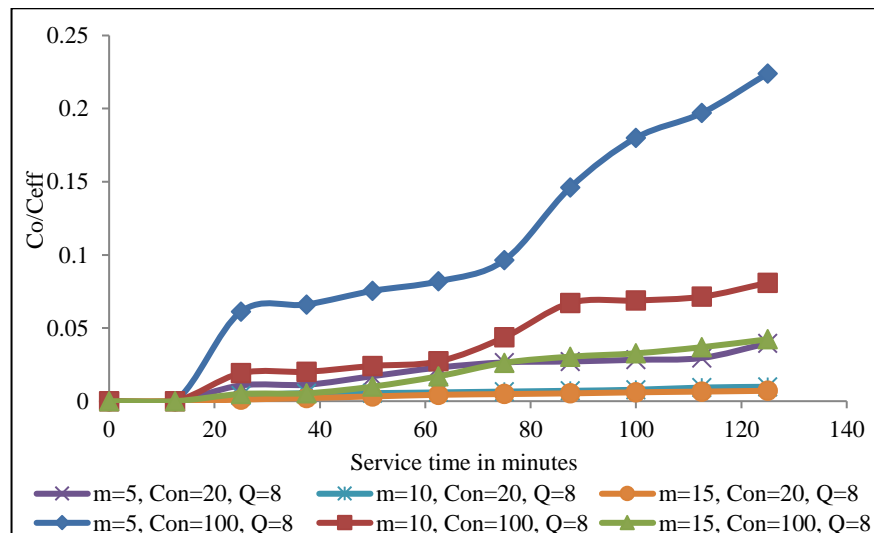


Fig. 3.29 Effect of concentration 20, 100 mg L<sup>-1</sup>, flow rate 8 ml/min, different bed heights. (Felgyő compost, Cd<sup>2+</sup> treated)

### 3.2.3.4 Effect of bed depth on breakthrough curves.

#### 3.2.3.4.1 Effect of bed depth on breakthrough curve after $\text{Cu}^{2+}$ treated using Garé compost

The breakthrough curves at different bed height (2.4, 3.1 and 6.5 cm) are shown in Fig. 3.30 and 3.31, using a constant influent concentration of  $20 \text{ mg L}^{-1}$  with a flow rate of 4 and  $8 \text{ mL min}^{-1}$ , and Fig 3.32 and 3.33 using  $100 \text{ mg L}^{-1}$  concentration while changing the rate flow from 4 to  $8 \text{ mL min}^{-1}$ , it is clear that the shape and slope of curves are changing with the discrepancy of the bed depth. The breakthrough time increases at higher bed depth of adsorbent. The slope of the breakthrough curve decreases with the increase in bed height, which result in a higher mass transfer zone (Ahmad and Hameed, 2010). The column parameters obtained from the effect of bed height is listed in table 3.6. As stated in table 3.6, when the bed height–increases, the removal percentage increases from 86 to 97% and the maximum adsorption capacity of the column is also increased, a similar trend was observed by (Mishra et al. 2016). A correlation is found between the reduction of bed height and the lower retention of metallic ions in consequence of this is because the adsorbent has insufficient contact time to attract the adsorbate  $\text{Cu}^{2+}$ .

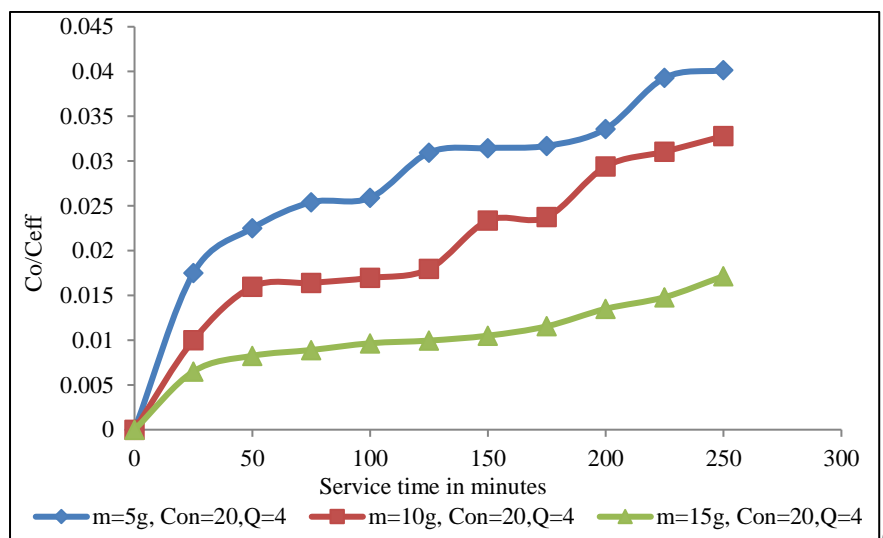


Fig. 3.30 Effect of bed height (Garé compost,  $\text{Cu}^{2+}$  treated) at concentration  $20 \text{ mg L}^{-1}$  and  $4 \text{ mL min}^{-1}$  flow rate

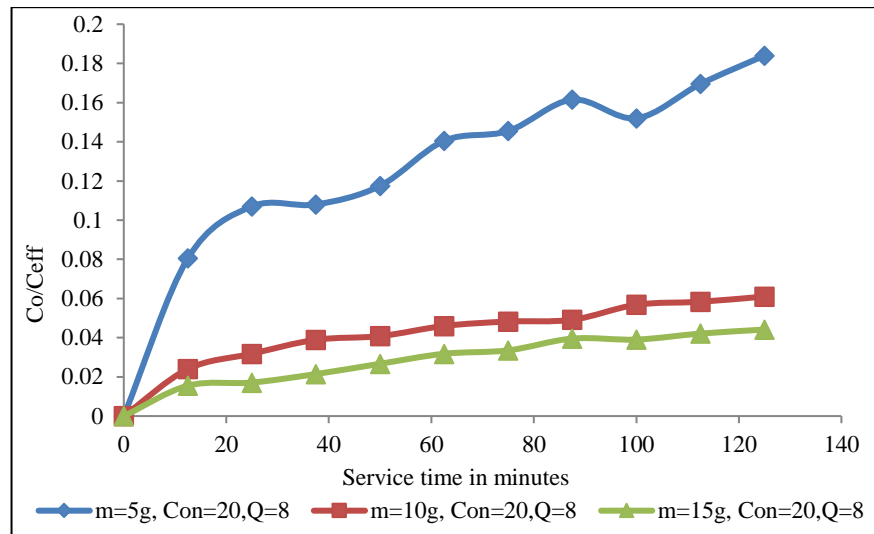


Fig. 3.31 Effect of bed height (Garé compost,  $\text{Cu}^{2+}$  treated) at concentration  $20 \text{ mg L}^{-1}$  and  $8 \text{ mL min}^{-1}$  flow rate

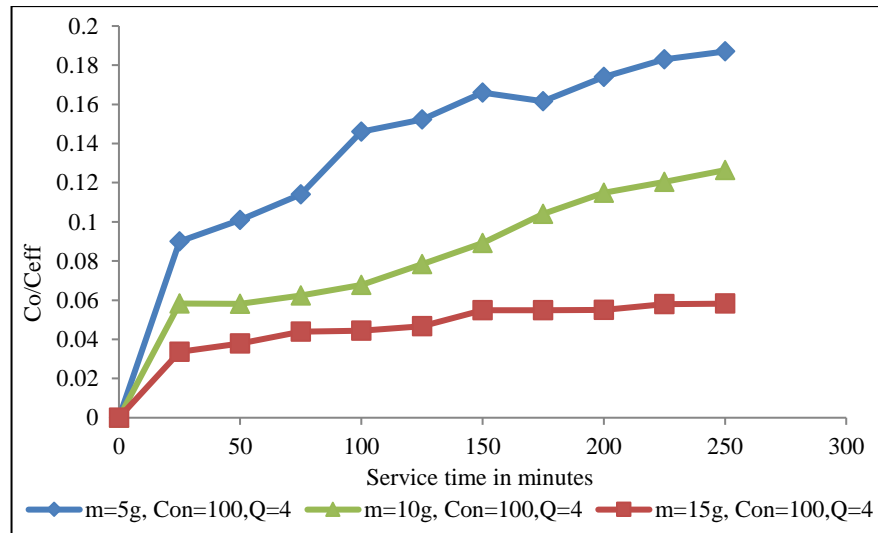


Fig. 3.32 Effect of bed height (Garé compost,  $\text{Cu}^{2+}$  treated) at concentration  $100 \text{ mg L}^{-1}$  and  $4 \text{ mL min}^{-1}$  flow rate

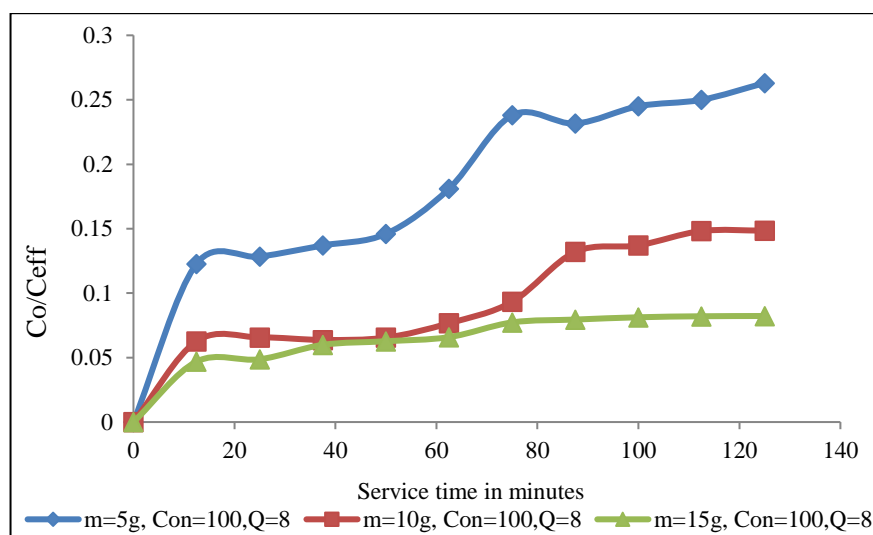


Fig. 3.33 Effect of bed height (Garé compost,  $\text{Cu}^{2+}$  treated) at concentration  $100 \text{ mg L}^{-1}$  and  $8 \text{ mL min}^{-1}$  flow rate

#### 3.2.3.4.2 Effect of bed depth on breakthrough curve after $\text{Cu}^{2+}$ treated using Felgyó compost

From Fig 3.34 to 3.37, the profile and slope of each curve are different with the variation of the bed depth. The breakthrough time increases at the greater bed depth of adsorbent. The breakthrough curve was steeper at lower bed height. The slope of the breakthrough curve decreased with an increase in bed height, which resulted in a higher mass transfer zone. The shape of the breakthrough curves was altered slightly from sharp concave to flat concave as the fixed-bed column length improved from 1.1 to 3.1 cm. This was attributed to the more adsorbent-specific surface and more available metal binding sites at higher bed height, which meant that consequently, the total adsorbed metal ions increased (Abdolali et al. 2017). According to table 3.7 when the bed height is increased, the removal percentage is improved, and the maximum adsorption capacity of the column is also increased. For a taller bed, a larger volume of the metal solution could be treated, and a higher percentage of metal removal was obtained (Muhamad et al. 2010). The longer bed delayed the exhaustion time of the adsorbent, which means the bed is able to operate for a longer period without changing the adsorbent, while for the shorter bed, the exhaustion approached faster; hence, the performance declined (Xu et al. 2013).

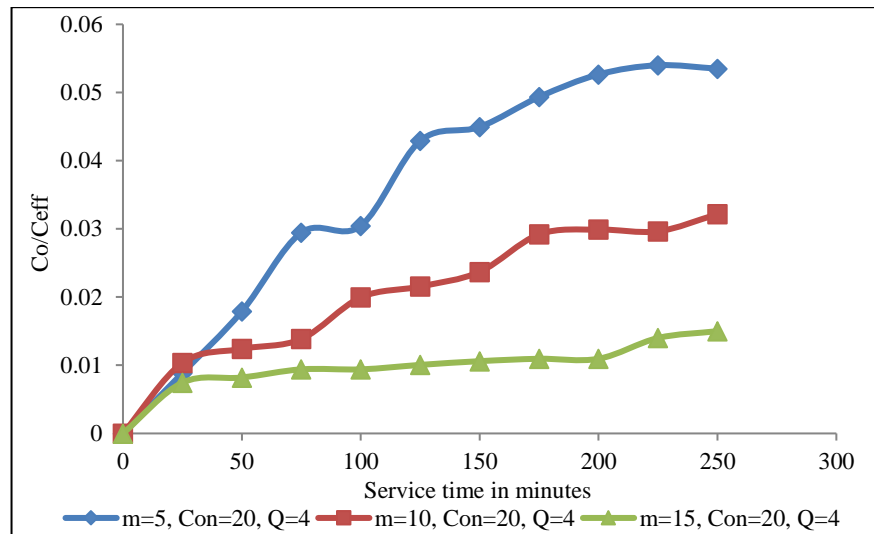


Fig. 3.34 Effect of bed height at concentration 20 mg L<sup>-1</sup> and 4 mL min<sup>-1</sup> flow rate, (Felgyő compost, Cu<sup>2+</sup> adsorbed)

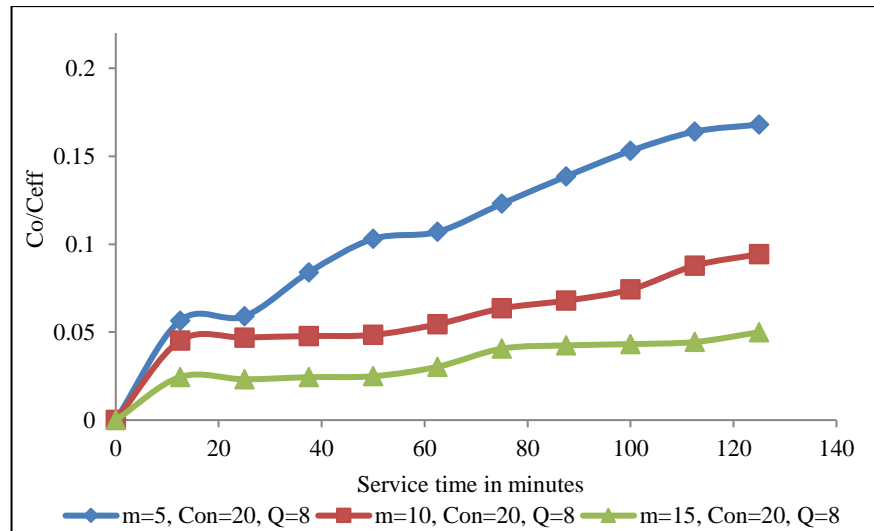


Fig. 3.35 Effect of bed height at concentration 20 mg L<sup>-1</sup> and 8 mL min<sup>-1</sup> flow rate (Felgyő compost, Cu<sup>2+</sup> adsorbed)

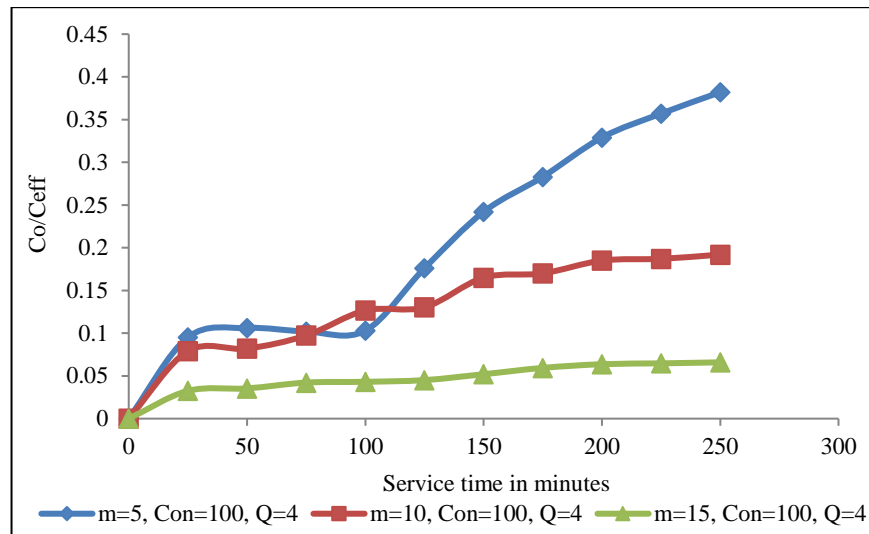


Fig. 3.36 Effect of bed height at concentration 100 mg L<sup>-1</sup> and 4 mL min<sup>-1</sup> flow rate (Felgyó compost, Cu<sup>2+</sup> adsorbed)

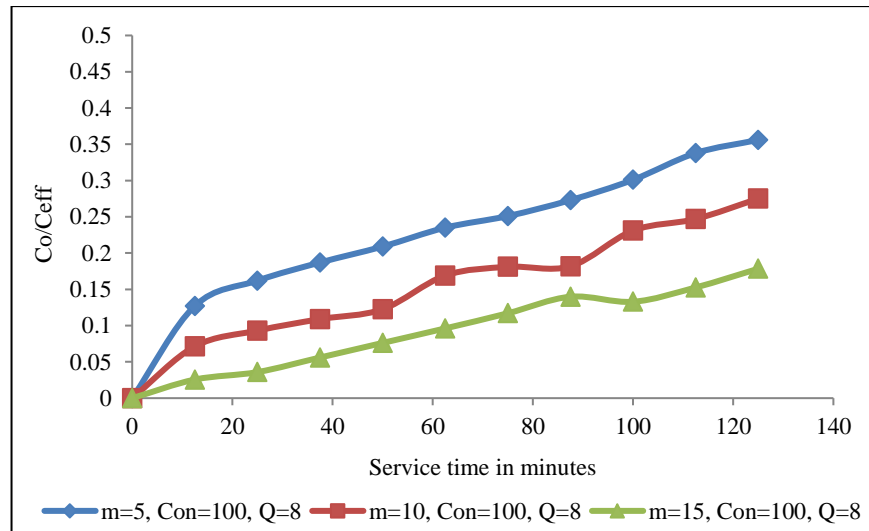


Fig. 3.37 Effect of bed height at concentration 100 mg L<sup>-1</sup> and 8 mL min<sup>-1</sup> flow rate (Felgyó compost, Cu<sup>2+</sup> adsorbed)

### 3.2.3.4.3 Effect of bed depth on breakthrough curve after Cd<sup>2+</sup> treated using Felgyó compost

The breakthrough curves at different bed depths (1.1, 2.1 and 3 cm) are shown in Fig. 3.38 to 3.41. From this figure, using a constant effluent concentration of 20 and 100 mg L<sup>-1</sup> with a flow rate of 4 and 8 mL min<sup>-1</sup>, we can see that the shape and slope of each curve are different with the variation of the bed depth. The breakthrough time increases at a higher bed depth of adsorbent. The breakthrough curve was steeper at lower bed height (Jing et al. 2011). The slope of the breakthrough curve decreased with an increase

in bed height, which resulted in a higher mass transfer zone. The shape of the breakthrough curves was changed slightly from steep concave to flat concave as the fixed-bed column height increased from 1.1 to .3.1 cm, leading to a broadened mass transfer zone. The column parameters gained from the effect of bed height is listed in table 3.8 and 3.9 for Felgyő and Garé compost respectively. In addition, as seen in Figs. 3.38 to 3.41 the breakthrough curve does not follow a characteristic ‘‘S’’ shape profile produced in ideal adsorption systems which is also noticed by Rouf and Nagapadma (2015). In consonance with Table 3.8, when the bed height is increased, the elimination percentage is increased and the maximum adsorption capacity of the column is also increased, a comparable tendency was experimental with (Jain et al. 2013). When the bed depth is reduced, axial dispersion phenomena predominate in the mass transfer and reduce the diffusion of metallic ions. The solute (metallic ions) does not have sufficient time to distribute into the total adsorbent mass (Mobasherpour et al. 2014).

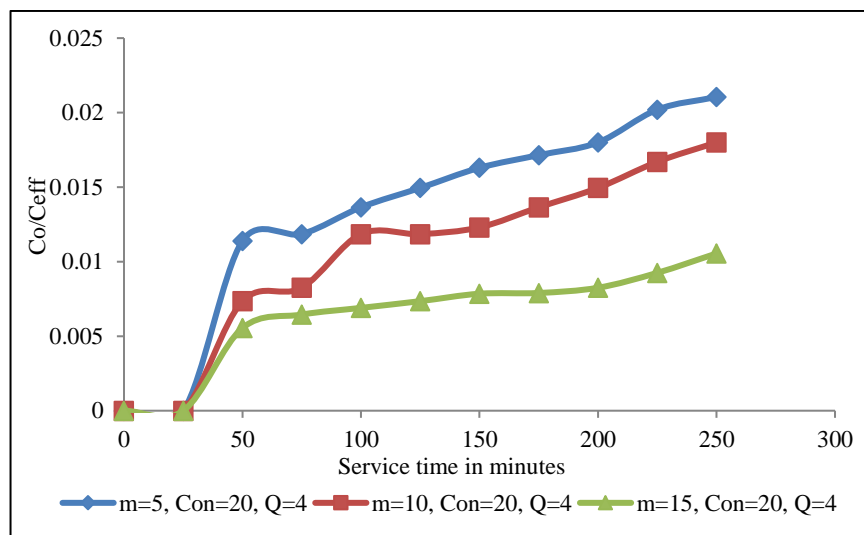


Fig.3.38 Effect of bed height when concentration  $20 \text{ mg L}^{-1}$  and flow rate  $4 \text{ mL min}^{-1}$ . (Felgyő compost,  $\text{Cd}^{2+}$  treated)

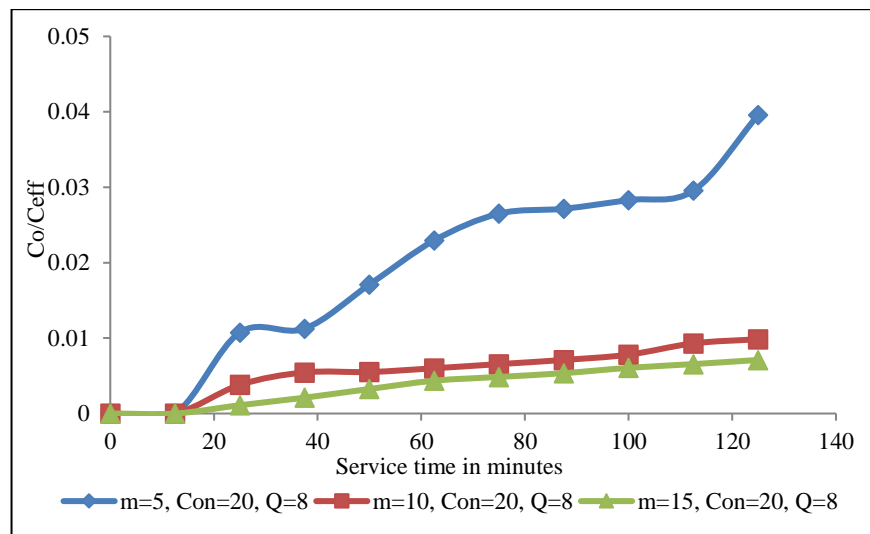


Fig. 3.39 Effect of bed height when concentration  $20 \text{ mg L}^{-1}$  and flow rate  $8 \text{ mL min}^{-1}$ . (Felgyó compost,  $\text{Cd}^{2+}$  treated)

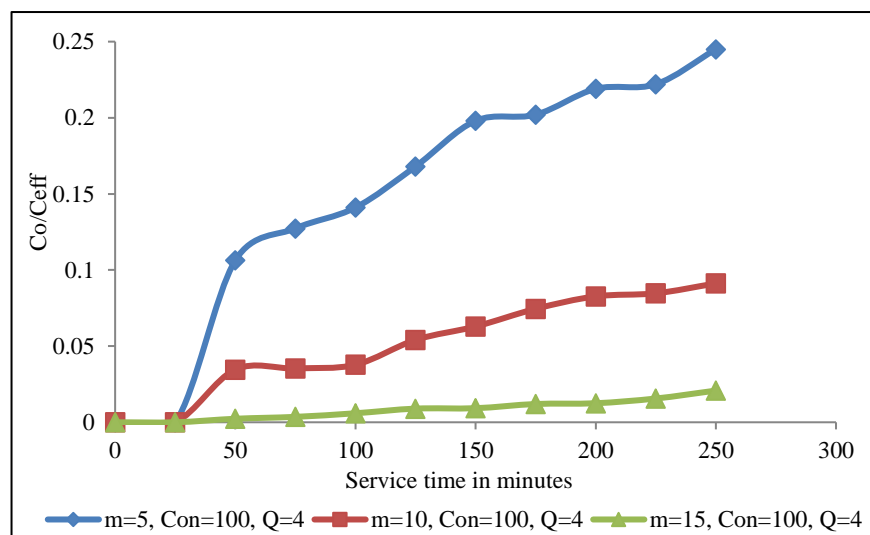


Fig. 3.40 Effect of bed height when concentration  $100 \text{ mg L}^{-1}$  and flow rate  $4 \text{ mL min}^{-1}$

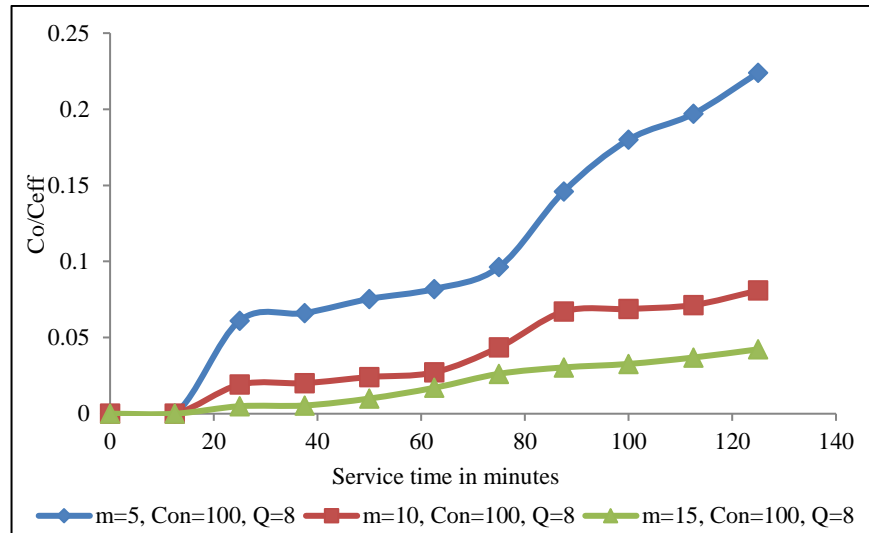


Fig. 3.41 Effect of bed height when concentration  $100 \text{ mg L}^{-1}$  and flow rate  $8 \text{ mL min}^{-1}$ . (Felgyő compost,  $\text{Cd}^{2+}$  treated)

Table 3.6. Mathematical description of column parameters (Garé compost,  $\text{Cu}^{2+}$  treated)

Q / $\text{mL min}^{-1}$	Bed Height / cm	$C_0 / \text{mg L}^{-1}$	Amount / g	$q_{\text{total}} / \text{mg}$	$q_{\text{exp}} / \text{mg g}^{-1}$	Total Removal / (%)
4	2.4	20	5 g	19.17	3.84	96
4	3.1	20	10 g	19.55	1.95	98
4	6.5	20	15 g	19.78	1.31	99
8	2.4	20	5 g	17.68	3.53	88
8	3.1	20	10 g	18.76	1.87	94
8	6.5	20	15 g	19.3	1.28	97
4	2.4	100	5 g	78.24	15.6	78
4	3.1	100	10 g	85.86	8.58	86
4	6.5	100	15 g	95.1	6.34	95
8	2.4	100	5 g	75.61	15.1	76
8	3.1	100	10 g	83.19	8.31	83
8	6.5	100	15 g	89.89	5.99	90

Table 3.7. Mathematical description of column parameters (Felgyő compost, Cu<sup>2+</sup> treated)

Q / mL min <sup>-1</sup>	Bed Height / cm	C <sub>0</sub> / mg L <sup>-1</sup>	Amount / g	q <sub>total</sub> / mg	q <sub>exp</sub> / mg g <sup>-1</sup>	Total Removal / %
4	1.1	20	5 g	19.4	3.88	97
4	2	20	10 g	19.56	1.95	86
4	3.1	20	15 g	19.77	1.31	84
8	1.1	20	5 g	17.26	3.45	80
8	2	20	10 g	19.08	1.98	97
8	3.1	20	15 g	19.37	1.29	95
4	1.1	100	5 g	85.25	17.55	91
4	2	100	10 g	91.22	9.12	90
4	3.1	100	15 g	95.12	6.34	98
8	1.1	100	5 g	80.57	16.14	96
8	2	100	10 g	90.06	9.66	95
8	3.1	100	15 g	93.13	6.29	93

Table 3.8. Mathematical description of column parameters (Felgyő compost, Cd<sup>2+</sup> treated)

Q / mL min <sup>-1</sup>	Bed Height / cm	C <sub>0</sub> / mg L <sup>-1</sup>	Wight / g	q <sub>total</sub> / mg	q <sub>eq</sub> / mg g <sup>-1</sup>	Total Removal / %
4	1.1	20	5 g	19.65	3.93	98
4	2	20	10 g	19.73	1.97	98
4	3.1	20	15 g	19.83	1.32	99
8	1.1	20	5 g	19.48	3.89	97
8	2	20	10 g	19.85	1.98	99
8	3.1	20	15 g	19.9	1.32	99
4	1.1	100	5 g	81.07	16.2	81
4	2	100	10 g	93.49	9.34	93
4	3.1	100	15 g	98.82	6.58	98
8	1.1	100	5 g	86.04	17.2	86
8	2	100	10 g	94.71	9.47	94
8	3.1	100	15 g	97.33	6.48	97

Table 3.9. Mathematical description of column parameters (Garé compost, Cd<sup>2+</sup> treated)

Q / mL min <sup>-1</sup>	Bed Height / cm	C <sub>0</sub> / mg L <sup>-1</sup>	Weight / g	q <sub>total</sub> / mg	q <sub>eq</sub> / mg g <sup>-1</sup>	Total Removal / %
4	2.4	20	5g	19.81	3.96	99
4	3.1	20	10g	19.84	1.98	99
4	6.5	20	15g	19.86	1.32	99
8	2.4	20	5g	19.84	3.96	99
8	3.1	20	10g	19.88	1.98	99
8	6.5	20	15g	19.9	1.32	99
4	2.4	100	5g	93.91	18.7	93
4	3.1	100	10g	98.12	9.81	98
4	6.5	100	15g	99.57	6.63	99
8	2.4	100	5g	95.55	19.1	95
8	3.1	100	10g	97.14	9.71	97
8	6.5	100	15g	99.62	6.64	99

### 3.2.4 Kinetic models of fixed bed column adsorption

The experimental data attained from the continuous adsorption system were fitted to the most commonly used kinetic models for adsorption in a fixed bed. Models were used to predict the dynamic behavior of the adsorbent-adsorbate system in this study, in addition, is to calculate the column kinetic constants and evaluate the fixed-bed columns' adsorption capacity. Authors have used different models for Cu<sup>2+</sup> and Cd<sup>2+</sup> adsorption onto different adsorbents. In order to describe the fixed bed column performance and to scale it up for industrial applications, three models were implied. (Bohart and Adams, 1920), (Yoon and Nelson, 1984) and (Thomas 1940) models were used to analyse the behaviour of adsorbent–adsorbate adsorption in this research.

#### 3.2.4.1 Adams –Bohart model.

The Adams–Bohart adsorption model was applied to experimental data for the description of the initial part zone of the breakthrough curve. Plotting  $\ln C_0/C_{eff}$  against  $t$ , using linear regression analysis on all breakthrough curves have been plotted, the respective values of  $k_{AB}$  and  $N_0$  were calculated and presented in table 3.10, 3.11 and 3.12. This model assumed that the biosorption rate is proportional to the residual

capacity of the solids and the concentration of the sorbent substances (Calero et al. 2009). The Adam's–Bohart model is used for the description of the initial part of the breakthrough curve.

The Adams-Bohart is given in equation 3.10 as:

$$\ln \left[ \frac{C_0}{C_{eff}} \right] = k_{AB} C_0 t - \frac{K_{AB} N_0 Z}{U_0} \quad (3.10)$$

Where  $C_0$  = influent concentration ( $\text{mg L}^{-1}$ );  $C_{eff}$  = effluent concentration ( $\text{mg/L}$ );  $k_{AB}$  = adsorption rate coefficient ( $\text{L mg min}^{-1}$ );  $N_0$  = adsorption capacity coefficient ( $\text{mg L}^{-1}$ );  $Z$  = bed depth ( $\text{cm}$ );  $U_0$  = linear velocity ( $\text{cm min}^{-1}$ ); and  $t$  = time ( $\text{min}$ ). The amount of metal concentration adsorbed  $\text{mg/g}$  is calculated through the factor  $N_0$  (adsorption capacity coefficient in  $\text{mg L}^{-1}$ ). The kinetic constant value of  $k_{AB}$  and  $N_0$  are determined from the slope and intercept of  $\ln(C_0/C_{eff})$  versus  $t$ .

#### 3.2.4.1.1 Adams –Bohart model fitted for $\text{Cu}^{2+}$ adsorbed by Garé compost

Adams-Bohart model results indicated that there was a decline with  $K_{AB}$  which dropped from 0.000235 to 0.000032  $\text{L min}^{-1} \text{mg}^{-1}$  when the initial concentration improved as given in table 3.10. The adsorption rate coefficient  $k_{AB}$  is an indication of the volume of influent treated by the unit amount of adsorbent at a unit time. The adsorption capacity coefficient ( $N_0$ ) increases with the increase of the influent concentration from 45.5 to 351  $\text{mg L}^{-1}$ , a similar trend observed by (Bulgariu and Bulgariu, 2013). These results are accounted for on the basis that the greater availability of solute molecules on an adsorbent surface will affect higher uptake of  $\text{Cu}^{2+}$  molecules by a unit mass of adsorbent. When the concentration is increasing, more solute molecules form greater concentration gradients, which ultimately reduce the adsorption rate coefficient. When the flow rate increased from 4 to 8  $\text{mL min}^{-1}$  the adsorption rate coefficient increased and  $N_0$  decreased, this is in agreement with (Cheraghi et al. 2016), the decrease in adsorption capacity is because of the lower residence time of solute in the column. Both  $k_{AB}$  and  $N_0$  did not show any precise tendency with the changes of bed heights. Fig 3.42 to 3.45 are Adams - Bohart linear illustration for  $\text{Cu}^{2+}$  treated by Garé compost in deferent conditions.

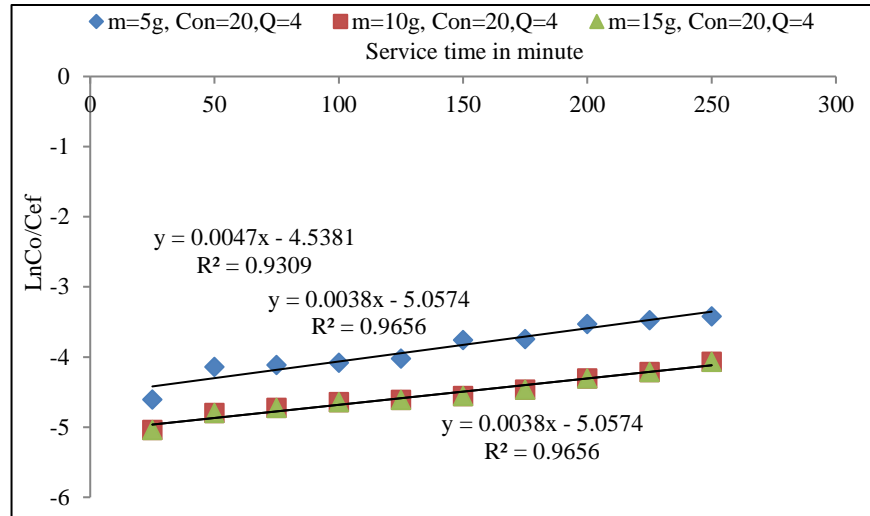


Fig. 3.42 Adams–Bohart plot (Garé compost,  $\text{Cu}^{2+}$  treated) concentration  $20 \text{ mg L}^{-1}$  and  $4 \text{ mL min}^{-1}$  flow rate and different bed heights

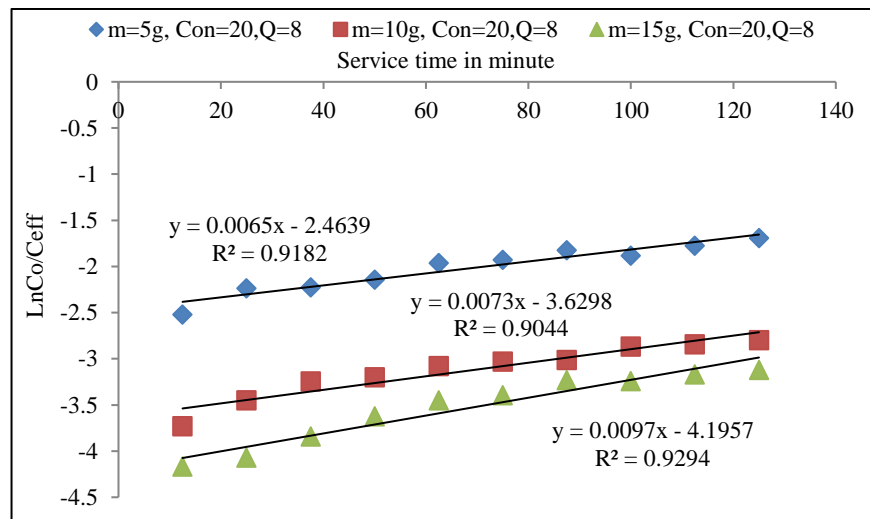


Fig. 3.43 Adams–Bohart plot (Garé compost,  $\text{Cu}^{2+}$  treated) concentration  $20 \text{ mg L}^{-1}$  and  $8 \text{ mL min}^{-1}$  flow rate and different bed heights

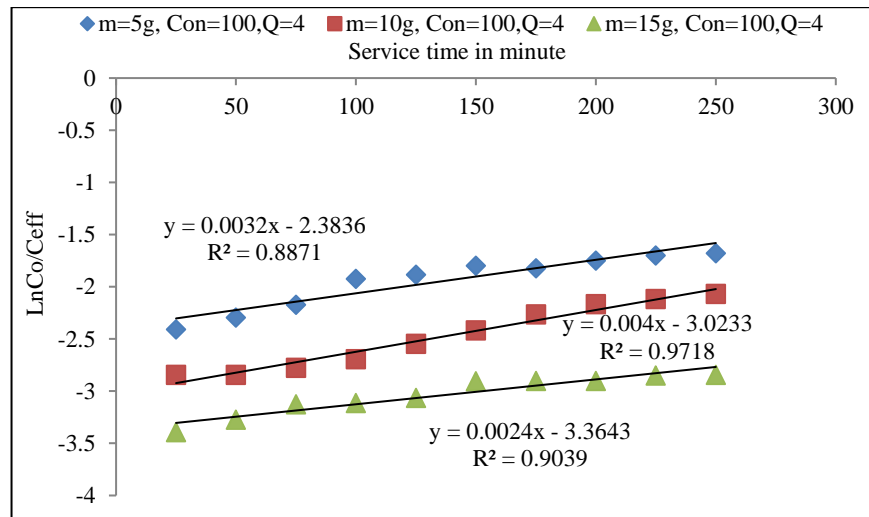


Fig. 3.44 Adams-Bohart plot (Garé compost,  $\text{Cu}^{2+}$  treated) concentration  $100 \text{ mg L}^{-1}$  and  $4 \text{ mL min}^{-1}$  flow rate and different bed heights

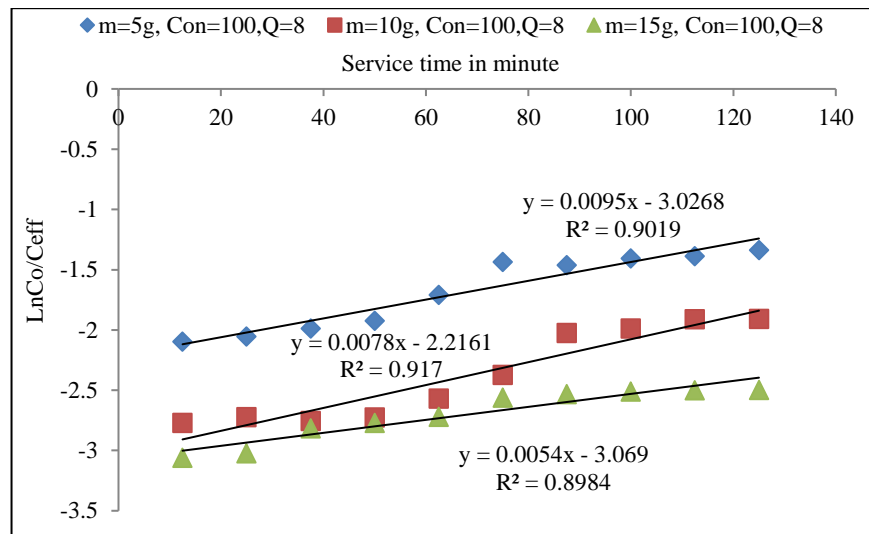


Fig. 3.45 Adams-Bohart plot (Garé compost,  $\text{Cu}^{2+}$  treated) concentration  $100 \text{ mg L}^{-1}$  and  $4 \text{ mL min}^{-1}$  flow rate and different bed heights

Table 3.10. Parameters predicted by Adam-Bohart model (Garé compost, Cu<sup>2+</sup> treated)

Column Parameters				Bohart Parameters		
C <sub>0</sub> / mg L <sup>-1</sup>	Weight / g	Bed heights / cm	Q / mL min <sup>-1</sup>	K <sub>AB</sub> / L min <sup>-1</sup> mg <sup>-1</sup>	N <sup>0</sup> / mg L <sup>-1</sup>	R <sup>2</sup>
20	5	2.4	4	0.000235	45.5	0.93
20	10	3.1	4	0.00019	48.5	0.96
20	15	6.5	4	0.00019	23.1	0.96
20	5	2.4	8	0.000325	17.8	0.91
20	10	3.1	8	0.000365	18.1	0.9
20	15	6.5	8	0.000485	7.53	0.92
100	5	2.4	4	0.000032	351	0.88
100	10	3.1	4	0.00004	275	0.97
100	15	6.5	4	0.000024	244	0.9
100	5	2.4	8	0.000078	134	0.91
100	10	3.1	8	0.000095	116	0.9
100	15	6.5	8	0.000054	98.9	0.89

### 3.2.4.1.2 Bohart model fitted for Cu<sup>2+</sup> adsorbed by Felgyő compost

The adsorption rate coefficient illustrated in table 3.11 ( $K_{AB}$ ) decreases on increasing the influent concentration from 0.0003 to 0.000073 L min<sup>-1</sup> mg<sup>-1</sup>. The adsorption capacity coefficient ( $N_0$ ) increases while increasing the influent concentration from 64.51 to 377 mg L<sup>-1</sup>. When the concentration is increased, more solute molecules from greater concentration gradients, which ultimately reduce the adsorption rate coefficient. The adsorption rate coefficient  $K_{AB}$  is an indication of the volume of influent treated by a unit amount of adsorbent at a unit time. When the flow rate increased from 4 to 8 mg L<sup>-1</sup> the adsorption rate coefficient decrease, the decrease in adsorption capacity is because of the lower residence time of solute in the column. As the bed height increased the adsorption capacity decrease along with adsorption rate coefficient ( $K_{AB}$ ), a similar tendency was observed for all parameters by (Cheraghi et al. 2016). Adams–Bohart model was able to describe the column initial part of the breakthrough curve and fit the experimental data with the regression coefficient of 0.90 to 0.98 as shown in Fig 3.46 to 3.49. Therefore, such fit of the experimental data on Bohart model ( $R^2$  range from 0.82 to 0.95) validates the simplistic modeling approach and suggests that the overall system kinetics can be controlled by external mass transfer in the initial zone of adsorption in the fixed-bed column (Chen et al. 2012).

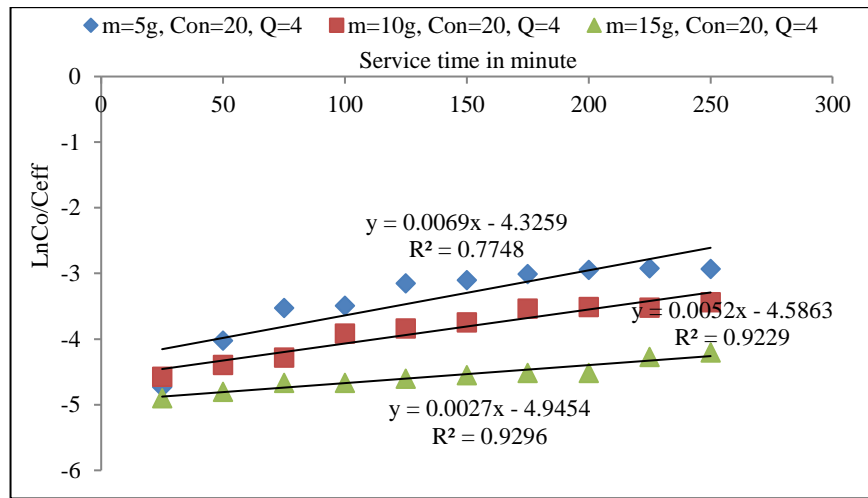


Fig. 3.46 Adams-Bohart plot of Felgyő compost,  $\text{Cu}^{2+}$  concentration  $20 \text{ mg L}^{-1}$  and  $4 \text{ mL min}^{-1}$  flow rate and different bed heights

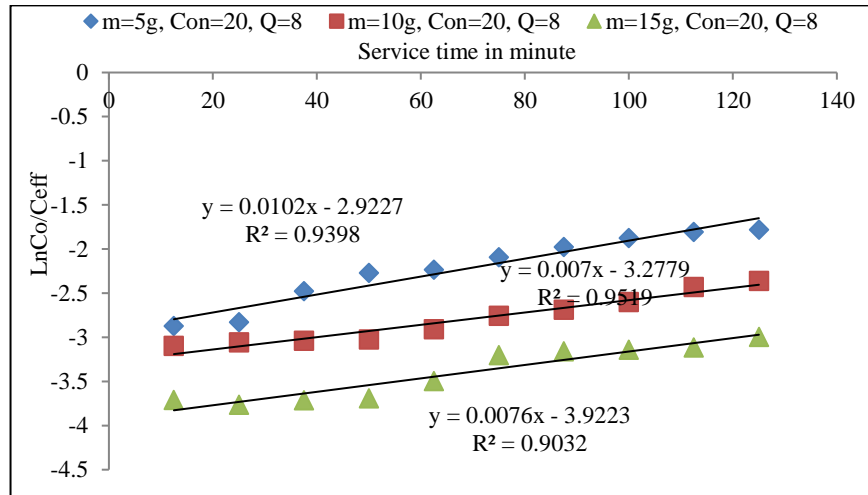


Fig. 3.47 Adams-Bohart plot of Felgyő compost,  $\text{Cu}^{2+}$  concentration  $20 \text{ mg L}^{-1}$  and  $8 \text{ mL min}^{-1}$  flow rate and different bed heights

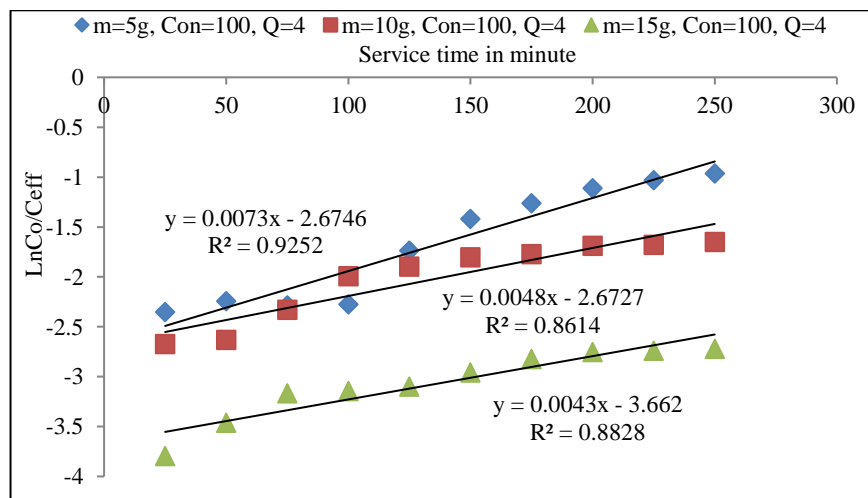


Fig. 3.48 Adams-Bohart plot of Felgyő compost,  $\text{Cu}^{2+}$  concentration  $100 \text{ mg L}^{-1}$  and  $4 \text{ mL min}^{-1}$  flow rate and different bed heights

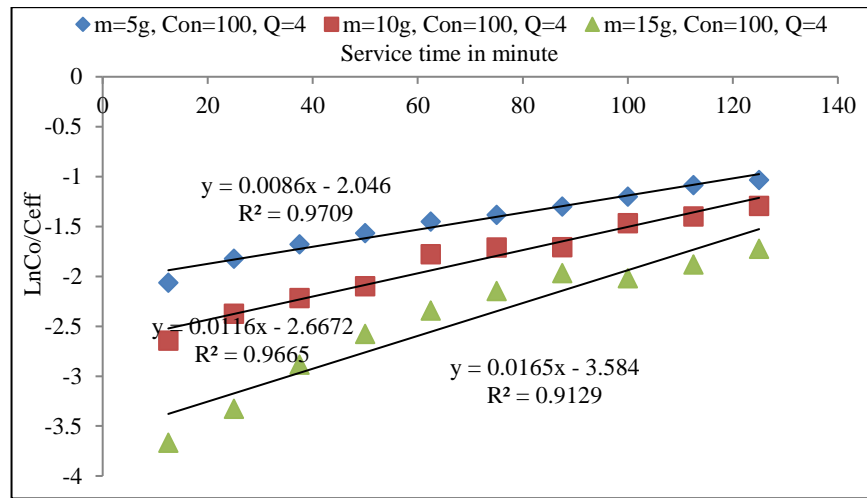


Fig. 3.49 Adams–Bohart plot of Felgyó compost,  $\text{Cu}^{2+}$  concentration  $100 \text{ mg L}^{-1}$  and  $4 \text{ mL min}^{-1}$  flow rate and different bed heights

Table 3.11. Bohart-Adams parameters for Felgyó compost,  $\text{Cu}^{2+}$  treated

Column Parameters				Bohart Parameters		
$C_0 / \text{mg L}^{-1}$	Weight / g	Bed heights / cm	$Q / \text{mL min}^{-1}$	$K_{AB} / \text{L min}^{-1} \text{mg}^{-1}$	$N_0 / \text{mg L}^{-1}$	$R^2$
20	5	1.1	4	0.000185	103.64	0.91
20	10	2	4	0.00026	49.92	0.92
20	15	3.1	4	0.000135	66.88	0.92
20	5	1.1	8	0.00051	29.48	0.93
20	10	2	8	0.000425	22.74	0.98
20	15	3.1	8	0.00038	18.84	0.9
100	5	1.1	4	0.000073	377.04	0.92
100	10	2	4	0.000044	335.66	0.92
100	15	3.1	4	0.000033	384.51	0.96
100	5	1.1	8	0.000086	244.82	0.97
100	10	2	8	0.000116	130.14	0.96
100	15	3.1	8	0.000165	79.31	0.91

### 3.2.4.1.3 Adams–Bohart model fitted for $\text{Cd}^{2+}$ adsorbed by Felgyó compost

The kinetic values of  $k_{AB}$  and  $N_0$  are determined from the slope and intercept of  $\ln(C_0/C_{eff})$  versus  $t$  as shown in Fig 3.50 to 3.53. The adsorption rate coefficient  $k_{AB}$  decreases on increasing the influent concentration from 0.000765 to 0.000222 as given in table 3.12. The adsorption capacity coefficient ( $N_0$ ) increases while increasing the influent concentration from 43.77 to 390.6  $\text{mg L}^{-1}$ . When the flow rate increased from 4 to 8  $\text{mL min}^{-1}$  the adsorption rate coefficient decreased, this also occurs with the decrease in adsorption capacity because of the lower residence time of solute in the

column. As the bed height increased the adsorption capacity decreased, along with the adsorption rate coefficient ( $k_{AB}$ ). A similar tendency was observed for all parameters by (Baral et al. 2009 ).

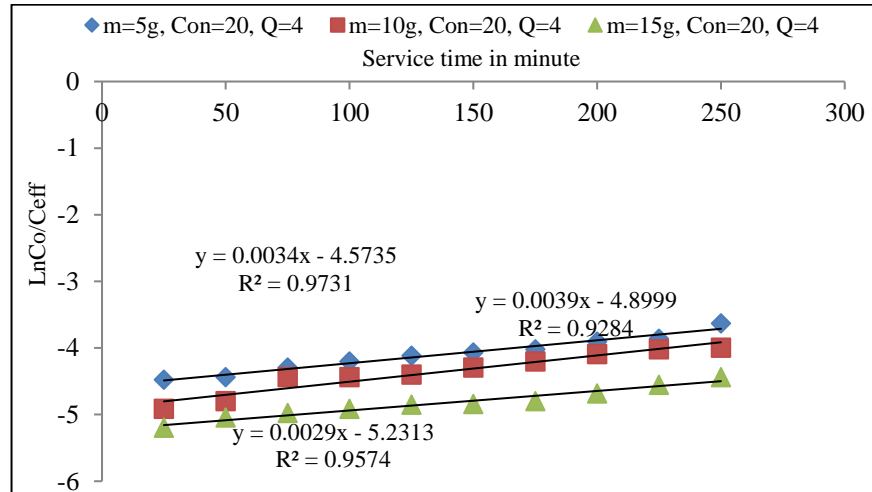


Fig. 3.50 Bohart–Adams plot of Felgyő compost,  $Cd^{2+}$  treated concentration  $20 \text{ mg L}^{-1}$  and  $4 \text{ mL min}^{-1}$  flow rate and different bed heights

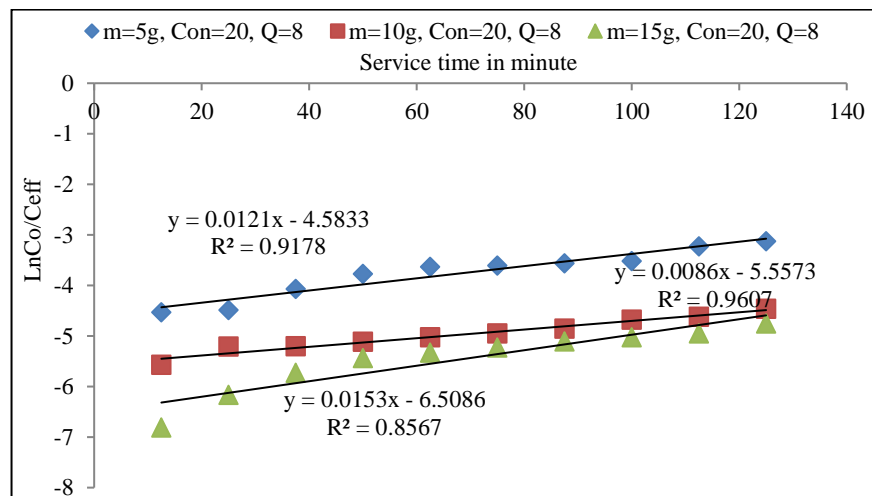


Fig. 3.51 Bohart–Adams plot of (Felgyő compost,  $Cd^{2+}$  treated) concentration  $20 \text{ mg L}^{-1}$  and  $8 \text{ mL min}^{-1}$  flow rate and different bed heights

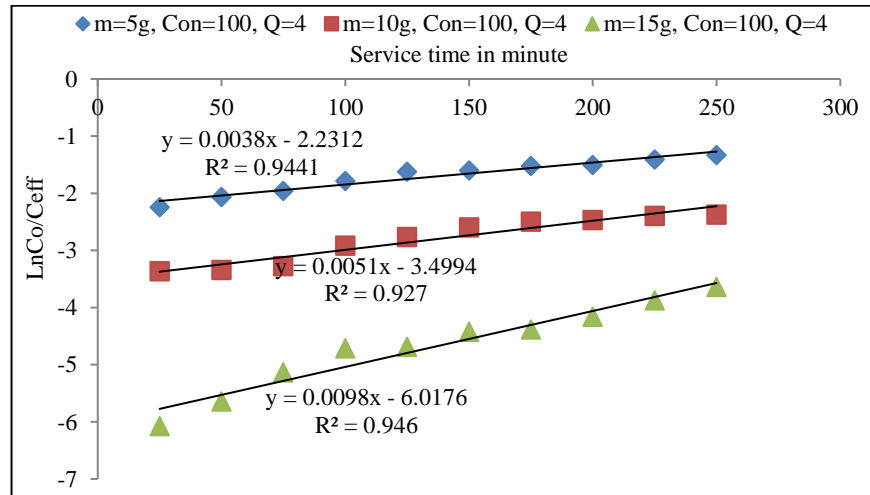


Fig. 3.52 Bohart–Adams plot of (Felgyő compost,  $\text{Cd}^{2+}$  treated) concentration  $20 \text{ mg L}^{-1}$  and  $4 \text{ mL min}^{-1}$  flow rate and different bed heights

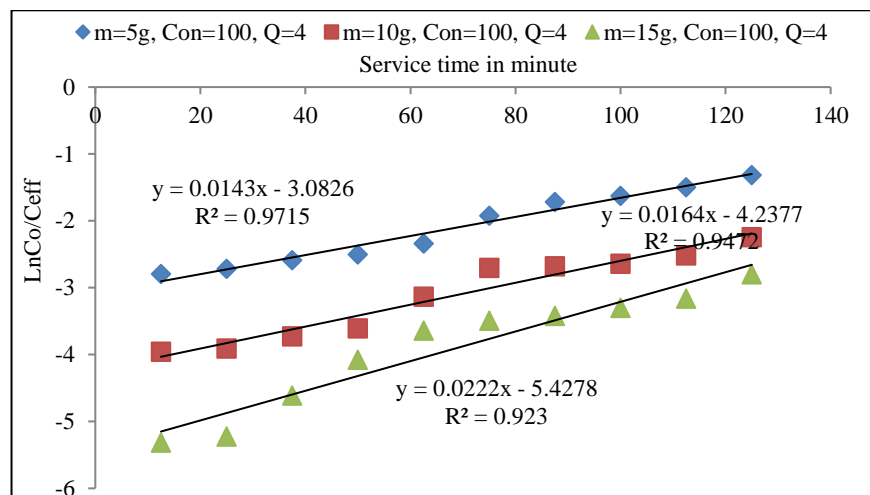


Fig. 3.53 Bohart–Adams plot of (Felgyő compost,  $\text{Cd}^{2+}$  treated) concentration  $20 \text{ mg L}^{-1}$  and  $4 \text{ mL min}^{-1}$  flow rate and different bed heights

Table 3.12. Parameters predicted by the Adam-Bohart model (Felgyő compost, Cd<sup>2+</sup> treated)

C <sub>0</sub> / mg L <sup>-1</sup>	Compost weight / g	Bed height / cm	Q / mL min <sup>-1</sup>	N <sub>0</sub> / mg g <sup>-1</sup>	K <sub>AB</sub> / L min <sup>-1</sup> mg	R <sup>2</sup>
20	5g	1.1	4	43.77	0.000765	0.97
20	10g	2	4	33.23	0.00019	0.92
20	15g	3.1	4	25.05	0.000255	0.95
20	5g	1.1	8	63.19	0.00049	0.91
20	10g	2	8	12.2	0.000715	0.96
20	15g	3.1	8	9.435	0.00082	0.85
100	5g	1.1	4	390.6	0.000222	0.94
100	10g	2	4	120.7	0.000051	0.92
100	15g	3.1	4	98.98	0.000098	0.94
100	5g	1.1	8	368.8	0.000143	0.97
100	10g	2	8	206.7	0.000164	0.94
100	15g	3.1	8	120.1	0.000222	0.92

### 3.2.4.2 Thomas model kinetics

Thomas model assumes plug flow behavior in the bed. This is most general and widely used to describe the performance theory of the sorption process in fixed-bed column (Sharma and Singh, 2013). This model was expressed through the second-order law of kinetic reaction without the presence of axial dispersion even when the bed depth was at the minimum and the breakthrough occurred immediately after the flow started (Apiratikul and Pavasant, 2008). The linearized form of this model can be described by the following expression:

$$\ln \left[ \frac{C_0}{C_{eff}} - 1 \right] = 1 + \frac{k_{th} q_0 m}{Q} - k_{th} q_0 t \quad (3.11)$$

Where  $C_0$  is the initial metal concentration (mg L<sup>-1</sup>),  $C_{eff}$  is effluent Cd<sup>2+</sup> concentration (mg L<sup>-1</sup>), at time  $t$ ,  $k_{th}$  is Thomas model constant, L min<sup>-1</sup>.mg.  $q_0$  is maximum Cu<sup>2+</sup> adsorption capacity (mg g<sup>-1</sup>),  $m$  is mass of the adsorbent (g) and  $Q$  is flow rate (ml/min). The kinetic coefficient  $k_{th}$  and the adsorption capacity of the column  $q_0$  can be determined from a plot of  $\ln \left[ \frac{C_0}{C_{eff}} - 1 \right]$  against  $t$  at a given flow rate using linear regression. A linear regression was then performed on each set to transform the data to determine the coefficient from the slope and the intercept. Inspection of the regressed

lines indicated that they were all acceptable fits with linear regression coefficients ranging from 0.90 to 0.99. Thomas model aims at calculating the adsorption rate constant of the solid phase concentration of the metals on the adsorbent from the continuous mode studies. All calculation was retrieved from Fig 3.54 to 3.65.

#### **3.2.4.2.1 Thomas model fitted for $\text{Cu}^{2+}$ adsorbed by Garé compost**

From the results of Thomas model, it is clear that the values of  $R^2$  range from 0.90 to 0.97 as shown in Fig 3.54 to 3.57. It can be observed from table 3.13, that the Thomas constant decreases with the increase of the initial  $\text{Cu}^{2+}$  concentration from 0.000185 to 0.000037  $\text{L mg}^{-1} \text{min}^{-1}$  at 20, 100  $\text{mg L}^{-1}$  respectively. In addition,  $q_0$  increased from 10.3 to 49.5  $\text{mg g}^{-1}$  at 20, 100  $\text{mg L}^{-1}$  correspondingly. The appearance of such results is due to the driving force for adsorption concentration differences between the solute on the adsorbent and the solute in the solution. In consequence, this high driving force is a result of the higher  $\text{Cu}^{2+}$  concentration, which in turn, resulted in better column performance. This behaviour can be attributed to the increases in concentration that leads to an increase in driving force for adsorption and will increase it. It can be observed that with the increases in flow rate, the maximum adsorption capacity is decreased and the coefficient  $K_{th}$  will also increase. This is because the residence time for the solute in the bed is less, a similar trend was observed by (Sarma et al. 2008). Overall the value of  $q_0$  decreased with an increase in bed height and corresponding  $K_{th}$  values increased in general. This is because, at higher bed heights, more reactive sites were available and driving force for adsorption increased.

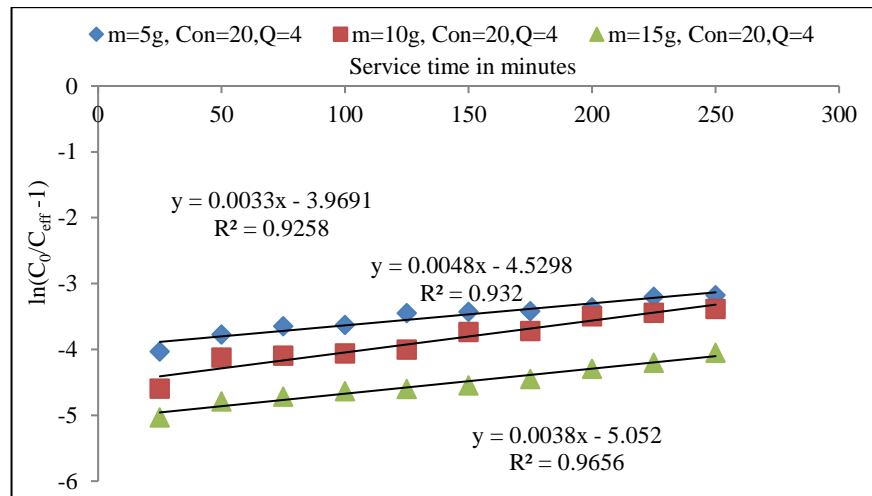


Fig. 3.54 Thomas plot (Garé compost,  $\text{Cu}^{2+}$  treated) concentration  $20 \text{ mg L}^{-1}$  and  $4 \text{ mL min}^{-1}$  flow rate and different bed heights

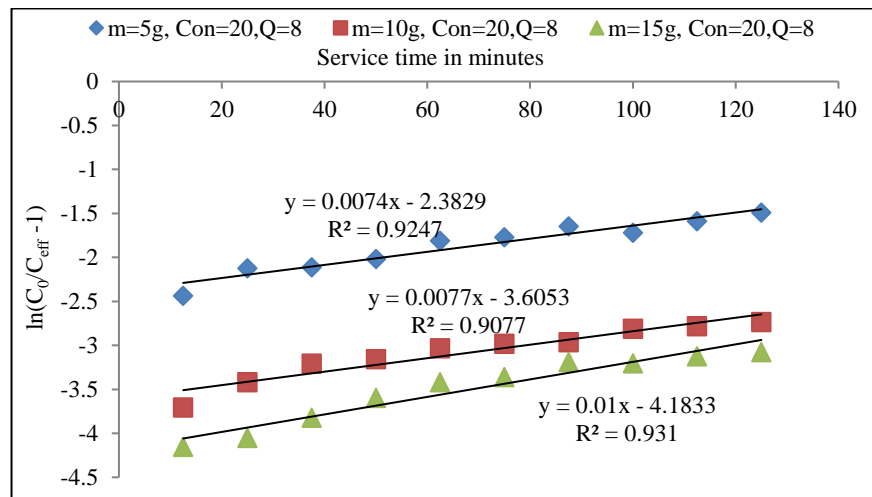


Fig. 3.55 Thomas plot (Garé compost,  $\text{Cu}^{2+}$  treated) concentration  $20 \text{ mg L}^{-1}$  and  $8 \text{ mL min}^{-1}$  flow rate and different bed heights

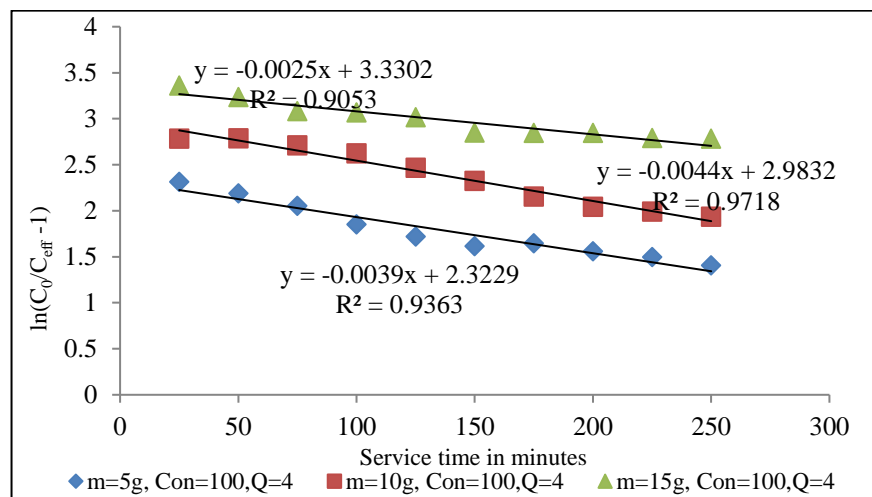


Fig. 3.56 Thomas plot (Garé compost,  $\text{Cu}^{2+}$  treated) concentration  $100 \text{ mg L}^{-1}$  and  $4 \text{ mL min}^{-1}$  flow rate and different bed heights

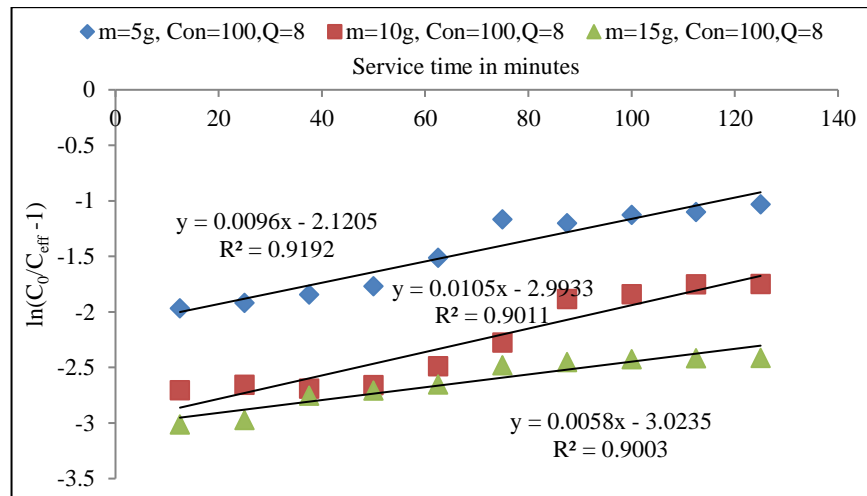


Fig. 3.57 Thomas plot (Garé compost, Cu<sup>2+</sup> treated) concentration 100 mg L<sup>-1</sup> and 4 mL min<sup>-1</sup> flow rate and different bed heights

Table 3.13. Parameters predicted by Thomas model (Garé compost, Cu<sup>2+</sup> treated)

Column Parameters				Thomas Parameters		
C <sub>0</sub> / mg L <sup>-1</sup>	Compost weight / g	Bed height / cm	Q / mL min <sup>-1</sup>	q <sub>0</sub> / mg g <sup>-1</sup>	K <sub>th</sub> / mL min <sup>-1</sup> .mg	R <sup>2</sup>
20	5	2.4	4	10.3	0.0002	0.92
20	10	3.1	4	7.59	0.0002	0.9
20	15	6.5	4	4.46	0.00025	0.93
20	5	2.4	8	10.3	0.00037	0.92
20	10	3.1	8	7.49	0.000385	0.9
20	15	6.5	8	4.46	0.0005	0.93
100	5	2.4	4	49.5	0.000037	0.93
100	10	3.1	4	27.1	0.000044	0.97
100	15	6.5	4	35.5	0.000025	0.95
100	5	2.4	8	35.3	0.000096	0.91
100	10	3.1	8	22.8	0.000105	0.9
100	15	6.5	8	27.8	0.000058	0.9

### 3.2.4.2.2 Thomas model fitted for Cu<sup>2+</sup> adsorbed by Felgyó compost

The Thomas constant decrease on increasing the initial Cu<sup>2+</sup> concentration from 0.00019 to 0.000093 L mg<sup>-1</sup> min<sup>-1</sup> at 20, 100 mg L<sup>-1</sup> respectively, in addition, q<sub>0</sub> increased from 15.6 to 23.89 mg g<sup>-1</sup> at 20, 100 mg L<sup>-1</sup> respectively, These results are illustrated in table 3.16 and also further noticed by (Aziz et al. 2014). It can be observed that with the increase in flow rate, the maximum adsorption capacity decreased and coefficient (K<sub>th</sub>) increased. This is because the residence time of solute in the bed was less. The value of q<sub>0</sub> increase with an increase in bed height and corresponding K<sub>th</sub> values decreased in

general, this is in agreement with (Uddin et al. 2009). At higher bed heights, more reactive sites were available and driving force for adsorption increased. The regression coefficients analyses reported in table 3.14 show that  $R^2$  ranging from 0.91 to 0.99. This well-fitting as shown in figure 3.58 to 3.61 of the empirical data on Thomas model showed that internal and external diffusions were not the rate-limiting steps (Rao et al. 2011).

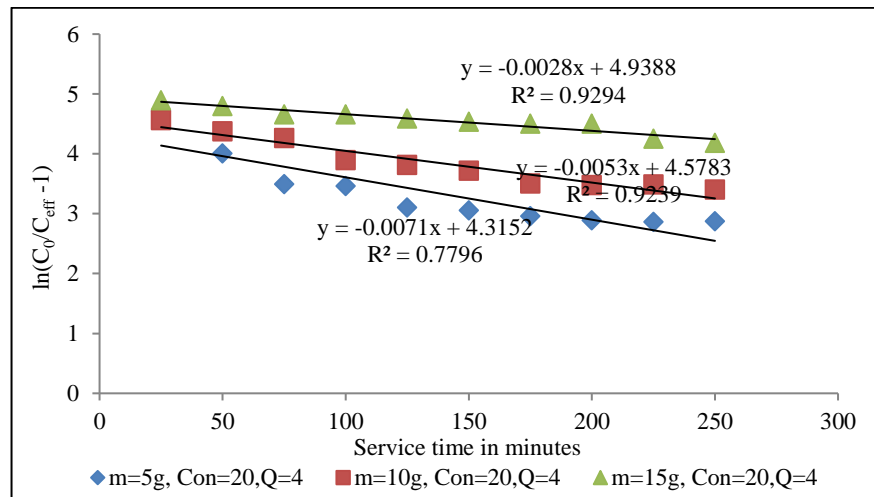


Fig. 3.58 Thomas plot of Felgyő compost,  $\text{Cu}^{2+}$  concentration 20 mg L<sup>-1</sup> and 4 mL min<sup>-1</sup> flow rate and different bed heights

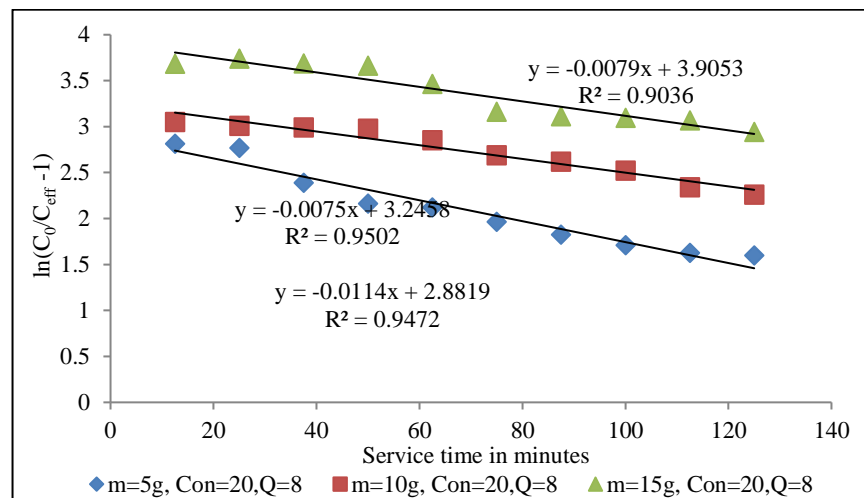


Fig. 3.59 Thomas plot of Felgyő compost,  $\text{Cu}^{2+}$  concentration 20 mg L<sup>-1</sup> and 8 mL min<sup>-1</sup> flow rate and different bed heights

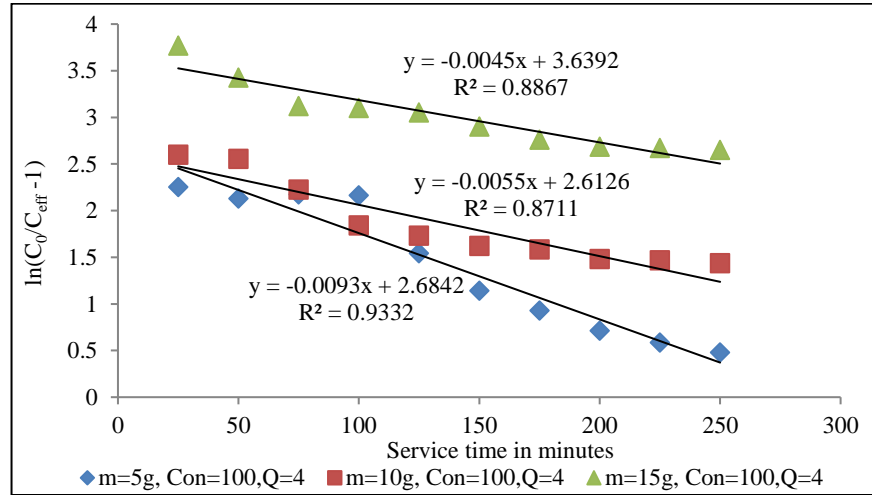


Fig. 3.60 Thomas plot of Felgyő compost,  $Cu^{2+}$  concentration  $100 \text{ mg L}^{-1}$  and  $4 \text{ mL min}^{-1}$  flow rate and different bed heights

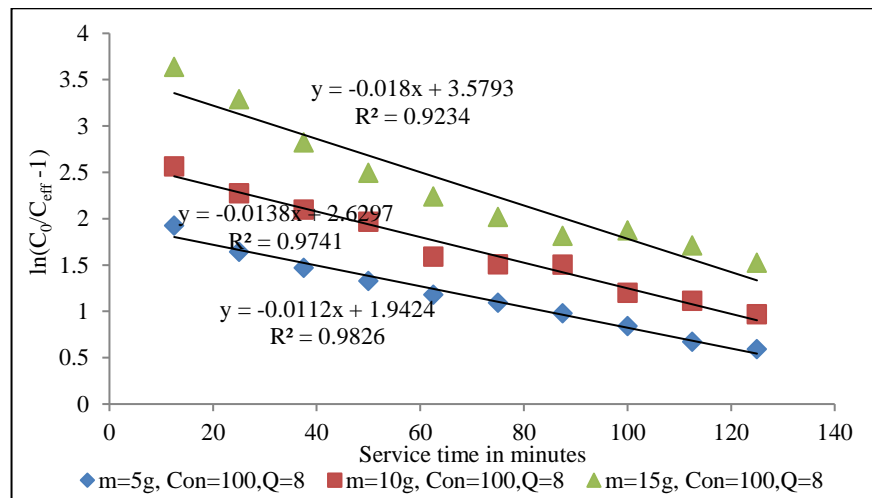


Fig. 3.61 Thomas plot of Felgyő compost,  $Cu^{2+}$  concentration  $100 \text{ mg L}^{-1}$  and  $4 \text{ mL min}^{-1}$  flow rate and different bed heights

Table 3.14. Parameters predicted by Thomas model (Felgyő compost loaded with  $\text{Cu}^{2+}$ )

Column Parameters				Thomas Parameters		
$C_0 / \text{mg L}^{-1}$	Weight / g	Bed heights / cm	$Q / \text{mL min}^{-1}$	$q_0 / \text{mg g}^{-1}$	$K_{th} / \text{L mg}^{-1} \text{min}^{-1}$	$R^2$
20	5	2.4	4	15.6	0.00019	0.91
20	10	3.1	4	6.91	0.000265	0.92
20	15	6.5	4	9.47	0.00014	0.92
20	5	2.4	8	8.08	0.00057	0.94
20	10	3.1	8	6.02	0.00045	0.99
20	15	6.5	8	5.27	0.000395	0.91
100	5	2.4	4	23.89	0.000093	0.93
100	10	3.1	4	20.37	0.00005	0.93
100	15	6.5	4	26.25	0.000035	0.96
100	5	2.4	8	27.74	0.000112	0.98
100	10	3.1	8	15.24	0.000138	0.97
100	15	6.5	8	10.65	0.00018	0.92

### 3.2.4.2.3 Thomas model fitted for $\text{Cd}^{2+}$ adsorbed by Felgyő compost

The values of  $K_{th}$  and  $q_0$  were influenced by both flow rate and influent concentration of  $\text{Cd}^{2+}$ . It can be observed from table 3.15, that the Thomas constant decrease on increasing the initial  $\text{Cd}^{2+}$  concentration from 0.000175 to 0.000047 at 20, 100  $\text{mg L}^{-1}$  respectively. In addition,  $q_0$  increased from 20.8 to 36.3  $\text{mg g}^{-1}$  at 20, 100  $\text{mg L}^{-1}$  respectively, it was observed also by (Bulgariu and Bulgariu, 2013). It can be deduced that with the increase in flow rate, the maximum adsorption capacity decreased and coefficient  $K_{th}$  increased. This is because the residence time of solute in the bed was less. The value of  $q_0$  increase with the increase of bed height, and corresponding  $K_{th}$  values which obtained from figure 3.62 to 3.65 decreased in general, Similar results have also been established by (Vijayaraghavan et al. 2006). This is because, at higher bed heights, more reactive sites were available and driving force for adsorption increased. From the results of Thomas model, it was seen that the values of  $R^2$  range from 0.91 to 0.97 which validates the fitting of the model for this study.

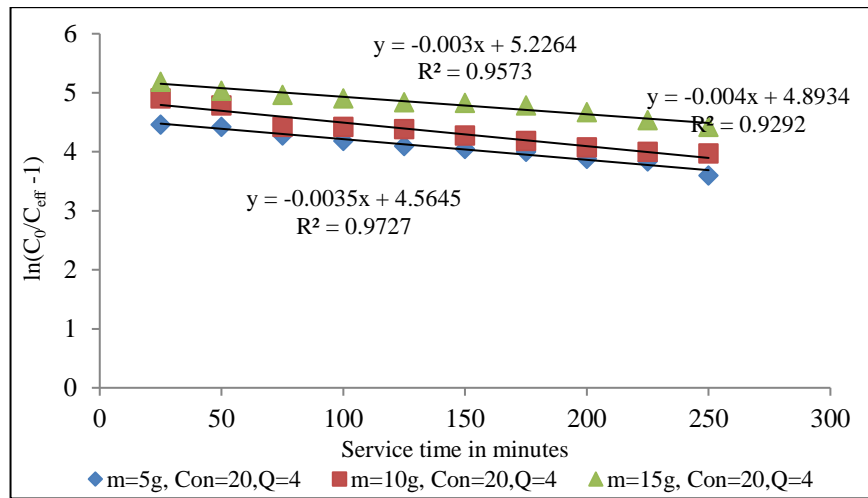


Fig. 3.62 Thomas plot of (Felgyő compost, Cd<sup>2+</sup> treated) concentration 20 mg L<sup>-1</sup> and 4 mL min<sup>-1</sup> flow rate and different bed heights

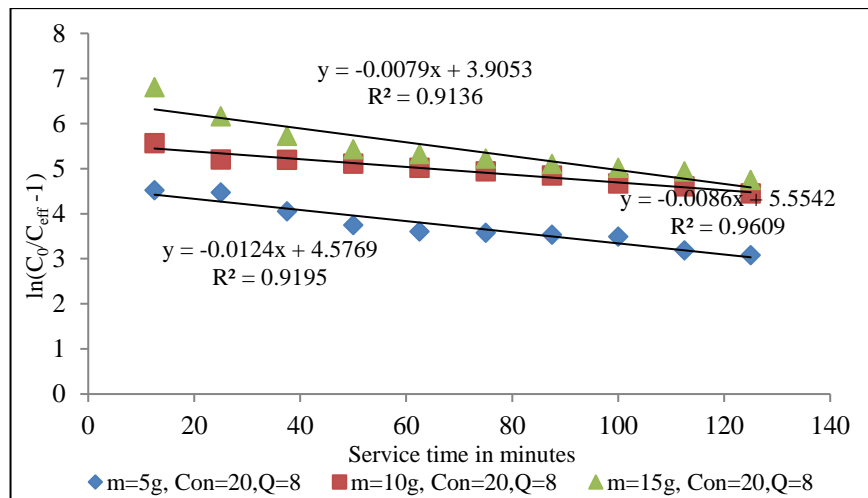


Fig. 3.63 Thomas plot of (Felgyő compost, Cd<sup>2+</sup> treated) concentration 20 mg L<sup>-1</sup> and 4 mL min<sup>-1</sup> flow rate and different bed heights

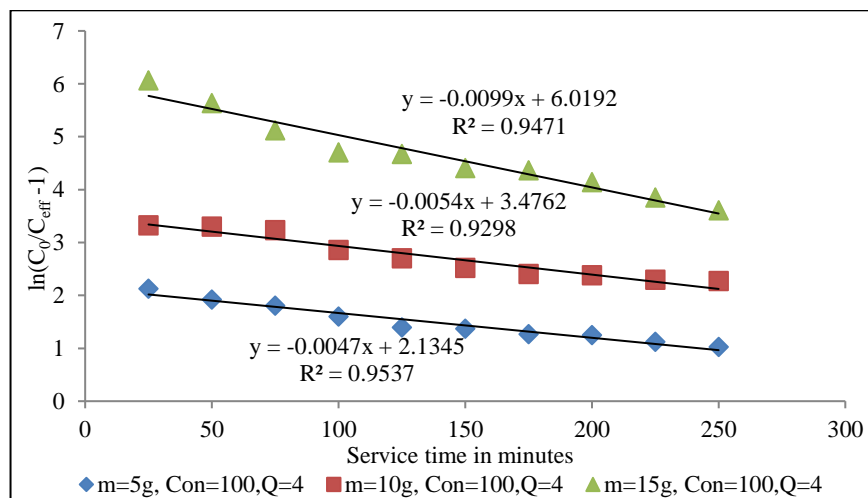


Fig. 3.64 Thomas plot of (Felgyő compost, Cd<sup>2+</sup> treated) concentration 20mg/l and 4 mL min<sup>-1</sup> flow rate and different bed heights

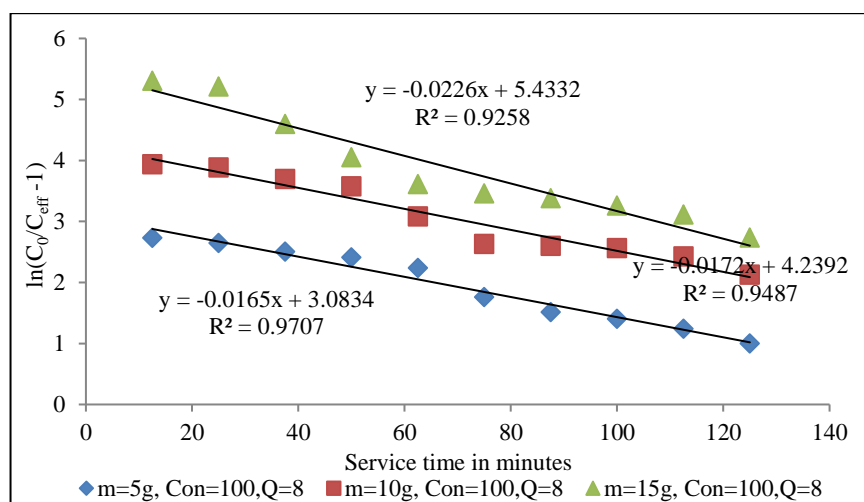


Fig. 3.65 Thomas plot of (Felgyó compost,  $\text{Cd}^{2+}$  treated) concentration  $20 \text{ mg L}^{-1}$  and  $4 \text{ mL min}^{-1}$  flow rate and different bed heights

Table 3.15. Parameters predicted by Thomas model (Felgyó compost,  $\text{Cd}^{2+}$  treated)

$C_0 / \text{mg L}^{-1}$	Compost weight / g	Bed height / cm	Flow rate / $\text{mL min}^{-1}$	$q_0 / \text{mg g}^{-1}$	$K_{th} / \text{mL min}^{-1} \cdot \text{mg}$	$R^2$
20	5g	1.1	4	20.8	0.000175	0.97
20	10g	2	4	9.78	0.0002	0.92
20	15g	3.1	4	9.29	0.00015	0.95
20	5g	1.1	8	11.8	0.00062	0.91
20	10g	2	8	10.3	0.00043	0.96
20	15g	3.1	8	5.27	0.000395	0.91
100	5g	1.1	4	36.3	0.000047	0.95
100	10g	2	4	25.7	0.000054	0.92
100	15g	3.1	4	16.2	0.000099	0.94
100	5g	1.1	8	29.8	0.000165	0.97
100	10g	2	8	19.7	0.000172	0.94
100	15g	3.1	8	12.8	0.000226	0.92

### 3.2.4.3 Yoon–Nelson kinetic model

The Yoon–Nelson model is based on the assumption that the rate of adsorption is decreasing in the probability of adsorption, of adsorbate molecules, and is proportional to the probability of the adsorbate adsorption and the adsorbate breakthrough on the adsorbent (Han et al. 2008). The values of  $(k_{YN})$  and  $\tau$  are determined from the slope and intercept of  $\ln(C_0/(C_0-C_{eff}))$  versus  $t$  and the results are given in Table 3.16, 3.17 and 3.18 for  $\text{Cu}^{2+}$  treated by Felgyó,  $\text{Cu}^{2+}$  treated by Garé and  $\text{Cd}^{2+}$  treated by Felgyó respectively. while figures 3.66 to 3.77 are depicted for Yoon models for  $\text{Cu}^{2+}$  treated by

Felgyő,  $\text{Cu}^{2+}$  treated by Garé and  $\text{Cd}^{2+}$  treated by Felgyő respectively. The Yoon Nelson model is given in equation 4.8.

$$\ln \left[ \frac{C_0}{C_0 - C_{eff}} \right] k_{YN} t - \tau k_{YN} \quad (3.12)$$

### 3.2.4.3.1 Yoon–Nelson model fitted for $\text{Cu}^{2+}$ adsorbed by Garé compost

Figures from 3.66 to 3.69 are illustration for Yoon–Nelson plot, from the calculation we could see the time required for 50% adsorbent breakthrough ( $\tau$ ), decreases from 285, 250, 333 to 212, 185, 101 min on increasing the initial metal concentration from 20 to 100 mg/L when the bed height set at 2.4, 3.1 and 6.5 cm respectively. In addition, it decreases from 303, 208, 263 to 135, 129, 100 min on the increasing flow rate from 4 to 8 mL/min, which can be attributed to the rapid saturation of bed with higher flow rates along, this is in a good agreement with the results obtained by (Acheampong et al. 2013). The increases in  $k_{YN}$  is in parallel with the increase of concentration and flow rate, however, there is no specific trend with increasing of bed heights. Furthermore,  $k_{YN}$  is in general, is increasing with the increases of bed height as depicted in table 3.16.

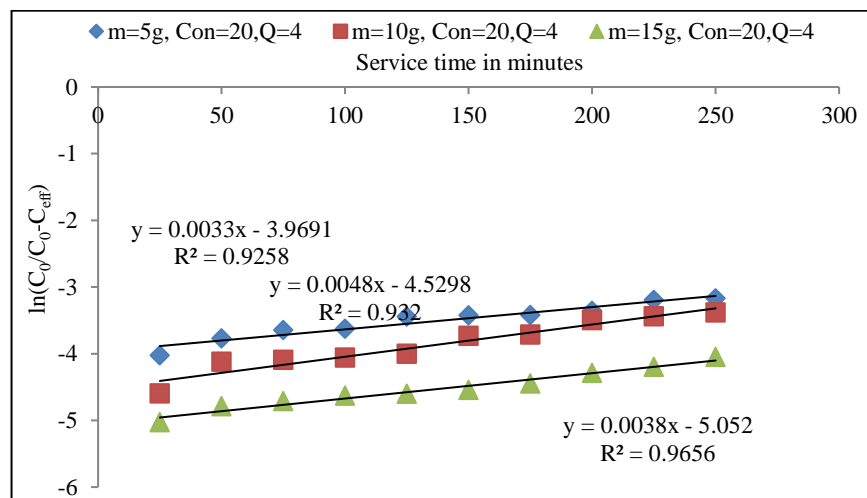


Fig. 3.66 Yoon–Nelson plot (Garé compost,  $\text{Cu}^{2+}$  treated) concentration  $20 \text{ mg L}^{-1}$  and  $4 \text{ mL min}^{-1}$  flow rate and different bed heights

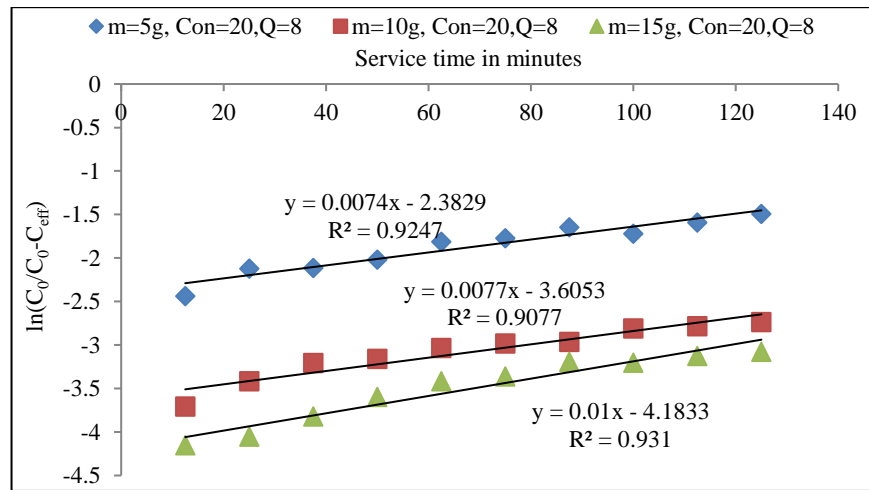


Fig. 3.67 Yoon–Nelson plot (Garé compost,  $\text{Cu}^{2+}$  treated) concentration  $20 \text{ mg L}^{-1}$  and  $8 \text{ mL min}^{-1}$  flow rate and different bed heights

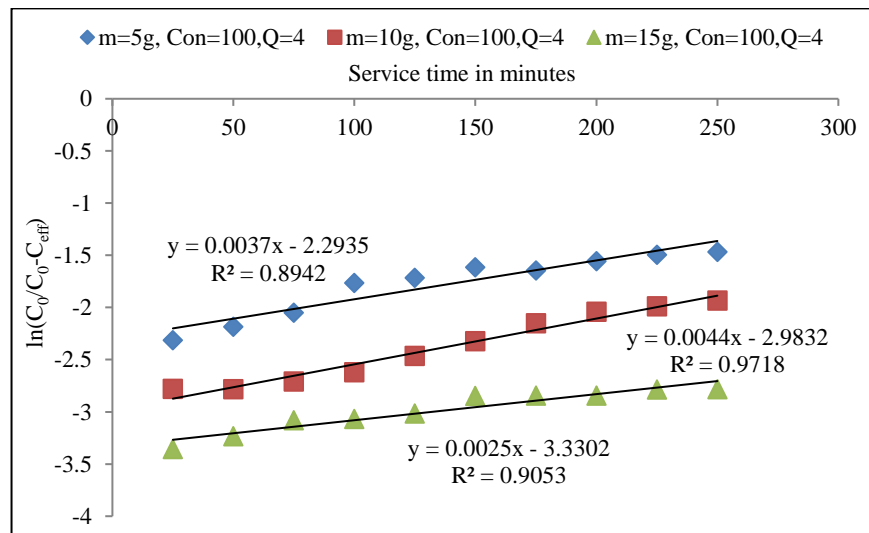


Fig. 3.68 Yoon–Nelson plot (Garé compost,  $\text{Cu}^{2+}$  treated) concentration  $100 \text{ mg L}^{-1}$  and  $4 \text{ mL min}^{-1}$  flow rate and different bed heights

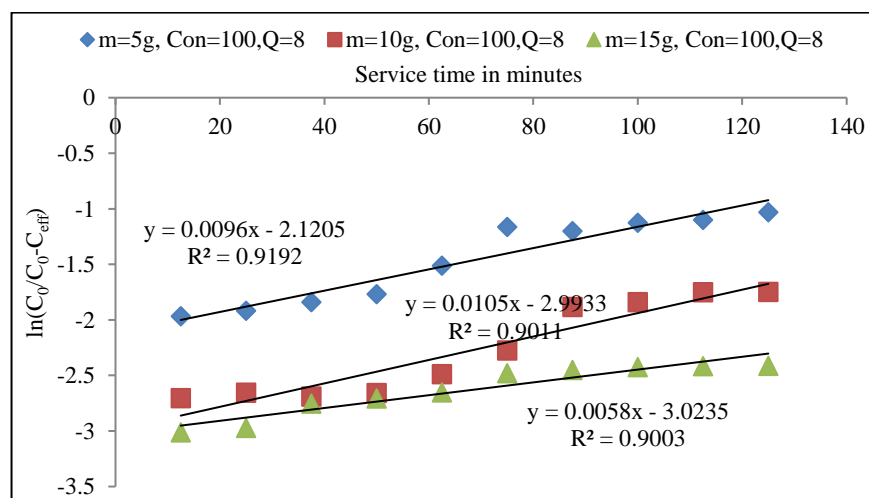


Fig. 3.69 Yoon–Nelson plot (Garé compost,  $\text{Cu}^{2+}$  treated) concentration  $100 \text{ mg L}^{-1}$  and  $4 \text{ mL min}^{-1}$  flow rate and different bed heights

Table 3.16. Parameters predicted by Yoon–Nelson model (Garé compost, Cu<sup>2+</sup> treated)

Column Parameters				Nelson Parameters		
C <sub>0</sub> / mg L <sup>-1</sup>	Weight / g	Bed heights / cm	Q / mL min <sup>-1</sup>	K <sub>YN</sub> / min <sup>-1</sup>	τ / min	R <sup>2</sup>
20	5	2.4	4	0.0033	303	0.92
20	10	3.1	4	0.0048	208	0.93
20	15	6.5	4	0.0038	263	0.96
20	5	2.4	8	0.0074	135	0.92
20	10	3.1	8	0.0077	129	0.9
20	15	6.5	8	0.01	100	0.93
100	5	2.4	4	0.0037	270	0.89
100	10	3.1	4	0.0044	400	0.97
100	15	6.5	4	0.0025	104	0.9
100	5	2.4	8	0.0096	95	0.91
100	10	3.1	8	0.0105	227	0.9
100	15	6.5	8	0.0058	174	0.9

### 3.2.4.3.2 Yoon–Nelson model fitted for Cu<sup>2+</sup> adsorbed by Felgyó compost

The time required for 50% adsorbent breakthrough ( $\tau$ ) decreases from 131, 144, 357 to 119, 75, 89 min on increasing the initial metal concentration from 20 to 100 mg L<sup>-1</sup> when the bed height set at 1, 1.2, and 3.1 cm respectively. In addition, it decreases from 119, 75, 89 to 34, 69, 31 min on increasing flow rate from 4 to 8 mg L<sup>-1</sup>, which can be attributed to the rapid saturation of bed in higher flow rates along with higher flow rate. The increase of  $K_{YN}$  in parallel with the increase in concentration and flow rate, the same trend was noticed by Aksu and Gönen (2004), while it did not show any specific trend with increasing of bed heights. Furthermore,  $K_{YN}$  is in general increased with the increase of bed height as depicted in table 3.17. The plots of Yoon-Nelson are shown in Fig 3.70 to 3.73 and all calculations are attained from these figures.

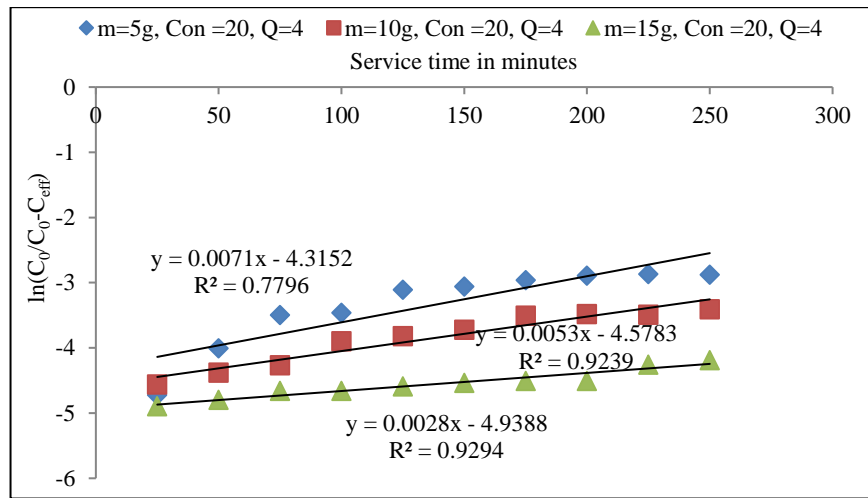


Fig. 3.70 Yoon–Nelson plot (Felgyő compost,  $Cu^{2+}$  treated)  $Cu^{2+}$  concentration  $20 \text{ mg L}^{-1}$  and  $4 \text{ mL min}^{-1}$  flow rate and different bed heights

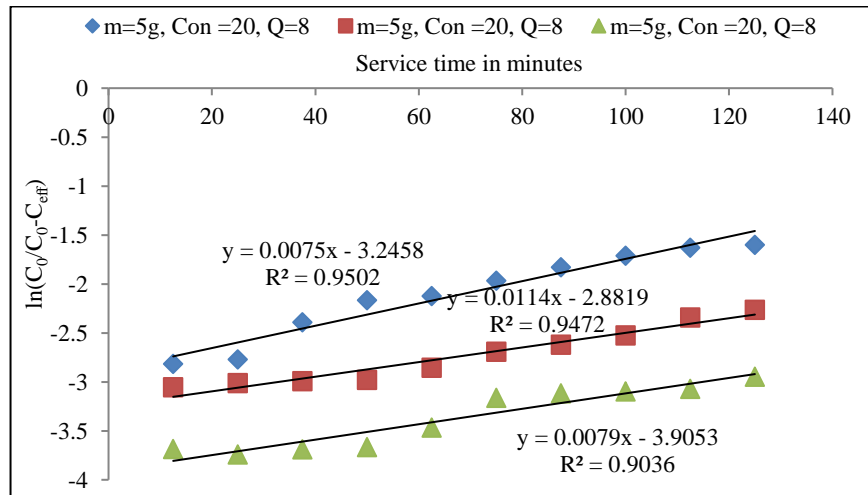


Fig. 3.71 Yoon–Nelson plot (Felgyő compost,  $Cu^{2+}$  treated)  $Cu^{2+}$  concentration  $20 \text{ mg L}^{-1}$  and  $8 \text{ mL min}^{-1}$  flow rate and different bed heights

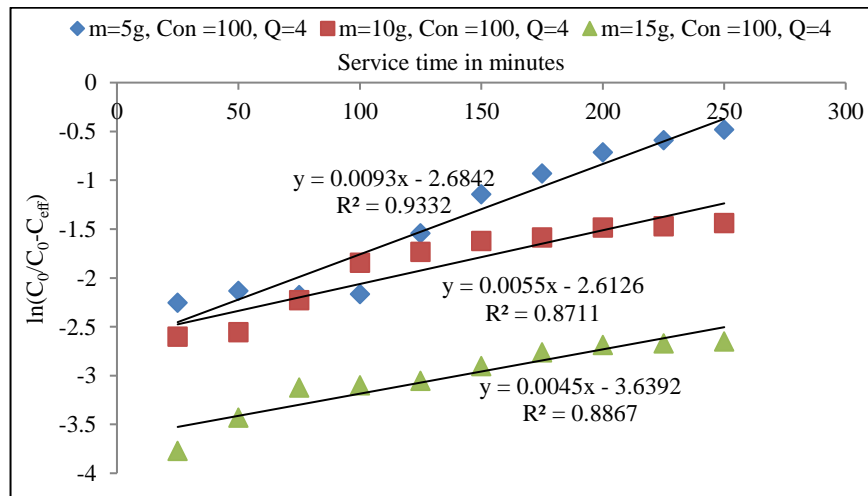


Fig. 3.72 Yoon–Nelson plot (Felgyő compost,  $Cu^{2+}$  treated)  $Cu^{2+}$  concentration  $100 \text{ mg L}^{-1}$  and  $4 \text{ mL min}^{-1}$  flow rate and different bed heights

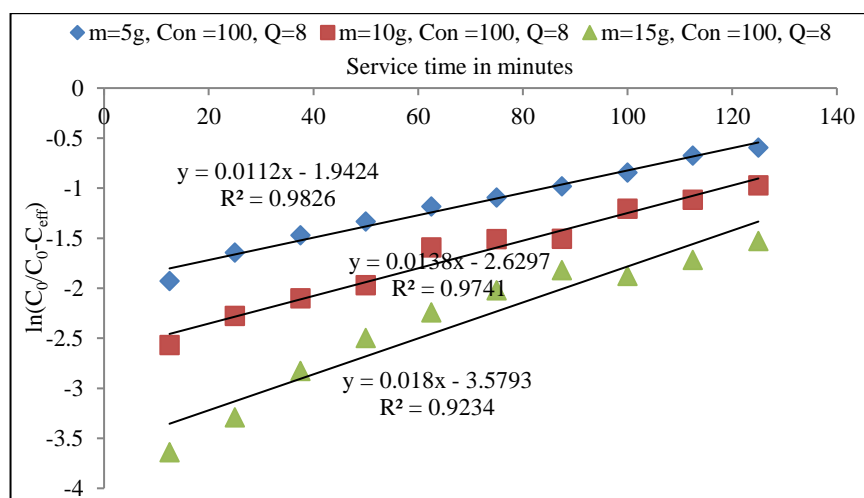


Fig. 3.73 Yoon–Nelson plot (Felgyó compost,  $\text{Cu}^{2+}$  treated)  $\text{Cu}^{2+}$  concentration 100 mg L<sup>-1</sup> and 4 mL min<sup>-1</sup> flow rate and different bed heights

Table 3.17. Parameters predicted by Yoon-Nelson model (Felgyó compost,  $\text{Cu}^{2+}$  treated)

Column Parameters				Nelson Parameters		
$C_0 / \text{mg L}^{-1}$	Weight / g	Bed heights / cm	$Q / \text{mL min}^{-1}$	$K_{YN} / \text{min}^{-1}$	$\tau / \text{min}$	$R^2$
20	5	2.4	4	263	0.0038	0.91
20	10	3.1	4	188	0.0053	0.92
20	15	6.5	4	357	0.0028	0.92
20	5	2.4	8	111	0.009	0.98
20	10	3.1	8	87	0.0114	0.94
20	15	6.5	8	126	0.0079	0.91
100	5	2.4	4	107	0.0093	0.93
100	10	3.1	4	200	0.005	0.93
100	15	6.5	4	285	0.0035	0.96
100	5	2.4	8	89	0.0112	0.91
100	10	3.1	8	72	0.0138	0.92
100	15	6.5	8	55	0.018	0.92

### 3.2.4.3.3 Yoon Nelson model fitted for $\text{Cd}^{2+}$ adsorbed by Felgyó compost

Yoon Nelson calculated results attained show that when the initial metal concentration rises from 20 to 100 mg L<sup>-1</sup>, the 50% adsorbent breakthrough ( $\tau$ ) decreases from 285, 250, 333 to 212, 185, 101 min once the bed height set at 1, 1.2, and 3.1 respectively. In addition, it declines from 116, 80, 64 to 60, 58, 44 min on increasing flow rate from 4 to 8 mL/min, which can be attributed to the rapid saturation of bed in higher flow rates along with higher flow rate; this is in agreement with the results obtained by (Sarma et

al. 2015). The increase of  $k_{YN}$  calculated from data that obtained from Fig 3.74 to 3.77 is found to be in parallel with the rise of concentration and flow rate while it did not show any particular tendency with increasing of bed heights. Furthermore,  $k_{YN}$  is in general increased with the increase of bed height as depicted in table 3.18. Nevertheless, the values of  $\tau$  were found to be higher in most cases than the  $t$  value at 50% breakthrough experimentally observed under all conditions estimated, this also concur with (V́ctor-ortega et al. 2016).

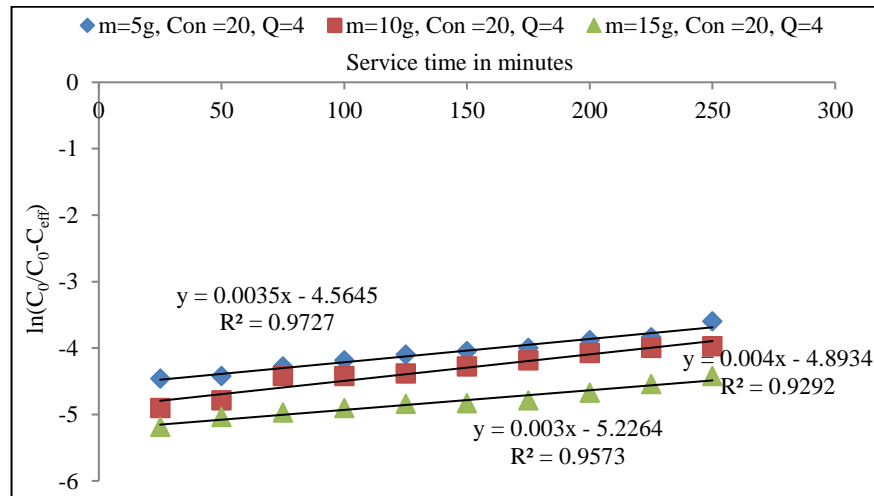


Fig. 3.74 Yoon–Nelson plot of (Felgyó compost, Cd<sup>2+</sup> treated) concentration 20 mg L<sup>-1</sup> and 4 mL min<sup>-1</sup> flow rate and different bed heights

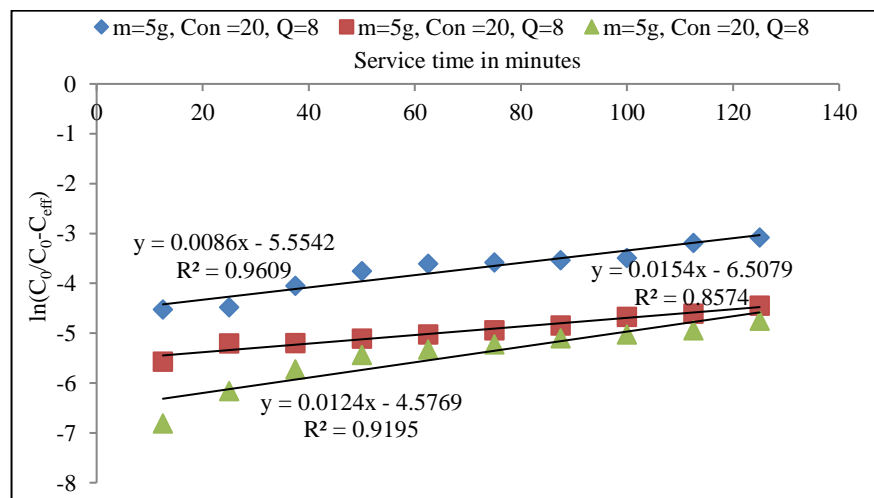


Fig. 3.75 Yoon–Nelson plot of (Felgyó compost, Cd<sup>2+</sup> treated) concentration 20 mg L<sup>-1</sup> and 4 mL min<sup>-1</sup> flow rate and different bed heights

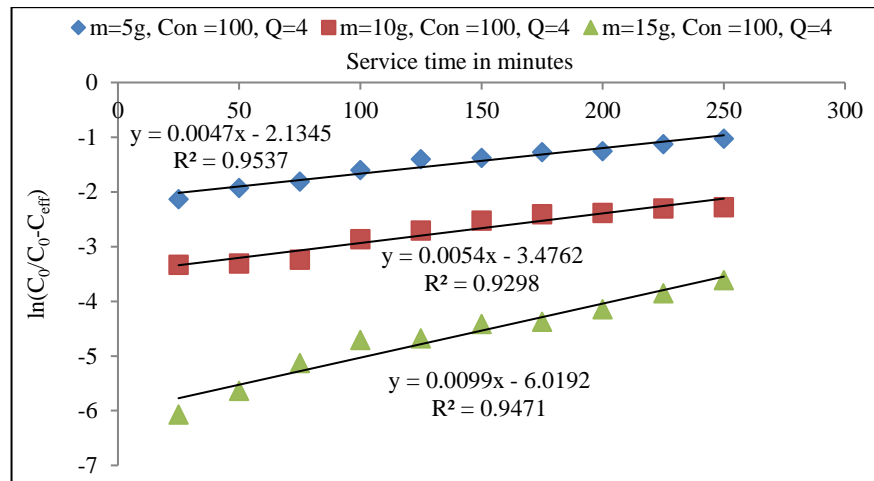


Fig. 3.76 Yoon–Nelson plot of (Felgyő compost,  $\text{Cd}^{2+}$  treated) concentration  $20 \text{ mg L}^{-1}$  and  $4 \text{ mL min}^{-1}$  flow rate and different bed heights

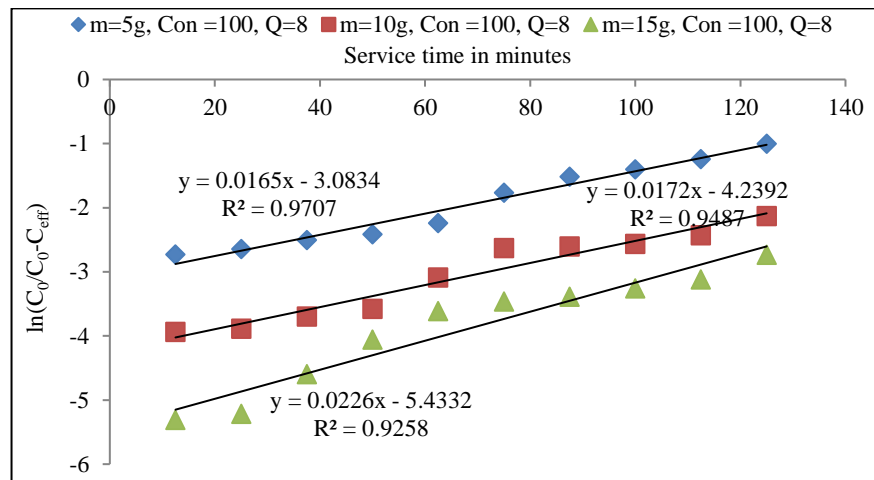


Fig. 3.77 Yoon–Nelson plot of (Felgyő compost,  $\text{Cd}^{2+}$  treated) concentration  $20 \text{ mg L}^{-1}$  and  $4 \text{ mL min}^{-1}$  flow rate and different bed heights

Table 3.18. Parameters predicted by Yoon-Nelson model (Felgyő compost,  $\text{Cd}^{2+}$  treated)

$C_0 / \text{mg L}^{-1}$	Weight / g	Bed heights / cm	$Q / \text{mL min}^{-1}$	$\tau / \text{min}$	$K_{YN} / \text{min}^{-1}$	$R^2$
20	5g	1.1	4	285	0.0035	0.97
20	10g	2	4	250	0.004	0.92
20	15g	3.1	4	333	0.003	0.95
20	5g	1.1	8	116	0.0086	0.96
20	10g	2	8	80	0.0124	0.91
20	15g	3.1	8	64	0.0154	0.85
100	5g	1.1	4	212	0.0047	0.95
100	10g	2	4	185	0.0054	0.92
100	15g	3.1	4	101	0.0099	0.94
100	5g	1.1	8	60	0.0165	0.97
100	10g	2	8	58	0.0172	0.94
100	15g	3.1	8	44	0.0226	0.92

#### 4. NEW SCIENTIFIC RESULTS

- I. This study proved that the compost material used for removing the heavy metal from contamination water has the capability of removing  $\text{Cu}^{2+}$  and  $\text{Cd}^{2+}$  in high percentages rate.
- II. Compost material used in this study is contained carboxyl functional groups which is supposed to interact with  $\text{Cu}^{2+}$  and  $\text{Cd}^{2+}$  ions for an ion exchange that leads to reduce heavy metal from contaminated water
- III. The bed column is significantly affected by the change of flow rate, metal concentration and bed heights.
- IV. Langmuir model can be used for compost material which is ununiformed and heterogeneous distributed, this model is to be used for uniform surface which is proved that is not valid.
- V. Thomas model used in the column experiment was performed well than Adams and Yoon models.

## 5. CONCLUSIONS AND SCOPE FOR FUTURE RESEARCH

### 5.1 CONCLUSIONS

- I. The results provide a good indication that all compost used in the batch experiment could remove  $\text{Cd}^{2+}$  and  $\text{Cu}^{2+}$  with favour for Garé compost and also favour for  $\text{Cu}^{2+}$ . All the 3 compost materials used for cleaning the water polluted in batch study could sorb practically the total amount of 100% of heavy metals up to  $10000 \mu\text{g g}^{-1}$  concentrations.
- II. Batch experiment could treat heavy metal in small volume, however in large volume, fixed bed is preferable.
- III. The results obtained from bed column showed that the adsorption of metals is affected by initial concentration, flow rate and bed height. The heavy metal removal yield decreased with increasing flow rate, bed depth and rise of metal concentration.
- IV. The total removal percentage acquired from fixed bed column is ranging from 88 to 99% at lower concentration; with higher concentration it could remove the heavy metal from 78 to 98%. The system required longer time for better performance.
- V. Among those models, the Thomas model was found to be most suitable to represent the kinetics of biosorption of the heavy metals.
- VI. Compost is proved to reduce heavy metal in very low level, therefore can be applied to remove other heavy metals from wastewaters.

### 5.2 Scope for future research

The following recommendations are the scope for future research:

- I. To explore the possibilities, modifications / pre-treatment of adsorbent to improve its adsorption capacity.
- II. Studies with actual industrial wastewater to evaluate parameters for field applications.

- III. Investigation of compost material adsorption capacity of removing other heavy metal from wastewaters.
- IV. Applying new and modifying mathematical models to evaluate their fitting with experimental data.
- V. Conducting experimental investigation in industrial scales to evaluate the applicability and capacity of compost material on removing heavy metals.
- VI. Designing continues fixed bed column system with computer stimulation programs.

## 6. Summary

Water pollution due to heavy metals is an issue of great environmental concern. Heavy metal ions are discharged into the water system from numerous manufacturing activities such as electroplating industries, electronic equipment manufacturing, and chemical processing plants. Due to the rapid development of industrial activities, the levels of heavy metals in water systems have significantly increased. The water-soluble forms of heavy metals can easily enter the food chain. Therefore various researchers conducted several experiments in order to remove a different type of heavy metal by applying different adsorbent materials. Most of the adsorption studies have been focused on low-cost adsorbents. Some of the advantages of using these materials for wastewater treatment include involvement of simple techniques requirement of very little processing, good adsorption capacity, selective adsorption of heavy metal ions, low cost, free availability. In this study conducted to remove tow heavy metals from contaminated water by using cost-effective techniques and effective adsorbent material. This study has gathered deep information about the usability of adsorption by different material and elimination of various heavy metals. The studies in the literature on adsorbents related to  $\text{Cd}^{2+}$   $\text{Cu}^{2+}$  ions were examined and compared with the values achieved in the current study. This research is aiming to try two different experimental methods, batch and continues column bed. The batch experiments carried out to evaluate three types of compost material and to test their ability to remove cadmium and copper. The results obtained from this study were satisfactory and encouraging to test other heavy metal with the same approach. Specifically, removal percentages attained from the results have shown the high affinity of these adsorbent materials and their capacity to remove cadmium and copper. The known Langmuir model fitted for batch experiments provides good adjustments to strongly favorable isotherms. One should bear in his mind that the Langmuir isotherm is derived assuming a uniform surface, which in many cases is not valid. This relation works fairly well, even with adsorbents with high heterogeneity such as compost, clays or activated carbon. The column bed aimed to test the compost material in continues flow by different bed heights, and high, low concentration of  $\text{Cd}^{2+}$  and  $\text{Cu}^{2+}$ . The parameters applied in the present study showed the influence on the breakthrough for heavy metal ions adsorption. Metal removal efficiencies and adsorbent adsorption capacities for each of the columns was estimated to assess the suitability of

these adsorption media and the preferred operating conditions for the treatment of cadmium and copper. The increase in bed height increased the amount of adsorbent used thus increasing the total removal of heavy metal removed and prolonged the lifespan of the compost column. However, the increase in flow rate and influent concentration resulted in the shortened lifespan of the column. Kinetic models applied in this study were useful tools to evaluate the column performance and the adsorption capacity; however different parameters of the column could be improved such as length of operation time. The analytical methods used in this study were accommodating tools to understand more about the adsorption process as indicated by FTIR for the presence of functional groups. The humic substances contain functional groups that are responsible for the sorption of metal ions; these functional groups are generally negatively charged which allows for the strong attraction of metal ions to compost. This work provides a better understanding of the processes and mechanisms involved in the sorption of pollutants on the environment in order to prevent their adverse consequences.

## 7. Összefoglalás

A nehézfémektől eredő vízszennyezés olyan probléma, ami komoly környezetvédelmi aggodalmakra ad okot. Nehézfém ionok többféle gyártó tevékenység kapcsán kerülhetnek bele a vízrendszerbe, például galvánozó üzemekből, villamos berendezések gyártóitól vagy vegyipari feldolgozó üzemekből. Az ipari tevékenységek gyors fejlődése miatt jelentősen megnöttek a vízrendszerekben a nehézfémek jelenlétének szintjei. A nehézfémek vízben oldódó megjelenési formái könnyen bejuthatnak az élelmiszer láncba. Ezért a kutatók sok kísérletet lefolytattak már, melynek során különböző adszorbens anyagok alkalmazásával próbálták eltávolítani nehézfémeket. Az adszorpcióval foglalkozó vizsgálatok többnyire kis költségű adszorbensekre fókuszáltak eddig. Az ilyen anyagok szennyvíztisztításban való alkalmazásának egyik előnye, egyebek között, hogy egyszerűek az eljárások, termék/anyag feldolgozást alig tartalmaznak, jó az ilyen anyagok adszorpciós képessége, szelektív módon szívják fel a nehézfém ionokat, alacsony költségűek és szabadon hozzáférhetőek. A szóban forgó vizsgálatban a költséghatékony technikákkal és hatékony adszorbens anyagokkal végezték a szennyezett vizek csöveken befolyó nehézfémektől való megtisztítását. A tanulmány nagy mennyiségben gyűjtött információt a különböző anyagok adszorpciós képességeinek kihasználásáról és a nehézfémek eliminálásáról. Tanulmányozták a szakirodalomban a  $\text{Cd}^{2+}$ ,  $\text{Cu}^{2+}$  ionokkal összekapcsolható adszorbensekről szóló vizsgálatok leírásait, és összehasonlították a jelen vizsgálatban elért eredményekkel. Ez a kutatás két kísérleti módszer kipróbálását tűzte célul - az egyik a csoportos, kötegben való elhelyezés, amit az oszlopágyas módszer követ. A „kötegelt” kísérletek háromféle kompozitanyagot értékelték azt vizsgálva, hogy milyen mértékben képesek kadmiumot és rézet eltávolítani. Ebből a vizsgálatból kielégítő eredmények születtek, melyek arra bátorítják a kutatókat, hogy ugyanezt a módszert próbálják ki más nehézfémeken is. Közelebbről, az eredmények alapján elért eltávolítási százalékok mutatják ezeknek az adszorbens anyagoknak a nagy kémiai affinitását és azt, hogy képesek kivonni a kadmiumot és a rézet. Az ismert Langmuir-féle modell ráillet a kötegelt kísérletekre, és ez jó adalékokkal szolgál az erőteljesen favorizál izotermák körüli módosításokra. Szem előtt kell tartanunk, hogy a Langmuir-izoterma egységes felület feltételezéséből származik, ami sok esetben nem érvényes. Ez a viszony jól működik még az olyan nagy heterogenitású adszorbensek esetében is, mint amilyen a kompozit, a különféle agyagok

és az aktív szén. Az oszlopággal az volt a cél, hogy tesztelje a komposztanyagot állandó áramlás mellett, eltérő ágymagasságokban, a  $\text{Cd}^{2+}$  és  $\text{Cu}^{2+}$  nagy és alacsony koncentrációi mellett. A fémeltávolítás hatékonysága és az adszorbens adszorpciós képessége becsléssel lett megállapítva minden egyes oszlop esetében, hogy fel lehessen mérni ezen adszorbeáló közegek alkalmasságát és a kívánatos üzemi körülményeket a kadmium és a réz kezeléséhez. Az ágymagasság növelése javította a felhasznált adszorpciós anyag mennyiségét, miáltal nőtt az összesen eltávolított nehézfém mennyisége is, és megnőtt a komposztos oszlop hasznos élettartama. Ugyanakkor az áramlási sebesség és a befolyó anyag koncentrációjának növelése rövidítette az oszlop üzemi élettartamát. A vizsgálatban felhasznált kinetikai modellek hasznosnak bizonyultak az oszlop teljesítményének és elnyelési kapacitásának értékelésére, miközben az oszlop paramétereit javítani lehetett olyan elemekkel, mint az üzemidő növelése. A vizsgálatban alkalmazott analitikai módszerek megfelelő eszközök voltak ahhoz, hogy jobban meg lehessen érteni az adszorpció folyamatát, amint azt az FTIR-spektroszkópia mutatta a funkcionális csoportok jelenlétére vonatkozóan. A nedves anyagok olyan funkcionális csoportokat tartalmaznak, melyek a fém ionok szorpcióáért felelnek; ezek a funkcionális csoportok rendszerint negatív töltésűek, ami alkalmassá teszi őket arra, hogy erőteljesen vonzzák a fémionokat a komposztba. A dolgozatból világosabban megértjük a szennyező anyagok szorpciójával együtt járó folyamatokat és mechanizmusokat és azok környezetre gyakorolt hatásait, miáltal megelőzhető a kedvezőtlen hatásuk.

## 8. References

- Abdolali, A., Ngo, H., Guo, W., Zhou, J., Zhang, J., Liang, S., Chang, S., Nguyen, D. & Liu, Y. (2017). Application of A Breakthrough Biosorbent for Removing Heavy Metals from Synthetic and Real Wastewaters in A Lab-Scale Continuous Fixed-Bed Column. *Bioresource Technology*, 229, pp. 78-87.
- Acheampong, A., Pakshirajan, K., Annachhatre, P. & Lens, N. (2013b). Removal of Cu (II) By Biosorption onto Coconut Shell in Fixed-Bed Column Systems. *Journal of Industrial and Engineering Chemistry*, 19(3), pp. 841-848
- Adil, M. (2006). Preparation, Modification and Characterization of Activated Carbons For Batch Adsorption Studies on The Removal of Selected Metal Ions. *M.Sc Thesis, University Technology, Malaysia*
- Ahluwalia, S. & Goyal, D. (2007). Microbial and Plant Derived Biomass for Removal of Heavy Metals from Waste Water. *Bioresource Technology*, 98(12), pp. 2243–2257.
- Ahmad, A. & Hameed, B. (2010a). Fixed-bed adsorption of reactive azo dye onto granular activated carbon prepared from waste. *Journal of Hazardous Materials*, 175(1-3), pp. 298-303.
- Ajmal, M. Rao., R. Ahmad., R. & Khan, A. (2006). Adsorption Studies on Parthenium Hysterophrous Weed: Removal and Recovery of Cd (II) from Wastewater. *Journal of Hazardous Materials*, 135(1-3), pp. 242–248.
- Aksu, Z, & Gönen, F. (2004). Biosorption Of Phenol By Immobilized Activated Sludge In A Continuous Packed Bed: Prediction of Breakthrough Curves. *Process Biochemistry*, 39(3), pp. 599–613.
- Alexander, M. (1994). Biodegradation and Bioremediation, Academic Press. San Diego San Diego, California, USA. 56 p.
- Amarasinghe, B, & Williams, T. (2007). Tea Waste as a Low Cost Adsorbent for the Removal of Cu and Pb from West Water. *Chemical Engineering Journal*, 132(1-3), pp. 299-309.

Anastopoulos, I., Massas, I. & Ehaliotis, C. (2013). Composting Improves Biosorption of  $Pb^{2+}$  and  $Ni^{2+}$  by Renewable Lignocellulosic Materials. Characteristics and Mechanisms Involved. *Chemical Engineering Journal*, 231, pp. 245–254.

Apiratikul, R. & Pavasant, P. (2008). Batch And Column Studies Of Biosorption Of Heavy Metals By *Caulerpa Lentillifera*. *Bioresource Technology*, 99(8), pp. 2766-2777.

Aranda, V., Macci, C., Peruzzi. & Masciandaro, G. (2015). Biochemical Activity and Chemical-Structural Properties of Soil Organic Matter after 17 Years of Amendments with Olive-Mill Pomace Co-compost. *Journal of Environmental Management*, 147, pp. 278–285.

Aziz, A.S., Manaf., L.A., Man., H.C. & Kumar, N.S. (2014). Column Dynamic Studies And Breakthrough Curve Analysis for Cd (II) and Cu (II) Ions Adsorption Onto Palm Oil Boiler Mill Fly Ash (POFA). *Environmental Science and Pollution Research*, 21 (13), pp. 7996–8005.

Baek, K., Song, S., Kang, S., Rhee, Y., Lee, C., Lee, B., Hudson, S. & Hwang, T. (2007). Adsorption kinetics of boron by anion exchange resin in packed column bed. *Journal of Industrial and Engineering Chemistry*, 13(3), pp. 452-456.

Banerjee, S.S. & Chen, D.H. (2007). Fast Removal of Copper Ions by Gum Arabic Modified Magnetic Nano-Adsorbent. *Journal of Hazardous Materials*, 147(3), pp. 792–799.

Barakat, A. (2011). New Trends in Removing Heavy Metals from Industrial Wastewater. *Arabian Journal of Chemistry*, 4(4), pp. 361- 377.

Baral, S., Das, N., Ramulu, T., Sahoo, S., Das, S. & Chaudhury, G. (2009). Removal of Cr(VI) By Thermally Activated Weed (*Salvinia Cucullata*) in a Fixed-Bed Column. *Journal of Hazardous Materials*, **161** (2-3), pp. 1427-1435.

Basci, N., Kocadagistan, E. & Kocadagistan, B. (2003). Biosorption of Cu II from Aqueous Solutions by Wheat Shells. *Desalination*, 164(2), pp. 135–140

- Benaissa, H. (2006). Screening of New Sorbent Materials for Cadmium Removal from Aqueous Solutions. *Journal of Hazardous Materials*, 132(2-3), pp. 189–195.
- Bhattacharyya, K. G. & Sharma, A. (2003). Adsorption Characteristics of the Dye, Brilliant Green on Neem Leaf Powder. *Dyes and Pigments*, 57(3), pp. 211-222.
- Biswas, S. & Mishra, U. (2015). Continuous Fixed-Bed Column Study And Adsorption Modeling: Removal of Lead Ion from Aqueous Solution by Charcoal Originated from Chemical Carbonization of Rubber Wood Sawdust. *Journal of Chemistry*, 2015, pp. 1-9.
- Bohart, G. & Adams, E. (1920). Some Aspects of The Behavior of Charcoal with Respect of Chlorine. *American Chemical Society*, 42 (30), pp. 523–544.
- Bulgariu, D. & Bulgariu, L. (2013) Sorption of Pb(II) onto a Mixture of Algae Waste Biomass and Anion Exchanger Resin in a Packed-Bed Column. *Bioresource Technology*, 129, pp. 374–380.
- Cai, Q. Y., Mo, C. H., Wu, Q. T., Zeng, Q. Y. & Katsoyiannis, A. (2007). Concentration and Speciation of Heavy Metals in Six Different Sewage Sludge-Composts. *Journal of Hazardous Materials*, 147 (3) pp. 1063–1072.
- Calero, M., Hernainz, F., Blazques, G., Tenorio, G. & Martin-Lara, M. (2009). Study of Cr (III) Biosorption in a Fixed-Bed Column. *Journal of Hazardous Materials*, 171(1-3), pp. 886–893.
- Castaldi, P., Santona, L. & Melis, P. (2006) Evolution of heavy metals mobility during municipal solid waste composting. *Fresenius Environmental Bulletin*, 15(9), pp. 1133–1140.
- Chao, H., Chang, C. & Nieva, A. (2014). Biosorption of Heavy Metals on *Citrus Maxima* Peel, Passion Fruit Shell, and Sugarcane Bagasse in a Fixed-Bed Column. *Journal of Industrial and Engineering Chemistry*, 20 (5), pp. 3408-3414.
- Chen, S., Yue, Q., Gao, B., Li, Q., Xu, X. & Fu, K. (2012). Adsorption of Hexavalent Chromium from Aqueous Solution by Modified Corn Stalk: a Fixed-Bed Column Study. *Bioresource Technology*, 113, pp. 114-120.

Cheraghi, E., Ameri, E. & Moheb, A. (2016). Continuous Biosorption of Cd(II) Ions from Aqueous Solutions by Sesame Waste: Thermodynamics and Fixed-Bed Column Studies. *Desalination and Water Treatment*, 57(15), pp. 6936-6949.

Christoforidis, A., Orfanidis, S., Papageorgiou, S., Lazaridou, A., Favvas, E. & Mitropoulos, A. (2015). Study of Cu(II) removal by *Cystoseira Crinitophylla* biomass in batch and continuous flow biosorption. *Chemical Engineering Journal*, 277, pp. 334–340.

Cole, M.A., X. Liu. & L. Zhang. (1994). Plant and Microbial Establishment in Pesticide Contaminated Soils Amended With Compost.” In *Bioremediation through Rhizosphere Technology*, edited by T.A. Anderson and J.R. Coats, 210-222. Washington, DC: *American Chemical Society*.

Covelo, F., Andrade, L. & Vega, A. (2004). Heavy Metal Adsorption by Humic Umbrilsols: Selectivity Sequences and Competitive Sorption Kinetics. *Colloid and Interface Science*, 280(1), pp. 1–8.

Dabrowski, A. (2001). Adsorption from Theory to Practice. *Advance in Colloid Interface Science*, 93(1-3), pp. 135-224.

Eccles, H. (1999). Treatment of Metal-Contaminated Wastes: Why Select a Biological Process?. *Trends in Biotechnology*, 17(12), pp. 462–465.

Elham Farouk Mohamed (2011): Removal Of Organic Compounds From Water By Adsorption And Photocatalytic Oxidation. PhD thesis, Institut National Polytechnique de Toulouse, France.

Finstein, M.S. & Morris, M.L. (1975). Microbiology of Municipal Solid Waste Composting. *Advances in Applied Microbiology*, 19, pp. 113-151.

Foo, Y., Lee, K. & Hameed, H. (2013). Preparation of Tamarind Fruit Seed Activated Carbon by Microwave Heating for the Adsorptive Treatment of Landfill Leachate: a Laboratory Column Evaluation. *Bioresource Technology*, **133**, pp. 599-605

Freundlich, F. (1906). Over the Adsorption in Solution. *The Journal of Physical Chemistry*, 56, pp. 385- 471

Fuentes. M., Baigorri, R., González-gaitano, G. & Garcia-Mina, M. (2007). The Complementary Use of <sup>1</sup>H Nmr, <sup>13</sup>C Nmr, Ftir and Size Exclusion Chromatography to Investigate the Principal Structural Changes Associated with Composting of Organic Materials with Diverse Origin. *Organic Geochemistry*, 38(12), pp. 2012–2023.

Gardea-Torresdey, L., Tiemann, J., Armendariz, V., Bess-Oberto, L., Chianelli, R., Rios, J., Parsons, G. & Gamez, G. (2000). Characterization of Chromium (Vi) Binding and Reduction to Chromium (III) by The Agricultural Byproduct of Avena Monida (Oat) Biomass. *Journal of Hazardous Materials*, 80(1-3), pp. 175–188.

Ghasemia, M., Keshtkarb, A., Dabbaghc, R. & Safdari, J. (2011). Biosorption of uranium (VI) from aqueous solutions by Ca-pretreated *Cystoseira indica* alga: Breakthrough curves studies and modelling. *Journal of Hazardous Materials*, 189(1-2), pp. 141–149.

Gupta, V.K. (1998). Equilibrium uptake, sorption dynamics, process development, and column operations for the removal of copper and nickel from aqueous solution and wastewater using activated slag, a low-cost adsorbent. *Industrial & Engineering Chemistry Research*, 37(1), pp. 192–202.

Gupta, V.K., Bakshi, M.P.S. & Langar, P.N. (1987). Microbiological Changes During Natural Fermentation of Urea-Wheat Straw. *Biological Wastes*, 21(4), pp. 291-299.

Han, R., Ding, D., Xu, Y., Zou, W., Wang, Y., Li, Y. & Zou, L. (2008). Use of Rice Husk for the Adsorption of Congo Red from Aqueous Solution In Column Mode. *Bioresource Technology*, 99(8), pp. 2938–2946.

Hanc, A., Szakova, J. & Svehla, P. (2012). Effect of Composting on the Mobility of Arsenic, Chromium and Nickel Contained in Kitchen and Garden Waste. *Bioresource Technology*, 126, pp. 444–452.

Haroun, M., Idris, A. & Omar, S. (2007). A Study of Heavy Metals and Their Fate in the Composting of Tannery Sludge. *Waste Management*, 27(11), pp. 1541–1550.

- Horsfall, M. & Spiff, A. (2005). Effect of Metal Ion Concentration on the Biosorption of  $Pb^{2+}$  and  $Cd^{2+}$  by *Caladium Bicolor* (Wild Cocoyam), *African Journal of Biotechnology*, 4(2), pp. 191–196.
- Huang, F. Wu, T. Wong, W. & Nagar, B. (2006). Transformation of Organic Matter During Co-Composting of Pig Manure with Sawdust. *Bioresource Technology*, 97(15), pp. 834–1842.
- Huang, X., Sillanpää, M., Dou, B. & Gjessing, T. (2008). Water Quality in the Tibetan Plateau: Metal Contents of four Selected Rivers. *Environmental Pollution*, 156(2), pp. 270–277.
- Ikedo, M., Zhang, W., Shimbo, S., Watanabe, T., Nakatsuka, H., Moon, S., Matsuda-Inoguchi, N. & Higashikawa, K. (2000). Urban Population Exposure to Lead and Cadmium in East and South-East Asia. *Science of the Total Environment*, 249(1-3), pp. 373-384.
- Jahangiri-rad, M., Jamshidi, A., Rafiee, M. & Nabizadeh, R. (2014). Adsorption performance of packed bed column for nitrate removal using PAN oxime-nano  $Fe_2O_3$ . *Journal of Environmental Health Science & Engineering*, 12(1), pp. 12-90.
- Jain, M., Garg, V. & Kadirvelu, K. (2013). Cadmium(II) Sorption and Desorption in a Fixed Bed Column Using Sunflower Waste Carbon Calcium-Alginate Beads. *Bioresource Technology*, 129, pp. 242–248.
- Jing, X., Cao, Y., Zhang, X., Wang, D., Wu, X. & Xu, H. (2011). Biosorption Of Cr(VI) From Simulated Wastewater Using A Cationic Surfactant Modified Spent Mushroom. *Desalination*, 269(1-3), pp. 120–127.
- Kamari, A. S.N.M., Yusoff, S. F., Abdullah, F. W.P. & Putra, W. (2014). Biosorptive Removal Of Cu(II), Ni(II) And Pb(II) Ions From Aqueous Solutions Using Coconut Dregs Residue: Adsorption And Characterisation Studies. *Journal of Environmental Chemical Engineering*, 2(4), pp. 21912–1919.
- Kamble, K. & Patil, R. (2001). Removal of Heavy Metals from Waste Water of Thermal Power Station by Water-Hyacinths. *Indian Journal of Environmental Protection*, 21(7), pp. 623–626.

- Kananpanah, S., Ayazi, M. & Abolghasemi, H. (2009). Breakthrough curve studies of purolite A-400 in an adsorption column. *Petroleum and Coal*, 51(3), pp. 189-192.
- Keskinkan, O., Goksu, M.Z.L., Yuceer, A., Basibuyuk, M. & Foster, C. F. (2003). Heavy Metal Adsorption Characteristics of a Submerged Aquatic Plant (*Myriophyllum spicatum*). *Process Biochemistry*, 39(2), pp. 179-183
- Ko, D., Potter, J. & Mackay, G. (2000). Optimised Correlations for the Fixed Bed Adsorption of Metal Ions on Bone Char. *Chemical Engineering Science*, 55(23), pp. 5819–5829.
- Kovacs, H. & Szemmelveisz, K. (2017). Disposal Options for Polluted Plants Grown on Heavy Metal Contaminated Brownfield Lands - A Review. *Chemosphere*, 166, pp. 8-20.
- Kratochvil, D. & Volesky, B. (1998). Advances In Biosorption Of Heavy Metals. *Trends in Biotechnology*, 16(7), pp. 291-300.
- Krishnan, K.A. & Anirudhan, T. (2003). Removal of Cadmium (II) from Aqueous Solutions by Steam-Activated Sulphurised Carbon Prepared from Sugar Cane Bagasse Pith: Kinetics and Equilibrium Studies. *Water SA*, 29(2), pp. 147–156.
- Kumar, D., Pansy, L. & Gaur, J. (2016). Metal Sorption by Algal Biomass: From Batch to Continuous System. *Algal Research*, **18**, pp. 95-109
- Kumar, R., Bhatia, R., Singh, Dv Rani, R. & Bishnoia, S. (2011). Sorption of Heavy Metals From Electroplating Effluent Using Immobilized Biomass *Trichoderma Viride* In A Continuous Packed-Bed Column. *International Biodeterioration & Biodegradation*, **65** (8) 1133-1139
- Kumar, U. & Bandyopadhyay, M. (2006). Sorption of Cd from Aqueous Solution Using Pretreated Rice Husk. *Bioresource Technology*, 97(1), pp. 104–109.
- Langmuir, I. (1918). The Adsorption of Gases on Plane Surfaces of Glass, Mica and Platinum. *Journal of the American Chemical Society*, 40(9) 1361-1403
- Laniyan, T., Kehinde, A., Phillips, O. & Elesha, L. (2011). Hazards of Heavy Metal Contamination on the Groundwater Around A Municipal Dumpsite in Lagos,

Southwestern Nigeria, *International Journal of Engineering & Technology*. 11(5), pp. 61-70.

Li, C. & Champagne, P. (2009). Fixed-Bed Column Study for The Removal Of Cadmium (II) and Nickel (II) Ions from Aqueous Solutions Using Peat and Mollusk Shells. *Journal of Hazardous Materials*, 171(1-3), pp. 872–878.

Li, Y., Yue, Y. & Gao, B.Y. (2010). Adsorption Kinetics and Desorption of Cu(II) and Zn(II) from Aqueous Solution onto Humic Acid. *Journal of Hazardous Materials*, 178(1-3), pp. 455–461.

Lim, A. & Aris, A. (2014). Continuous Fixed-Bed Column Study And Adsorption Modeling: Removal Of Cadmium (II) And Lead (II) Ions In Aqueous Solution By Dead Calcareous Skeletons. *Biochemical Engineering Journal*, 87, pp. 50–61.

Ling, C., Ai, I., Tan, W., Lik, L. & Lim, P. (2016). Fixed-Bed Column Study For Adsorption Of Cadmium On Oil Palm Shell-Derived Activated Carbon. *Journal of Applied Science & Process Engineering*, 3(2), pp. 60–71.

Liu, L., Guo, X., Zhang, C., Luo, C., Xiao, C. & Li, R. (2018) Adsorption Behaviours and Mechanisms of Heavy Metal Ions' Impact on Municipal Waste Composts with Different Degree of Maturity. *Environmental Technology*, 0, pp 1–15.

Luo, X., Deng, Z., Lin, X. & Zhang, C. (2011). Fixed-Bed Column Study For Cu<sup>2+</sup> Removal From Solution Using Expanding Rice Husk. *Journal of Hazardous Materials*, 187(1-3), pp. 182–189.

Ma, W., Hung, L. & Chen, C. (2006). A Systemic Health Risk Assessment for the Chromium Cycle in Taiwan. *Environment International*, 33(2), pp. 206-218.

Macauley, B.J., Stone, B., Iiyama, K., Harper, E.R. & Miller, F.C. (1993). Compost Research Runs "Hot" and "Cold" at La Trobe University. *Compost Science and Utilization*, 1, pp. 6-12.

Martín-Lara, M., Blázquez, G., Calero, M., Almendros, A. & Ronda, A. (2016a). Binary Biosorption of Copper and Lead onto Pine Cone Shell in Batch Reactors and in Fixed Bed Columns. *International Journal of Mineral Processing*, 148, pp. 72–82.

- McCabe, W. L., Smith, J.C. & Harriot, P. (2001). Unit Operations of Chemical Engineering, McGraw-Hill International Ed., 6th ed., New York, USA. 165 p.
- McKay, G. & Bino, J. (1990). Fixed Bed Adsorption for the Removal of Pollutants from Water. *Environmental Pollution*, 66(1), pp. 33–53.
- Mehta, S.K. & Gaur, J.P. (2005). Use of Algae for Removing Heavy Metal Ions from Wastewater: Progress and Prospects, Crit. Rev. *Biotechnology*, 25(3), pp. 113–152.
- Merrill, D.T., Maltby C.V., Kahmark, K., Gerhardt, M. & Melecer, H. (2001). Evaluating Treatment Process to Reduce Metals Concentration in Pulp And Paper Mill Waste Waters to Extremely Low Values. *Tappi Journal*, 84, pp. 52-58.
- Mishra, A., Tripathi, B. & Rai, A. (2016). Packed-Bed Column Biosorption Of Chromium(Vi) And Nickel(Ii) Onto Fenton Modified Hydrilla Verticillata Dried Biomass. *Ecotoxicology and Environmental Safety*, 132, pp. 420–428.
- Mobasherpour, E., Salahi, A. & Asjodi, A. (2014). Research on the Batch and Fixed-Bed Column Performance of Red Mud Adsorbents for Lead Removal. *Canadian Chemical Transactions*, 2(1), pp. 83–96.
- Mohammadi, T., Moheb, A., Sadrzadeh, M. & Razmi, A. (2005). Modeling of Metal Ions Removal from Wastewater by Electrodialysis. *Separation and Purification Technology*, 41(1), pp. 73–82.
- Mohan, D. & Singh, P. (2002). Single and Multi-Component Adsorption of Cadmium and Zinc Using Activated Carbon Derived from Bagasse-An Agricultural Waste. *Water Research*, 36(9), pp. 2304–2318.
- Mohee, R. & Soobhany, N. (2014). Comparison of Heavy Metals Content in Compost Against Vermin Compost of Organic Solid Waste: Past and Present. *Resources, Conservation and Recycling*, 92, pp. 206–213.
- Montanher, F., Oliveira, A. & Rollemberg, C. (2005). Removal of Metal Ions from Aqueous Solutions by Sorption Onto Rice Bran. *Journal of Hazardous Materials*, 117(2-3), pp. 207–211.

Mourao, P., Carrott, P. & Carrott, M. (2006). Application of Different Equations to Adsorption Isotherms of Phenolic Compounds on Activated Carbons prepared from Cork. *Carbon*, 44(12), pp. 2422-2429.

Moyo, M., Guyo, U., Mawenyiyo, G., Kwethu, N.P., Zinyama, P. & Nyamunda, C. (2015). Marula seed husk (*Sclerocarya birrea*) biomass as a low cost biosorbent for removal of Pb(II) and Cu(II) from aqueous solution. *Journal of Industrial and Engineering Chemistry*, 27, pp. 126–132.

Muchuweti, M., Birkett, W., Chinyanga, E., Zvauya, R., Scrimshaw, D. & Lester, N. (2006). Heavy Metal Content of Vegetables Irrigated with Mixture of Wastewater and Sewage Sludge in Zimbabwe: Implications for Human Health. *Agriculture Ecosystem and Environment*, 112, (1), pp. 41-48..

Muhamad, H.H., Doan, H. & Lohi, A. (2010b). Batch and Continuous Fixed-Bed Column Biosorption of Cd<sup>2+</sup> and Cu<sup>2+</sup>. *Chemical Engineering Journal*, 158(3), pp. 369–377.

Murthy, R & Srinivas, T. (2016) Removal of Cu (II) and Cd (II) from Synthetic Effluents Using Low Cost Adsorbents by Continuous Flow Operation. *World Applied Sciences Journal*, 34 (2), pp. 164-173.

Nasir, H., Nadeem, R., Akhtar, K., Hanif, A. & Khalid, M. (2007). Efficacy of Modified Distillation Sludge of Rose (*Rosa Centifolia*) Petals for Lead and Zinc Removal from Aqueous Solutions. *Journal of Hazardous Materials*, 147(3), pp. 1006–1014.

National Research Council (NRC), 1983. Risk Assessment in the Federal Government: Managing the Process. NAS-NRC Committee on the Institutional Means for Assessment of Risks to Public Health. National Academy Press, Washington, DC.

Neklyudov, A. D., Fedotov, G. N. & Ivankin, A. N. (2008). Intensification of Composting Processes by Aerobic Microorganisms: A Review. *Applied Biochemistry and Microbiology*, 44(1), pp. 6–18.

Nguyen, T., Loganathan, P., Nguyen, T., Vigneswaran, S., Kandasamy, J. & Naidu, R. (2015). Simultaneous Adsorption of Cd, Cr, Cu, Pb, And Zn By An Iron-Coated

Australian Zeolite In Batch And Fixed-Bed Column Studies. *Chemical Engineering Journal*, 270, pp. 393–404.

Oguz, E. & Ersoy, M. (2014). Biosorption of Cobalt(II) with Sunflower Biomass from Aqueous Solutions in A Fixed Bed Column and Neural Networks Modelling. *Ecotoxicology and Environmental Safety*, 99, pp. 54–60.

Ozdemir, O., Turan, M., Turan, A., Faki, A. & Engin, A. (2009). Feasibility Analysis of Color Removal From Textile Dyeing Wastewater in A Fixed-Bed Column System by Surfactant-Modified Zeolite (SMZ). *Journal of Hazardous Materials*, 166(2-3), pp. 647–654.

Pardo, T., Clemente, R. & Bernal, M. P. (2011). Effects of Compost, Pig Slurry and Lime on Trace Element Solubility and Toxicity in Two Soils Differently Affected by Mining Activities. *Chemosphere*, 84(5), pp. 642–650.

Paulino, A., Minasse, F., Guilherme, M., Reis, A., Muniz, E. & Nozaki, J. (2006). Novel Adsorbent Based on Silkworm Chrysalides for Removal of Heavy Metals from Wastewaters. *Journal of Colloid and Interface Science*, 301(2), pp. 2479-487.

Pino, G.H., De Mesquita, L.M.S., Torem, M.L. & Pinto, G.A.S. (2006). Biosorption Of Heavy Metals By Powder Of Green Coconut Shell. *Separation Science and Technology*, 41(14), pp. 3141-3153.

Rajaie, M., Karimian, N., Maftoun, M., Yasrebi, J. & Assad, T. (2006). Chemical forms of Cadmium in Two Calcareous Soil Textural Classes as Affected by Application of Cadmium-Enriched Compost and Incubation Time. *Geoderma*, 136(3), pp. 533–541.

Rao, K., Anand, S. & Venkateswarlu, P. (2011). Modeling the Kinetics of Cd (II) Adsorption on *Syzygium Cumini L* Leaf Powder in a Fixed Bed Mini Column. *Journal of Industrial and Engineering Chemistry*, 17 (2), pp. 174-181.

Rattan, K., Datta, P., Chhonkar, K., Suribabu, K. & Singh, K. (2005). Long-Term Impact of Irrigation with Sewage Effluents on Heavy Metal Content in Soils, Crops and Groundwater-A Case Study. *Agriculture Ecosystem and Environment*, 109(3-4), pp. 310-322.

- Redlich O. & Peterson, L. (1959). A useful adsorption isotherm. *The Journal of Physical Chemistry*, 63, 1024-1029.
- Riazi, M., Keshtkar, A. & Moosavian, M. (2016). Biosorption of Th (IV) in A Fixed-Bed Column by Ca-Pretreated *Cystoseira Indica*. *Environmental Chemical Engineering*, 4(2), pp. 1890–1898.
- Robinson, S., Arnold, W. & Byers, C. (1994). Mass-Transfer Mechanisms for Zeolite Ion Exchange in Wastewater Treatment. *AIChE*, 40(12), pp. 2045–2053.
- Rothenberg, E., Du, X., Zhu, G. & Jay, A. (2007). The Impact of Sewage Irrigation on the Uptake of Mercury in Corn Plants (*Zea Mays*) from Suburban Beijing. *Environmental Pollution*, 149, 246(2), pp. 251.
- Rouf, S. & Nagapadma, M. (2015). Modeling of Fixed Bed Column Studies for Adsorption of Azo Dye on Chitosan Impregnated With a Cationic Surfactant. *International Journal of Scientific and Engineering Research*, 6, pp. 538–545.
- Saeed, A. & Iqbal, M. (2003). Bioremoval of Cd from aqueous solution by black gram husk (*Cicer arietinum*). *Water Research*, 37(14), pp. 3472–3480.
- Sarma, R., Kumar, J. & Pakshirajan, K. (2015). Batch and Continuous Removal of Copper and Lead from Aqueous Solution Using Cheaply Available Agricultural Waste Materials. *International Journal of Environmental Research*, 9(2), pp. 635–648.
- Sas-Nowosielska, A., Kucharski, R., Malkowski, E., Pogrzeba, M., Kuperberg, J. & Krynski, K. (2004). Phytoextraction Crop Disposal an Unsolved Problem. *Environmental Pollution*, 128(3), pp. 373–379.
- Semerjian, L. (2010). Equilibrium and Kinetics of Cadmium Adsorption from Aqueous Solutions Using Untreated *Pinus Halepensis* Sawdust. *Journal of Hazardous Materials*, 173(1-3), pp. 236-242.
- Sharma, R. & Singh, B. (2013). Removal of Ni (II) Ions from Aqueous Solutions Using Modified Rice Straw in a Fixed Bed Column. *Bioresource Technology*, 146, pp. 519–524.

Silva, A., Cossich, E., Tavares, C., Cardozo, L. & Guirardello, R. (2002a). Modeling of Copper (II) Biosorption by Marine Alga *Sargassum* sp. In fixed Bed Column. *Process Biochemistry*, 38 (5), pp. 791–799.

Silva, E., Tavares, C., Barros, M., Arroyo, P., Schneider, R. & Suszek, M. (2003b). Modeling and Experimental  $\text{Cr}^{+3}$  Uptake Using Naxzeolite, In: Sixth Italian Conference on Chemical and Process Engineering (2003), Pisa, Italy. *Chemical Engineering Transactions*, 3, pp. 303–308.

Singh, K. K., Rastogi, R. & Hasan, S.H. (2005). Removal of Cadmium From Waste Water Using Agricultural Waste Using Rice Polish. *Journal of Hazardous Materials*, 121(1-3), pp. 51–58.

Singh, O., Labana, S., Pandey, G., Budhiraja, R. & Jain, R. (2003). Phytoremediation: An Overview of Metallic Ion Decontamination from Soil. *Applied Microbiology and Biotechnology*, 61(5-6), pp. 405–412.

Sivakumar, P. & Palanisamy, N. (2009). Adsorption studies of basic Red 29 by a non-conventional activated carbon prepared from *Euphorbia antiquorum* L. *International Journal of Chemtehc Research*, 1 (3), pp. 502-510.

Spaccini, R. & Piccolo, A. (2009). Molecular Characteristics of Humic Acids Extracted from Compost at Increasing Maturity Stages. *Soil Biology and Biochemistry*, 41(6), pp. 1164–1172.

Srivastava, S., Ahmed, H. & Thakur, S. (2007). Removal of Chromium and Pentachlorophenol from Tannery Effluent. *Bioresource Technology*, 98, (5), pp. 1128–1132.

Subbaiah, M, V., Vijaya, Y., Reddy, A, S., Yuvaraja, G. & Krishnaiah. A. (2011). Equilibrium, Kinetic And Thermodynamic Studies On The Biosorption Of Cu(II) Onto *Trametes Versicolor* Biomass. *Desalination*, 276 (1–3), pp. 310-316.

Sud, D., Mahajan, G. & Kaur, M. (2008). Agricultural Waste Material as Potential Adsorbent for Sequestering Heavy Metal Ions from Aqueous Solutions—A Review. *Bioresource Technology*, 99 (14) 6017–6027.

Sud, D., Mahajan, G. & Kaur, M.P. (2008). Agricultural Waste material as Potential Adsorbent for Sequestering Heavy Metal Ions from Aqueous Solutions—A review. *Bioresour Technology*, 99(14), pp. 6017–6027.

Suksabye, P., Thiravetyan, P. & Nakbanpote, W. (2008). Column Study of Chromium (VI) Adsorption from Electroplating Industry by Coconut Coir Pith. *Journal of Hazardous Materials*, 160 (1), pp. 56-62

Sun, F., Imai, T., Sekine, M., Higuchi, T., Yamamoto, K., Kanno, A. & Nakazono, S. (2014). Adsorption of Phosphate Using Calcined Mg<sub>3</sub>-Fe Layered Double Hydroxides in A Fixed-Bed Column Study. *Journal of Industrial and Engineering Chemistry*, 20(5), pp. 3623–3630.

Sunarso, J. & Ismadji, S. (2009) Decontamination of Hazardous Substances From Solid Matrices and Liquids Using Supercritical Fluids Extraction: A Review. *Journal of Hazardous Materials*, 161(1), pp. 1-20.

Taty-Costodes, C., Fauduet, V., Porte, C. & Ho, Y. (2005). Removal of lead (II) ions from synthetic and real effluents using immobilized *Pinus sylvestris* sawdust: Adsorption on a fixed-bed column. *Journal of Hazardous Materials*, 123(1-3), pp. 135-144.

Thermo Fisher Scientific. (2013) FTIRB,asicshttps://www.thermofisher.com/fr/fr/home/industrial/spectroscopy-elemental-isotope-analysis/spectroscopy-elemental-isotope-analysis-learning-center/molecular-spectroscopy-information/ftir-information/ftir-basics.html. Search engine: Google. Key words: FTIR Basics. Date of search: 2018.05.10

Thomas, H. (1944) Heterogeneous Ion Exchange in a Flowing System. *American Chemical Society*, 66 (10), pp. 1664–1666.

Türkdoğan, K., Fevzi, K., Kazim, K., Ilyas, T. & Ismail, U. (2003). Heavy Metals in Soil, Vegetables and Fruits in the Endemic Upper Gastrointestinal Cancer Region of Turkey. *Environmental Toxicology and Pharmacology*, 13(3), pp. 175-179.

Uddin, M., Rukanuzzaman, M., Khan, M. & Islam, A. (2009). Adsorption of Methylene Blue from Aqueous Solution By Jac kfruit (*Artocarpus Heteropyllus*) Leaf Powder: A

Fixed-Bed Column Study. *Journal of Environmental Management*, 90 (11), pp. 3443-3450.

Upadhyaya, R., Pankaj, K. & Pardeepc, P. (2017). Adsorption of Cu (II) and Cr (VI) by zeolite in batch and column mode, *Materials Today: Proceedings* 4, pp. 10504–10508.

Veeken, A., Nierop, K., Wilde, D. & Hamelers, B. (2000). Characterisation of NaOH-Extracted Humic Acids During Composting of a Biowaste. *Bioresource Technology*, 72(1), pp. 33–41.

Víctor-ortega, M., Ochand-pulid, J. & Martínez, A. (2016). Modeling of Fixed Bed Column Studies for Iron Removal from Industrial Effluents Through Ion Exchange Process, *Chemical. Engineering Transactions*, 47, pp. 277–282.

Vieira, M., Neto, A., da Silva, M., Carneiro, C. & Filho, A. (2014 ). Adsorption of Lead And Copper Ions from Aqueous Effluents on Rice Husk Ash in a Dynamic System. *Brazilian Journal of Chemical Engineering*, 31(2) ,pp. 519–529.

Viel, M., Sayag, D., Peyre, A. & André, L. (1987). Optimization of In-Vessel Co-Composting Through Heat Recovery. *Biological Wastes*, 20(3), pp. 167-185.

Vijayaraghavan, K., Palanivelu, K. & Velan, M. (2006) Biosorption Of Copper(II) And Cobalt(II) From Aqueous Solutions By Crab Shell Particles. *Bioresource Technology*, 97(12), pp. 1411–1419

Vimala, R., Charumathi, D. & Das, N. (2011). Packed Bed Column Studies on Cd(II) Removal from Industrial Wastewater by Macrofungus *Pleurotus Platypus*. *Desalination*, 275(1-3), pp. 291–296.

Volesky, B. & Holan, Z. (1995). Biosorption of Heavy Metals. *Biotechnology Progress*, 11(3), pp. 235–250.

Xu, X., Gao, B., Tan, T., Zhang, X., Yue, Q., Wang, Y. & Li, Q. (2013). Nitrate adsorption by stratified wheat straw resin in lab-scale columns. *Chemical Engineering Journal*, 226, pp. 1-6.

Yoon, Y. & Nelson, J. (1984). Application Of Gas Adsorption Kinetics — II. A Theoretical Model for Respirator Cartridge Service Life and Its Practical Applications. *American Industrial Hygiene Association Journal*, 45(8), pp. 509–516.

Zorpas, A. A., Constantinides, T., Vlyssides, A. G., Haralambous, I. & Loizidou, M. (2000). Heavy Metal Uptake by Natural Zeolite and Metals Partitioning in Sewage Sludge Compost. *Bioresour Technology*, 72 (2), pp. 113-119.

Zulkali, D., Ahmed, C. & Norulakmal, H. (2006). Oriza Sativa Husk as Heavy Metal Adsorbent: Optimization with Lead as Model Solution. *Bioresource Technology*, 97(1), pp. 21–25.

## 9. ACKNOWLEDGMENTS

I would like to express my sincere gratitude to my thesis advisor Dr. László Tolner, I appreciate all his contributions of time, ideas, comments and suggestions to make my PhD experience productive and stimulating. I extend thanks to my opponent members who assisted me with their insightful comments and suggestions.

I would also like to thank my research lab colleagues and school staff for their support and assistance when was needed, for their expertise and suggestions pertaining to my project, as well as their enjoyable presence in the lab.

I must express my profound gratitude for my family, for their continual support and motivation throughout my many years of school. I am also grateful for my friends who supported me during this time. This accomplishment would not have possible without them!

Also, thanks to everyone who encouraged me, helped me, and gave me passion and encouragement when I was down and lost.

I gratefully acknowledge the financial support received from my country, Libya. Finally, I must thank God for giving me the ability and intelligence to complete this accomplishment.

## 10. RELATED PUBLICATIONS

### Journal articles with IF

#### 1. Published Article:

- Kinetics Study of the Ability of Compost Material for Removing  $\text{Cu}^{2+}$  from Wastewater. Ramadan Benjreid, Mohammed Matouq, Mutaz Al-Alawi, Füleky György. Global nest Journal. DOI: <https://doi.org/10.30955/gnj.002865>

#### 2. Articles in provisional submission:

- Fixed Bed Adsorption Column Studies for the Removal of Cd (II) Using compost Material. Ramadan. Benjreid, Mutaz Al-Alawi, György. Füleky, Prokainé. Ágnes. Desalination and Water Treatment.
- Evaluation of the performance of encapsulated lifting system composting technology with a GORE(R) cover membrane: physico-chemical properties and spectroscopic analysis" Environmental Engineering Research.

### Conference proceedings:

- Title: “Cleaning Heavy Metal Pollution of Wastewater with Compost Application” Ramadan Benjared, György Füleky. International Youth Science Forum “LITTERIS ET ARTIBUS” 24–26 November 2016, LVIV, UKRAINE 498 – 501.
- Title: “Examination of Zinc Adsorption Capacity of Soils Treated with Different Pyrolysis Products”. Acta CTA Universitatis Sapientiae Agriculture and Environment. Cluj Napoca, Romania, 6(2014) 33– 38.

### International conferences:

- I. Title: “Cadmium Copper and Zink Sorption on Compost Materials. ORBIT 2016, 10<sup>th</sup> International Conference on Circular Economy and Organic Waste, Heraklion, Crete, Greece. 25-28 of May 2016.

- II. Title: “Soil Quality Improvement Using Natural Materials”. The 2016 ESSC International Conference. Babeş-Bolyai University, Cluj Napoca, Romania. 15-18 June 2016.
- III. Title: “KOMPOSZTANYAGOK KADMIUM, RÉZ ÉS CINK MEGKÖTŐ KÉPESSÉGE” Talajtani Vándorgyűlést. Debrecen, Hungary. 1-3 September 2016.
- IV. Title: “Removal of Cu and Cd from wastewater by compost application” WORKSHOP SOIL WASTE WATER 2018. Reusing wastewater and solid residues in agriculture, Landau in der Pfalz , Germany. 26th – 28th of March 2018.
- V. Title: “Cleaning heavy metal pollution of wastewater with compost application” XIV. Kárpát-medencei Környezettudományi Konferencia, Gödöllő, Hungary. 5-7 April 2018.
- VI. Title: “Ólom és cink megkötés komposztokon” LVIII Georgikon Napok, International Scientific Conference. University of Pannonia, Keszthely, Hungary 29-30. Sept 2016.

## 11. Declaration

I, Ramadan Benjreid, hereby declare that the effort presented in the Ph.D. thesis entitled **“POLLUTED WATER TREATMENT USING COMPOST MATERIAL AS ADSORBENT: BATCH AND CONTINUES COLUMN STUDIES”** is based on the novel work done by me under the supervision of Prof. László Tolner and Prof. György Füleky, Department of Soil Science and Agrochemistry, (Institute of Environmental Science, Faculty of Agricultural and Environmental Science,) Szent István University. This thesis contains no material that has been submitted previously, in whole or in part, for the award of any other academic degree or diploma. This dissertation is my own work.